

This is to certify that the dissertation entitled

Novel Polymer Films for Separations in Nanofiltration

presented by

Matthew D. Miller

has been accepted towards fulfillment of the requirements for the

Doctoral	degree in		Chemistry
n	e 1 1	Lua	\
Major Professor's Signature			
	8/8	23/05	
		Date	

MSU is an Affirmative Action/Equal Opportunity Institution

LIBRARY
Michigan State
University

PLACE IN RETURN BOX to remove this checkout from your record. TO AVOID FINES return on or before date due. MAY BE RECALLED with earlier due date if requested.

DATE DUE	DATE DUE	DATE DUE

2/05 c:/CIRC/DateDue.indd-p.15

Novel Polymer Films for Separations in Nanofiltration

Ву

Matthew D. Miller

A DISSERTATION

Submitted to
Michigan State University
in partial fulfillment of the requirements
for the degree of

DOCTOR OF PHILOSOPHY

Department of Chemistry

2005

ABSTRACT

Novel Polymer Films for Separations in Nanofiltration

By

Matthew D. Miller

Nanofiltration (NF) is a powerful separation technique, capable of operation in both large- and small-scale applications. Despite extensive developments in the NF field, increased permeate fluxes as well as greater control over membrane properties are constant objectives. A common target for NF performance enhancement is the membrane, which is the selective barrier between the feed and permeate solutions. In this dissertation I detail how the deposition of ultrathin polymer films on porous supports yields selective, high flux membranes.

To form composite NF membranes with ultrathin polymer skins, I employ alternating adsorption of polycations and polyanions on a porous support. Separations can be optimized by varying the constituent polyelectrolytes, and in general, the use of polycations and polyanions with lower charge densities allows greater passage of larger analytes, presumably because ionic crosslinking decreases with decreasing charge density. In situ ellipsometry confirms that lower charge densities result in highly water-swollen films. Careful selection of polyelectrolytes results in membranes capable of separating salts, sugars, or, remarkably, even proteins such as myoglobin and bovine serum albumin.

Additionally, membrane transport characteristics such as rejection and solution flux can be optimized by simple changes in the film deposition process. Moreover, water fluxes through these films are 1.5-5 times greater than through commercial NF membranes.

To my mom and dad.

ACKNOWLEDGMENTS

I would first like to thank Professor Bruening for his guidance and assistance throughout the past four years. His ability to always have time for questions and discussion has made my tenure in graduate school an educational and enjoyable experience.

I also want to thank the members of the Bruening research group, past and present, as well as Dr. Baker, J.B., Bao, and Ying for their fruitful and insightful discussions. I especially thank Dan, Brian, Alex, and Rick for their friendship and conversation on topics ranging from the newest video cards to the sorry state of the Mets/Cubs/Tigers/Lions (depending on the year, of course—unless we were talking about the Tigers or Lions, which are of late always pretty sorry). I also greatly appreciate the initial nanofiltration research performed in the Bruening Group by Jeremy, Brian, and Xiaoyun; as well as their guidance in teaching me the equipment and analysis techniques.

I particularly want to thank my family (including Michelle's family!) and friends for all their love and support; they have kept me going strong for over 24 years. You have made me strive to be my best every day. Also, special thanks to mom and dad for not taking away my chemistry set after any of the countless mishaps in the garage. I promise to pay you back for all the structural damage to the house... eventually.

Last but certainly not least, I want to thank my fiancée Michelle for selflessly supporting me—her encouragement and presence lights my days.

TABLE OF CONTENTS

List of Table	es	viii
List of Figur	es	x
Key to Abbr	eviations	xiv
Chapter 1:	Introduction	1
	Membranes and Nanofiltration	2
1.2:	Multilayer Polyelectrolyte Films as Skin Layers in NF	
	Membranes	
	Outline of this Dissertation	
1.4:	Works Cited	24
Chapter 2:	The Nanofiltration Properties of Multilayer Polyelectrolyte	
	Membranes through Variation of Film Composition	32
2.1:	Introduction	33
	Experimental	
2.3:	Results and Discussion	42
2.4:	Conclusions	63
2.5:	Acknowledgements	63
2.6:	Works Cited	64
Chapter 3:	Correlation of the Swelling and Permeability of	
·	Polyelectrolyte Multilayer Films	67
3.1:	Introduction	68
	Experimental	
	Results and Discussion	
3.4:	Conclusions	96
	Acknowledgements	
3.6:	Works Cited	98

Chapter 4: Modified Polyelectrolyte Multilayer Films for Enhance Nanofiltration of Neutral and Charged Molecules	
4.1: Introduction	102
4.2: Experimental	106
4.3: Results and Discussion	
4.4: Conclusions	
4.5: Acknowledgements	123
4.6: Works Cited	
Chapter 5: Conclusions and Future Work	127
5.1: Conclusions	
5.2: Future Work	128
5.3: Works Cited	132

LIST OF TABLES

Table 2.1:	Molecular weights, aqueous diffusion coefficients (D), and Stokes' radii (r _s) of the neutral molecules used in transport studies.
Table 2.2:	Flux and selectivity values for diffusion dialysis of glycerol, glucose, sucrose, and raffinose through porous alumina coated with various PSS/PDADMAC films deposited from 0.5 M NaCl
Table 2.3:	Flux and selectivity values for diffusion dialysis of glycerol, glucose, sucrose, and raffinose through bare porous alumina and alumina coated with various PSS/PDADMAC films deposited from 0.1 M NaCl. 50
Table 2.4:	Rejections, water fluxes, and selectivities from nanofiltration of a series of neutral molecules using porous alumina coated with a variety of PEM films.
Table 2.5:	Rejections, water fluxes, and selectivities from nanofiltration of a series of neutral molecules using porous alumina coated with PSS/PDADMAC films deposited from 0.1 M NaCl
Table 2.6:	Rejections, water fluxes, and selectivities from nanofiltration of sucrose and NaCl by porous alumina coated with PSS/PDADMAC films.
Table 3.1:	Ellipsometric thicknesses of PEMs under nitrogen (<5% RH), water, or ethanol, and percent swelling in the two solvents82
Table 3.2:	Percent rejection in nanofiltration of glucose, sucrose, and raffinose dissolved in water. PSS/PDADMAC and HA/chitosan data are from Chapter 2. The swelling values are from analogous films (Table 3.1)
Table 3.3:	Fluxes in diffusion dialysis of glucose, sucrose, and raffinose (dissolved in water) through porous alumina coated with various polyelectrolyte films. The bare alumina and PSS/PDADMAC data are from Chapter 2. All film thicknesses were measured in a <5% RH nitrogen atmosphere except for that of [HA/chitosan] ₈ HA, which is an estimate based upon the thickness of 8-bilayer HA/chitosan films.

Table 3.4:	Fluxes in diffusion dialysis of 140 μM glucose, sucrose, and raffinose in ethanol through porous alumina coated with various polyelectrolyte films. All film thicknesses were measured in a <5% RH nitrogen atmosphere except for that of [HA/chitosan] ₈ HA, which is an estimate based upon the thickness of 8-bilayer HA/chitosan films.
Table 4.1:	Rejections, solution fluxes, and selectivities from nanofiltration of a series of neutral molecules using porous alumina coated with a variety of multilayer polyelectrolyte films. 6,7. 0.5 M NaCl was used in deposition of the PSS/PDADMAC layers. Films are given numbers to aid in discussion
Table 4.2:	Rejections, solution fluxes, and selectivities from nanofiltration of sucrose and NaCl by porous alumina coated with a variety of PEM films arranged in order of increasing NaCl/sucrose selectivity. 0.5 M NaCl was used in deposition of the PSS/PDADMAC layers. Films are numbered to aid in discussion
Table 4.3:	Rejections, solution fluxes, and selectivities from nanofiltration of BT and sodium sulfate using porous alumina coated with a variety of PEM films. All PSS/PDADMAC layers were deposited from 0.5 M NaCl unless indicated otherwise. Films are numbered to aid in discussion
Table 4.4 :	Rejections, solution fluxes, and selectivities from nanofiltration of BT and potassium phosphate at pH 8 using porous alumina coated with PEM films. All PSS/PDADMAC layers were deposited from 0.5 M NaCl. Films are numbered to aid in discussion

LIST OF FIGURES

Figure 1.1:	Schematic depiction of a pressure-driven, size-selective membrane separation	2
Figure 1.2:	Representation of the concentration profile in NF. Charge or size exclusion of the solute at the membrane-feed interface results in rejection.	5
Figure 1.3:	Illustration depicting the size-exclusion model described in Equation 1.6	7
Figure 1.4:	Schematic description of the layer-by-layer assembly of polyelectrolyte multilayer films. Counter-ions and intertwining of polymers are not shown for the sake of clarity.	5
Figure 2.1:	Schematic showing the NF unit used in this dissertation4	O
Figure 2.2:	Schematic diagram of a "nanofiltration cell" from Figure 2.1 showing the assembly of the cell components. From top to bottom: (1) and (2) are the inlet and outlet ports, (3) are the threads, (4) is the rubber O-ring, (5) is the membrane, (6) is the stainless steel frit that the membrane is placed on, (7) is the cap that holds the frit, and (8) is the bottom part of the cell that screws into the threads (3). This figure is adapted from Stanton et al. The arrow indicates flow direction through the cell.	1
Figure 2.3:	Structures of polyelectrolytes used in this study4	3
Figure 2.4:	SEM images of porous alumina coated with polyelectrolyte films. (a) cross section of a ~30 nm thick, 5-bilayer PSS/PDADMAC film deposited from 0.5 M NaCl. (b) top-down view of a 4.5-bilayer PSS/chitosan film	7
Figure 2.5:	NaCl flux and NaCl/Sucrose selectivity from DD through porous alumina coated with PSS/PDADMAC films deposited from 0.5 M NaCl. The arrows indicate which y-axis pertains to each data set. Flux was normalized by dividing by the source-phase concentration.	8

Figure 2.6:	NaCl flux and NaCl/Sucrose selectivity from diffusion dialysis through porous alumina coated with PSS/PDADMAC films deposited from 0.1 M NaCl. The arrows indicate which y-axis pertains to each data set. Flux was normalized by dividing by the source-phase concentration.
Figure 3.1:	Diagram depicting the model of light reflection used to fit ellipsometric data. The n and k terms describe the real and imaginary parts of the complex refractive indices, while d represents the layer thickness. The layers are not drawn to scale.
Figure 3.2:	Calculated Ψ and Δ values for a Si/SiO ₂ /film system (water as the ambient medium and a 2.0 nm silicon oxide layer) as a function of the refractive index and thickness of the film. The simulation was performed at a wavelength of 450.5 nm where the optical constants are: water - n=1.3395, silicon oxide - n=1.4644, k=0, and silicon - n=4.7108, and k=0.0963. The point with a thickness of 55 nm and a refractive index of 1.44 represents a 9.5-bilayer PSS/PDADAMC film deposited from 0.1 M NaCl, and the black lines through that point show the $\pm 0.3^{\circ}$ uncertainty in Ψ and Δ measurements. Enclosed data points correspond to identical thicknesses at different refractive indices.
Figure 3.3:	Calculated Ψ and Δ values for the system depicted in Figure 3.1 (nitrogen with <5% relative humidity as the ambient medium and a 2.0 nm silicon oxide layer) as a function of the refractive index, n_2 , and thickness, d_2 , of the film. The simulation was performed at a wavelength of 450.5 nm where the optical constants are n_1 =1.000, n_3 =1.4644, k_3 =0, n_4 =4.7108, and k_4 = 0.0963. The point with a thickness of 25 nm and a refractive index of 1.54 represents a 9.5-bilayer PSS/PDADAMC film deposited from 0.1 M NaCl, and the black lines through that point show the ±0.3° uncertainty in Ψ and Δ measurements. Enclosed data points correspond to identical thicknesses at different refractive indices

Figure 3.4:	Calculated Ψ and Δ values for the system depicted in Figure 3.1 (ethanol as the ambient medium and a 2.0 nm silicon oxide layer) as a function of the refractive index, n_2 , and thickness, d_2 , of the film. The simulation was performed at a wavelength of 480.2 nm where the optical constants are n_1 =1.3645, n_3 =1.4636, k_3 =0, n_4 =4.412, and k_4 = 0.0629. The point with a thickness of 50 nm and a refractive index of 1.47 represents a 9.5-bilayer PSS/PDADAMC film deposited from 0.1 M NaCl, and the black lines through that point show the ±0.3° uncertainty in Ψ and Δ measurements. Enclosed data points correspond to identical thicknesses at different refractive indices.	79
Figure 3.5:	A 3 x 25 µm AFM topographical image and the derived average line scan for thickness analysis of a [PSS/PDADMAC] ₁₀ film deposited from 0.1 M NaCl. The region between the two black arrows on the left determines the average film + wafer height, and the area between the two dark grey arrows on the right determines the height of the scratched Si wafer. The average PEM thickness for this particular scan is 28.3 nm.	81
Figure 3.6:	The experimental (dashed line) and generated (fit, solid line) Ψ and Δ ellipsometric data for a dry (under <5% RH nitrogen) 10-bilayer PSS/PDADMAC film deposited from 0.1 M NaCl. This fit corresponds to a film that is 24 nm thick and has a refractive index of 1.541 at 450.5 nm	83
Figure 3.7:	The experimental (dashed line) and generated (fit, solid line) Ψ and Δ ellipsometric data for a water-submerged 8-bilayer HA/chitosan film. This fit corresponds to a film that is 124 nm thick and has a refractive index of 1.389 at 450.5 nm	84
Figure 3.8:	The experimental (dashed line) and generated (fit, solid line) Ψ and Δ ellipsometric data for an ethanol-submerged 9.5-bilayer PSS/PDADMAC film deposited from 0.1 M NaCl. This fit corresponds to a film that is 52 nm thick and has a refractive index of 1.453 at 480.2 nm.	85
Figure 3.9:	Structures of the polyelectrolytes used in Chapter 3	87

Figure 4.1:	Schematic illustration of the concept of hybrid polyelectrolyte membranes containing PSS, PDADMAC, and PAH deposited onto a porous alumina support. The color-coded chemical structures of the individual polyelectrolytes are also shown. (The porous support is actually several orders of magnitude thicker than the polyelectrolyte film.)	
Figure 4.2:	Cross-sectional SEM image of a [PSS/PDADMAC] ₃ - [PSS/PAH]PSS* film deposited on porous alumina. The final PSS layer was deposited from 2.5 M MnCl ₂	
Figure 5.1:	Simplified mechanism for the crosslinking reaction of HA and chitosan by EDC/NHS coupling129	

LIST OF ABBREVIATIONS

Abbreviation Definition

AFM Atomic Force Microscopy

DD..... Diffusion Dialysis

EDC 1-Ethyl-3-(3-dimethylaminopropyl)-carbodiimide

FT-IR..... Fourier Transform Infrared

HA..... Hyaluronic Acid

M_W Molecular Weight

MWCO Molecular Weight Cutoff

NF Nanofiltration

NHS N-hydroxysuccinimide

PAA..... Poly(acrylic acid)

PAH Poly(allylamine hydrochloride)

PDADMAC Poly(diallyldimethylammonium chloride)

PEI Poly(ethylene imine)

PEM Polyelectrolyte Multilayer

PSS...... Poly(styrene sulfonate)

RH..... Relative Humidity

RO Reverse Osmosis

SEM Scanning Electron Microscope

Chapter 1

INTRODUCTION

Chemical separations are essential processes in diverse applications ranging from chromatographic analysis to petroleum refining to the isolation of pharmacologically active plant components. 1-3 Techniques employed in such recrystallization.7,8 separations include distillation.4-6 centrifugation. 9-11 sublimation, 12-14 dialysis, 15-17 and chromatography. 18-20 This research focuses specifically on nanofiltration (NF), which is a membrane-based process similar to reverse osmosis. Membrane separations are often employed in large-scale industrial processes such as desalination²¹ and gas separations, ²²⁻²⁴ though they are also important in small-scale applications such as membrane introduction mass spectrometry.^{25,26} These separations rely on the interaction of chemical compounds with a selective phase, the membrane, to effect separations. The selective phase is the foundation of these separations and should be amenable to key improvements that employ novel film chemistry.

This dissertation explores the use of multilayer polyelectrolyte multilayer (PEM) films as the discriminating layer in membranes. The minimal thickness of the polyelectrolyte films allows fluxes that are 1.5 to 5-fold greater than those through commercial membranes, and Chapter 2 discusses how careful selection of the constituent polycations and polyanions in these films allows development of membranes with a wide range of molecular weight cutoffs. Multilayer polyelectrolyte films are particularly promising for sugar and salt/sugar

separations. Chapter 3 discusses how the ellipsometrically measured swelling behavior of these films relates to their transport properties, and Chapter 4 investigates how slight changes to polyelectrolyte deposition systems can significantly enhance several practical separations.

To put these results in context, this introduction first briefly discusses separation mechanisms in the area of NF as well as some membrane synthesis methods. The next section describes prior research on the formation and structure of multilayer polyelectrolyte films. Finally, an outline for the other chapters of the dissertation is given.

1.1 Membranes and Nanofiltration

Membrane systems utilize a discriminating layer (the membrane) to allow selective transport between two phases as shown in Figure 1.1. Several forces can drive transport across this layer, including pressure differences. nanofiltration e.g., (NF),²⁷ reverse osmosis (RO),²¹ and separations: 22-24 gas а concentration gradient, e.g., dialysis:²⁸ or even an electrical

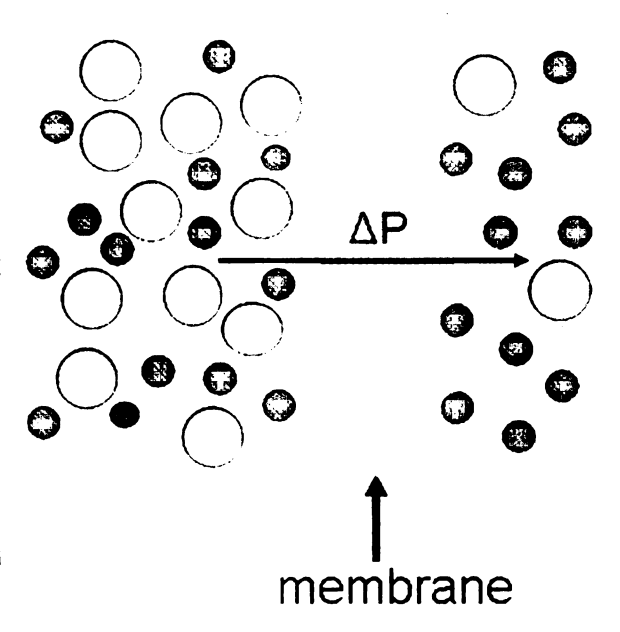


Figure 1.1: Schematic depiction of a pressure-driven, size-selective membrane separation

potential difference, e.g., electrodialysis.²⁹⁻³¹ Membrane separations can occur between two liquid phases,³² from a liquid to a gas phase (pervaporation),³³⁻³⁵ and between two gas-phases.³⁶⁻³⁸ This work focuses on liquid-liquid separations that include diffusion dialysis and NF, but the primary emphasis is on NF because of its higher fluxes and greater practicality. In this technique, pressure drives a solvent (with some accompanying solutes) across a membrane against a concentration gradient. NF is similar to reverse osmosis, but NF membranes are more permeable so lower pressures can be applied to achieve similar fluxes.^{32,39,40} The use of lower pressure makes NF more economical than RO for separations that do not require high NaCl rejections.

The term "nanofiltration" was initially coined by the membrane company FilmtecTM in the mid-1980s, but the name was retroactively applied to separations with water fluxes from 0.2-2 m³/(m² day bar) and NaCl rejections of 20-80%. The molecular weight cutoff (MWCO, solute molecular weight needed to achieve <10% passage of the solute through the membrane) of NF membranes is generally between 200-10000 g/mol, so NF applications include selective removal of molecules such as sugars, herbicides, for pesticides, and dyes. The largest application of NF is the softening of water (removal of Mg² and Ca² ions), and some plants have been built that can process 40 million gallons of water per day. Despite these applications, improved membranes with higher permeabilities, greater stabilities and lower propensities for fouling would certainly be beneficial for expanding the scope of this technique. Hence

the goal of this work is to develop a versatile method for forming ultrathin films that are capable of a wide range of high-flux separations.

Separation Mechanisms in NF. NF membranes rely primarily on two mechanisms for selective transport: charge exclusion and sieving. In both mechanisms, transport is often modeled by assuming equilibrium at the feed and permeate interfaces and allowing transport within the membrane to occur by convection and diffusion (Figure 1.2). In charge exclusion (also called Donnan exclusion), a high density of charge on the membrane surface results in exclusion of species in solution with a charge of the same sign. 49-53 Because exclusion increases with the charge on the species, this mechanism can separate singly and doubly charged species such as chloride and sulfate 50-53 or sodium and magnesium ions. 49

To understand how a charged membrane rejects ions, consider a membrane exposed to a solution of a single binary salt, $A_x B_y$, where z_A is the charge on the cation and z_B is the charge on the anion. Because of the fixed charge on the membrane, the concentrations of mobile cations and anions within the membrane are not the same. At equilibrium, this creates an electrical potential (the Donnan potential), which is described by Equation 1.1,⁵⁴ where Ψ_{Don} is the Donnan potential, R is the gas constant, T is temperature, F is Faraday's constant, a^M is the activity of the ion in the membrane, and a^S is

$$\Psi_{Don} = \left(\frac{RT}{z_B F}\right) \ln \left(\frac{a_B^S}{a_B^M}\right) \text{ and } \Psi_{Don} = \left(\frac{RT}{z_A F}\right) \ln \left(\frac{a_A^S}{a_A^M}\right)$$
(1.1)

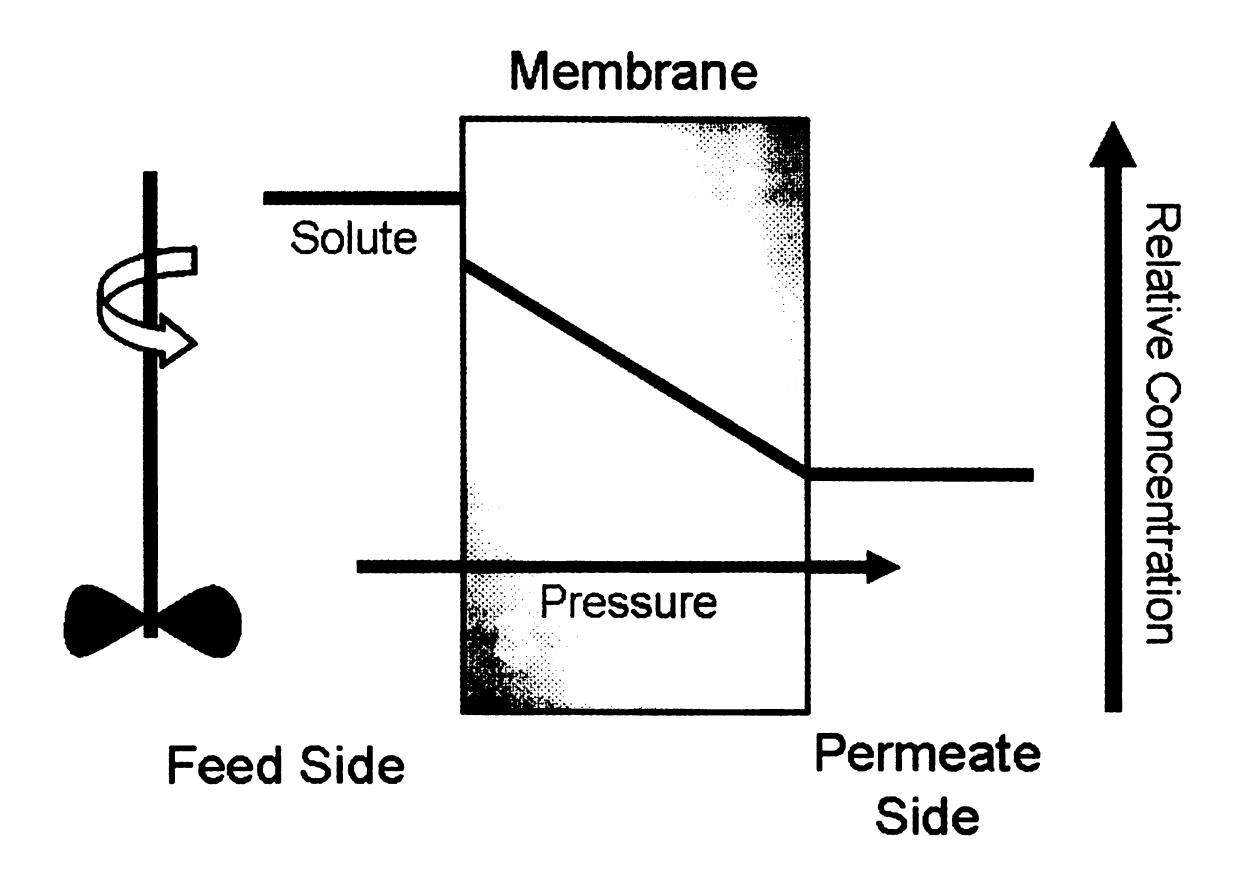


Figure 1.2: Representation of the concentration profile in NF. Charge or size exclusion of the solute at the membrane-feed interface results in rejection.

the activity of the ion in solution. This equation applies to both the cation and anion of the salt. Equating the Donnan potential for each species and assuming that solutions are sufficiently dilute that concentrations, c, equal activities yields Equation 1.2.

$$\frac{RT}{z_B F} \ln \left(\frac{c_B^S}{c_B^M} \right) = \frac{RT}{z_A F} \ln \left(\frac{c_A^S}{c_A^M} \right)$$
 (1.2)

The assumption of charge neutrality both in solution and in the membrane results in Equations 1.3 and 1.4, respectively, where c^S is the species concentration in bulk solution, c^M is the species concentration in the membrane, and c_X^M is the concentration of fixed charge due to the membrane material.

$$|z_A|C_A^S = |z_B|C_B^S \tag{1.3}$$

$$|z_A|C_A^M = |z_B|C_B^M + |z_X|C_X^M$$
(1.4)

Finally, substituting Equations 1.3 and 1.4 into Equation 1.2 leads to the distribution coefficient for the anion shown in Equation 1.5. A similar expression can be derived for the cation. In the case of a divalent and monovalent sodium salt and a negatively charged membrane, this equation will result in a much smaller distribution coefficient for the divalent anion.

$$\frac{C_B^M}{C_B^S} = \left\lceil \frac{|z_B|C_B^S}{|z_B|C_B^M + |z_X|C_X^M} \right\rceil^{\Lambda} \left| \frac{z_B}{z_A} \right| \tag{1.5}$$

For neutral molecules, the major separation mechanism in porous membranes is sieving, in which transport into membrane pores depends on solute dimensions. The most important variables for predicting the rejection properties of a sieving membrane are the radii of the solutes and membrane

simple partition model with spherical solutes and cylindrical pores used to estimate steric-based membrane rejection, where r is the radius of the solute and R is the radius of the pore (assuming a uniform pore-size). This model assumes that the closest a solute can approach the pore wall is the radius of that solute, r. Thus, the

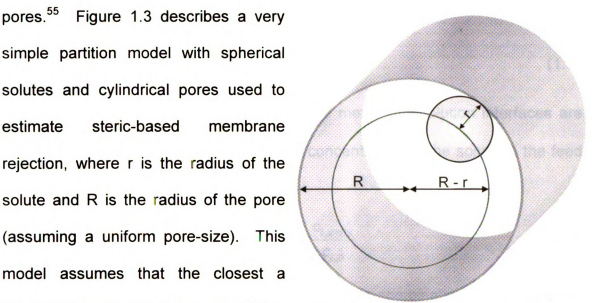


Figure 1.3: Illustration depicting the size-exclusion model described in Equation 1.6

center of the solute can only occupy a fraction of the cross-sectional area. (1r/R)² (also called Φ). Essentially, the ratio of solute to pore radius determines an effective partition coefficient, Φ , that dictates how well molecules can enter the membrane. If transport to the permeate side is primarily due to convection, the partition coefficient can also predict rejection as described by Equation 1.6.41,44,55 Hindered convection or diffusion will result in a more complicated model of transport.44,56,57

Percent Rejection =
$$\left[1 - \left(1 - \frac{r}{R}\right)^2\right] * 100\%$$
 (1.6)

Equation 1.7 (a form of Fick's first law) describes steady state diffusion through a membrane, where j_i is the solute flux, D_i is the diffusion coefficient of the solute through the membrane, $c_{i,x=0}$ and $c_{i,x=\Delta x}$ are the concentrations of the solute in the membrane at the feed and permeate sides of the film, respectively, and Δx is the thickness of the membrane.

$$j_i = -D_i \frac{c_{i,x=0} - c_{i,x=\Delta x}}{\Delta x}$$
 (1.7)

However, the concentrations of solute at the membrane/solution interfaces are controlled by Φ , where $c_{i,f}$ and $c_{i,p}$ are the concentration of the solute in the feed and permeate, as shown in Equation 1.8.

$$\Phi = \frac{c_{i,x=0}}{c_{i,f}} = \frac{c_{i,x=\Delta x}}{c_{i,p}}$$
 (1.8)

Also, the diffusion coefficient in Equation 1.7 is a combination of the diffusion coefficient of the solute at infinite dilution, $D_{i,inf}$, as well as the hindrance factor for diffusion, $K_{i,d}$, and the film porosity, ε , as shown in Equation 1.9.

$$D_i = D_{i,\inf} K_{i,d} \varepsilon \tag{1.9}$$

Note that $K_{i,d}$, assuming a homogeneous velocity across the membrane pores, is similar to the enhanced drag coefficient, K^1 , which is a function of the ratio of solute to pore radius, and expressions for calculating this value are available in literature. Substitution of Equations 1.8 and 1.9 into Equation 1.7 results in Equation 1.10, an expression for diffusive flux through a membrane.

$$j_i = -D_{i,inf} K_{i,d} \varepsilon \frac{\Phi(c_{i,f} - c_{i,p})}{\Lambda x}$$
 (1.10)

Solvent flux in pressure driven processes like NF is described by Equation 1.11, where η is the solvent viscosity, τ is the pore tortuosity, and ΔP is the pressure drop across the membrane.

$$J_{V} = \frac{\varepsilon R^{2} \Delta P}{8 \eta \tau \Delta X} \tag{1.11}$$

Including both hindered diffusion and hindered convection, $K_{i,c}$, the expression for solute flux in NF is shown in Equation 1.12.

$$j_i = K_{i,c}c_iJ_v - D_{i,\inf}K_{i,d}\varepsilon\frac{dc_i}{dx}$$
 (1.12)

The hindered convection term can be approximated by the lag coefficient, *G*, which is also a function of the ratio of solute to pore radius. Again, expressions for calculating this value are available in the literature.⁴⁴ Finally, integration of Equation 1.12 with the boundary conditions in Equation 1.13, results in an expression for rejection that combines hindered diffusion and convection with the ratio of solute to membrane pore radius, Equation 1.14.^{44,57} The partition expression does not factor into the solute concentration on the permeate side of the membrane in Equation 1.13 because that side is not stirred with the NF system discussed in this dissertation (only the feed side is stirred with our cross-flow equipment).

$$c_{i,f} \Phi = c_{i,x=0}; c_{i,p} = c_{i,x=\Delta x}$$
 (1.13)

Rejection =
$$1 - \frac{K_{i,c}\Phi}{1 - \exp\left(-\frac{K_{i,c}}{K_{i,d}}\frac{J_{v}\Delta x}{D_{i,\inf}\varepsilon}\right)\left(1 - K_{i,c}\right)}$$
 (1.14)

While the previous theoretical discussion describes the pore-flow model, it is also possible that a solution-diffusion mechanism influences solute and solvent transport. In this model, solute and solvent dissolve in the film, cross the membrane via diffusion, then desorb into the permeate. In the case of solution-diffusion, Equation 1.15 describes the *solvent* flux in NF (J_i), where D_i is the diffusion coefficient of solvent in the membrane, K_i is the sorption coefficient of the solvent, c_i is the concentration of the solvent, $\Delta \pi$ is the osmotic pressure, R is the gas constant, T is temperature, and v_i is the molar volume of the solvent.

$$J_{i} = \frac{D_{i}K_{i}C_{i}v_{i}(\Delta P - \Delta \pi)}{\Delta xRT}$$
 (1.15)

Equation 1.16 describes the solution-diffusion *solute* flux through the membrane where D_j is the diffusion coefficient of the solute, K is the sorption coefficient of the solute, and Δc is the concentration change of the solute across the membrane.

$$J_j = \frac{D_j K_j \Delta c_j}{\Delta x} \tag{1.16}$$

A more in-depth derivation of these equations is beyond the scope of this dissertation, though it is available elsewhere.⁴¹

It is often difficult to determine the contribution of solution-diffusion or transport through pores to the solute transport through the membranes described in this dissertation. Baker states that the transition between the two mechanisms occurs when the effective radii of membrane pores are between 0.25-0.5 nm.⁴¹ The pore size of the membranes described in this dissertation are likely above this threshold. A previous modeling study with similar, more rejecting films found

the average pore radius of the membranes to be between 0.4-0.5 nm.⁴⁴ An investigation of the local solute environment using a technique like fluorescence lifetime measurement⁵⁸ may elucidate if transport occurs through the water-filled pores or along the polymer backbone. Tedeschi et al. performed a similar study with PEMs utilizing pyrene fluorescence as a polarity sensitive probe,⁵⁹ but unfortunately most of their data were collected when the films were under varying degrees of relative humidity and not immersed in water.

Synthesis of NF membranes. Sieving properties of membranes are a function of pore size, and one of the largest factors that affect this variable is the method of membrane synthesis. Most current NF membranes are made by interfacial polymerization, phase inversion, or surface modification of preexisting membranes.60 Interfacial polymerization is the process of loading a porous support with a reactive species (such as a diamine) dissolved in solvent A, and then immersing it in a complementary reactive species (e.g., a di-acid chloride) dissolved in solvent B. The two solvents are immiscible so the polymerization occurs only at the solution A/solution B interface. 60 Such membranes are advantageous in that very little material is needed in the thin skin layer, so expensive, high-performance polymers can be employed to make the skins. Many recent membranes made by this process utilize trimesoylchloride as one of the reactive species. 61-63 This monomer is popular because it possesses three active sites that can be reacted to varying degrees depending on stoichiometric control. The unreacted groups are subsequently hydrolyzed, lending additional control over the hydrophilicity to the membrane. 60 The amine co-reactant is often *m*- or *p*-phenylenediamine, ^{62,63} however, bipiperidine or bisphenol derivatives are often used to increase chemical resistance. ⁶⁴⁻⁶⁶

Phase inversion is another popular technique, which yields asymmetrically skinned membranes. In general, these structures are made by the precipitation of a solvated polymer to form a membrane whose surface has very small pores and sits on top of a porous, spongy bulk. Some of the methods for producing these films include immersion of dissolved polymer into a solvent in which the polymer is not soluble, removal of solvent from a solution of a polymer in a solvent/non-solvent system, temperature reduction, and placement of a cast film in an atmosphere that contains non-solvent saturated with a solvent. The porosity of these films is controlled by a combination of the polymer type, casting solution, post-casting treatment, coagulation method, and post-precipitation treatment.

Loeb and Sourirajan pioneered the phase inversion technique and specialized in making membranes from cellulose acetate. Since cellulose acetate membranes suffer from chemical instability, so asymmetric membranes have since been produced from several different polymers, including polyamides, polyimides, sulfonated polysulfone, and brominated poly(phenylene oxide). Many recent phase inversion membranes involve copolymers of poly(vinylidene fluoride) (PVDF). Sor example, Jeon and coworkers cast a mixture of poly(vinylidene fluoride-co-hexafluoropropylene) and poly(ethylene oxide-co-ethylene carbonate) to form high flux, highly stable membranes for use in a polymer electrolyte system.

Zhai et al. involves membranes made from a co-polymer of PVDF and 2-(2-bromoisobutyryloxy)ethyl acrylate, the latter acting as an initiator for atom transfer radical polymerization.⁷⁷

The final general membrane preparation technique discussed here is the one used in this dissertation, the physiochemical modification of membrane surfaces. One such method involves the plasma treatment of polymeric membranes. This process can form groups that increase permeability or, depending on the type of plasma used, induce cross-linking to increase stability. Membranes can also be chemically treated to increase performance, i.e. sulfonation to increase water flux and ion rejection. Another surface modification technique involves the direct attachment of polymers to the membrane surface. Ulbricht and Yang demonstrated this method when they grew acrylic acid from initiators trapped at the surface of polypropylene membranes.

The specific surface modification method utilized here involves the layer-by-layer adsorption of anionic and cationic polyelectrolytes on a ceramic alumina membrane. More than 40 years ago, Michaels demonstrated that precipitated polycation/polyanion complexes are capable of selective separations, and a number of studies examined adsorption of single polyelectrolytes on the surface of separation membranes. However, deposition of multilayer polyelectrolyte films differs from adsorption of single polyelectrolytes in that the multilayer films do more than just modify the membrane, they become the selective layer. Moreover, in comparison to

precipitated polyelectrolyte complexes, the layer-by-layer process should provide much better control over both membrane thickness and permeability. The next section more thoroughly discusses the large body of research concerning the properties and structure of multilayer polyelectrolyte films.

1.2 Multilayer Polyelectrolyte Films as Skin Layers in NF Membranes

Multilayer assemblies formed via layer-by-layer deposition have been extensively explored in recent literature. 94-105 A variety of interactions can be used to assemble such films, including both covalent and hydrogen bonding 102-104 as well as donor-acceptor coupling. However, the most popular method for forming multilayer films employs electrostatic interactions between polycations and polyanions. Assembly of such films can occur using the simple "dip-and-rinse" procedure illustrated in Figure 1.4, where charged substrates are immersed in a polyelectrolyte solution, rinsed with water, immersed in a solution of oppositely charged polyelectrolyte, and rinsed again. This process is repeated until a film of desired thickness is produced. These films are attractive as skin layers of membranes because their thickness can be controlled simply by varying the number of deposited layers, and the use of a variety of constituent polyelectrolytes should allow control over film permeability.

PEM Assembly and Structure. Knowledge of the structure of PEMs will be vital to understanding their permeability, and a number

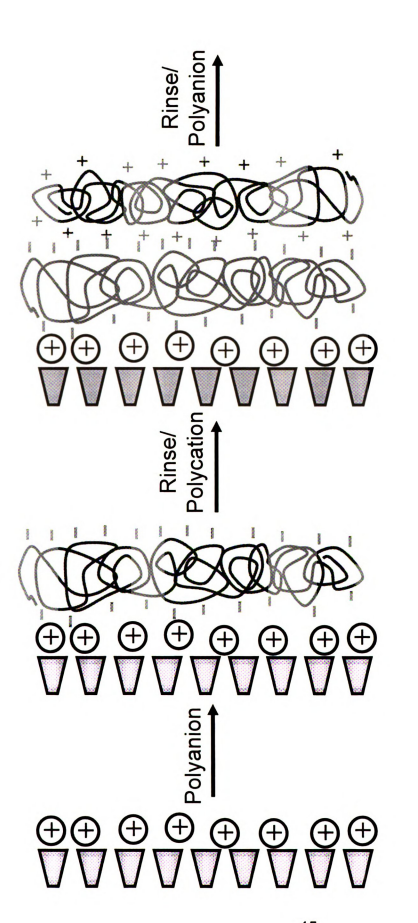


Figure 1.4: Schematic description of the layer-by-layer assembly of polyelectrolyte multilayer films. Counter-ions and intertwining of polymers are not shown for the sake of clarity.

of insightful studies have been performed in this regard. ^{100,108-121} Some of the earliest reports of PEMs by Decher and coworkers state that smooth, ordered films can be built up with over 100 layers with little to no change in adsorption characteristics. ¹⁰⁸ Additionally, these films do not exist in a discrete, layered structure, as interpenetration between the layers is estimated to be at least 4 polymer layers thick, ^{100,109} though this value can vary depending on film type and assembly conditions.

The structural properties of PEM films made with strong polyelectrolytes (polyelectrolyte repeat units that are fully ionized in solution) are heavily influenced by the salt concentration present during deposition. 110-112 concentrations of supporting electrolyte result in screening of the charges on the polyelectrolyte and lead to coiled polymer chains that form thick films. 110,111 For example, Dubas and Schlenoff demonstrated that there is a linear relationship between salt concentration in deposition solutions and the thickness of sulfonate) (PSS)/poly(diallyldimethylammonium chloride) poly(styrene (PDADMAC) films. 110 The structure of films made with weak polyelectrolytes (polyelectrolyte repeat units that are not completely ionized in solution, such as primary amines and carboxylic acids) is especially sensitive to deposition pH, which controls the degree of polyelectrolyte ionization. 113-115 Yoo et al. showed that bilayer composition, surface wettability, layer interpenetration, and layer thickness are all controlled by simply varying the polyelectrolyte deposition pH. 114

Interestingly, some polyelectrolyte systems grow exponentially (as opposed to linearly) with the number of added polymer layers. 116-121 This rapid

growth may occur because at least one of the polyelectrolytes is capable of penetrating and diffusing through the bulk of the film, as opposed to linearly growing films that interpenetrate only over a couple of bilayers. When the film is rinsed, polyelectrolytes that diffuse throughout the film are not readily removed, and when the membrane is brought into contact with a polyelectrolyte with opposing charge, the previously deposited polymer chains diffuse back towards the solution/film interface, precipitate with the new polyelectrolyte and form an extremely thick layer. Films constructed from hyaluronic acid (HA) and chitosan exhibit this non-linear growth behavior and possess very interesting permselectivity and swelling properties, as discussed in Chapters 2 and 3 of this dissertation.

Separations with PEMs. Careful consideration of properties such as polyelectrolyte type (strong or weak polyelectrolytes, linearly or exponentially growing) and deposition conditions (pH and salt concentration) should allow tailoring of the permeability of PEMs. 33,35,44,49,53,123 Many studies of transport through PEMs have been published, and include techniques like pervaporation, 33,34,124-127 NF, 44,53,123,128 and gas separation. 49,129 Krasemann and Tieke reported that 60-bilayer films exhibit a diffusional selectivity of over 100 for a mixture of Na⁺/Mg²⁺ and 45 for a mixture of Cl⁻ and SO₄²⁻. 130 However, these results were obtained with thick films that limited flux. Tieke's group also produced PEMs for NF that exhibited SO₄²⁻ rejections of up to 98.5%, but solution flux was only 0.003 m³/(m² day bar). 123 Stanton et al. used much thinner

PEM films to obtain a sulfate rejection of 95% with a solution flux of 0.4 m³/(m² day bar), a stark improvement in hydraulic permeability.⁵³

Despite their charged nature, PEMs are not limited to ionic separations. They recently found utility in pervaporation separations and are attractive for removing water from organic/water mixtures. 33,34,124,125,127 Very recent work by Schwarz and Malsch demonstrated that PEMs can separate cyclohexane and benzene via pervaporation. However, these separations are likely based upon solute solubility in the membrane material, so fractionation of molecules with similar polarities may be challenging.

This work explores the use of PEMs in NF of neutral molecules and in the separation of salts from neutral molecules. Although a few papers examined NF of salts using PEMs, only one study, published by our group, examined NF of neutral molecules with PEMs. 44 That work showed that high selectivities between glucose and sucrose are possible, but the high rejection of organic solutes (the rejection of even methanol is 70%) may limit the use of these membranes in applications where high solute recovery is desired. This work shows that both control over MWCO and increased NF fluxes are possible with appropriate selection of the polyelectrolytes in PEMs. Moreover, ellipsometric data demonstrate that film swelling in aqueous solutions increases with decreasing charge density of the constituent polyelectrolytes and correlates well with MWCO.

This dissertation also shows the promise of multilayer polyelectrolyte films for two specific applications: the fractionation of oligosaccharides and the

separation of salt from sugar. Process streams in sugar refining consist of a variety of sugar oligomers, such as glucose, sucrose, raffinose, and stachyose, that all fulfill various chemical and biological roles. 131-133 Ideally, membranes with carefully controlled MWCOs could fractionate these sugar oliogomers, which vary in molecular weight by 160-180 g/mol per additional ring unit. One commercial membrane utilized for this task, the DS-5-DL from Osmonics, exhibits a glucose/sucrose selectivity of about 40, but the solution flux through these films is less than 0.2 m³/(m² day bar). 131 The PEM NF membranes detailed in this dissertation are capable of achieving similar selectivities, but with twice the flux.

Another possible application of PEM membranes involves the separation of salt and sugar. During the sugar refining process, the feed is passed through a bed of anion exchange resin to remove color bodies and other impurities. Once the anion exchange resin reaches its total exchange capacity, it is subsequently regenerated with NaCl. The regeneration effluent contains a significant amount of sugar as well as excess salt not used in the regeneration process. This solution is usually considered waste, but NF membranes are capable of recovering the salt as well as the sugar for future use. NF45 membranes from Dow Chemical/Filmtec have been investigated for this separation, but they exhibit a water flux of only 0.1 m³/(m² day bar) and have a relatively high NaCl rejection of ~40%. The membranes in this dissertation can increase flux by a factor of 4 over commercial products as well as produce sucrose rejections greater than 99% with 75% NaCl recovery.

The above applications, in concert with several others discussed in this dissertation, demonstrate the power of PEMs as NF membranes. Interestingly, simple variation of constituent polyelectrolytes, deposition conditions, and capping layer results in films with diverse retention and flux properties. Utilizing all of these parameters, the PEMs presented in Chapters 2-4 are capable of effecting the selective separation of species ranging in size from salts to albumin $(M_W 70000)$.

1.3 Outline of this Dissertation

Chapter 2 of this dissertation shows how PEMs can be tailored for specific separations by varying film composition. Liu and Bruening previously demonstrated that in NF, PSS/poly(allylamine hydrochloride) (PAH) films exhibit alucose/sucrose selectivities in excess of 100. However, glucose passage in those experiments was <3%, limiting the potential for saccharide separations.44 The data in Chapter 2 show that changing the polycation from PAH to the less densely charged PDADMAC results in membranes that exhibit at least twice the flux of PSS/PAH films with glucose recoveries in excess of 40%. PSS/PDADMAC films also separate NaCl and sucrose with high recoveries of salt and fluxes 2-3 times greater than commercial membranes (Typical water fluxes through commercial membranes are about 0.9 m³/(m² day) at 5 bar.⁴⁰). Additional experiments show that these transport properties are highly dependent on top-layer choice, as PSS/PDADMAC films capped with PDADMAC exhibit raffinose dialysis fluxes 300 times greater than films with PSS as the terminating layer (the reason why this occurs is discussed in Chapter 3). Finally, the use of exponentially growing PEMs with even lower charge densities demonstrates the potential for high-resolution separations of the proteins myoglobin (M_W 17000) and bovine serum albumin (M_W 70000).

The results in Chapter 2 clearly show that variables such as constituent polyelectrolytes, top-layer charge, and deposition conditions directly affect transport properties. In an effort to better understand the permeability of polyelectrolyte films, Chapter 3 aims at correlating transport through PEMs with their swelling in aqueous and ethanolic solutions. PEM swelling has been previously investigated in several published reports. Wong et al. showed that swelling of PSS/PAH films is proportional to relative humidity. Hiller and Rubner reported that PSS/PAH films exhibit unique swelling behavior as a function of swellant pH, and Burke and Barrett observed that HA/PAH films swell as much as 8-times their dry thicknesses, one of the highest expansions reported. Despite the various reports describing PEM swelling, however, very few data correlate solvent uptake with transport.

The in-situ ellipsometry experiments discussed in Chapter 3 demonstrate that in water, permeability increases as film swelling increases. For example, HA/chitosan films swell 4 times more than PSS/PAH coatings, and in NF experiments, the HA/chitosan membranes permit a 250-fold greater fractional passage of sucrose. Similar results are seen for diffusion dialysis experiments. PEMs also display diverse swelling properties in ethanol, but transport rates do not correlate with ethanol uptake, most likely due to a complex interplay between hydrophobicity and ionic crosslinking.

Despite these advances in membrane performance by utilizing PEMs, further improvement is always desirable. Previously reported PSS/PAH films exhibit glucose/sucrose selectivities 6 times greater than the PSS/PDADMAC films described in Chapter 2,44 but PSS/PDADMAC films have solution fluxes 2-3 times greater than those through PSS/PAH films and 10-fold greater glucose recoveries. An "ideal" PEM for NF of sugars would combine the best features of both PSS/PAH and PSS/PDADMAC films to give high selectivity, flux, and glucose recovery. Chapter 4 describes two types of film modifications that are intended to improve performance: adsorption of the capping layer of PSS/PAH films from high ionic strength and deposition of highly selective PSS/PAH layers on high flux PSS/PDADMAC "gutter layers." Hybrid PSS/PAH/PSS/PDADMAC films are capable of improving selectivities in sugar and NaCl/sucrose separations compared to pure PSS/PDADMAC films. Interestingly, simply increasing the solution ionic strength during the deposition of the final PSS-layer in PSS/PAH films results in high selectivities coupled with greater fluxes than pure PSS/PAH assemblies. This increased performance is likely because the high ionic strength induces reorganization throughout the film. In addition to revisiting sugar/sugar and sugar/salt separations from Chapter 2, Chapter 4 presents results from the purification of an idealized fermentation broth mimic to show an example of a salt/neutral molecule separation where salts are the rejected species.

Finally, Chapter 5 brings together several conclusions about this work.

Overall, improvements in NF are possible through the use of novel polymeric

films. Polyelectrolyte multilayers can serve as highly tunable, selective skin layers for NF membranes and are capable of separating multiple types of analytes. Chapter 5 also briefly discusses possible future paths of research for PEMs in the field of separation science.

1.4 Works Cited

- (1) Wu, S.; Sun, A.; Liu, R. J. Chromatogr., A 2005, 1066, 243-247.
- (2) Page, M. M.; Page, C. L.; Shaw, S. J.; Sawada, S. *J. Sep. Sci.* **2005**, *28*, 471-476.
- (3) Chevron U.S.A, *Refining Process*, http://www.chevron.com/products/about/pascagoula/refiningprocess/proccrude.s http://www.chevron.com/products/about/pascagoula/refiningprocess/proccrude.s http://www.chevron.com/products/about/pascagoula/refiningprocess/proccrude.s http://www.chevron.com/products/about/pascagoula/refiningprocess/proccrude.s http://www.chevron.com/products/about/pascagoula/refiningprocess/proccrude.s http://www.chevron.com/products/about/pascagoula/refiningprocess/proccrude.s https://www.chevron.com/products/about/pascagoula/refiningprocess/proccrude.s https://www.chevron.com/products/about/pascagoula/refiningprocess/proccrude.s https://www.chevron.com/products/about/pascagoula/refiningprocess/proccrude.s https://www.chevron.com/products/about/pascagoula/refiningprocess/proccrude.s https://www.chevron.com/products/about/pascagoula/refiningprocess/proccrude.s <a href="https://www.chevron.com/products/about/pascagoula/refiningprocess/pascagoula/refiningprocess/pascagoula/refiningprocess/pascagoula/refiningp
- (4) Liu, K.; Tong, Z.; Liu, L.; Feng, X. J. Membr. Sci. 2005, 256, 193-201.
- (5) Singh, A.; Hiwale, R.; Mahajani, S. M.; Gudi, R. D.; Gangadwala, J.; Kienle, A. *Ind. Eng. Chem. Res.* **2005**, *44*, 3042-3052.
- (6) Skouras, S.; Skogestad, S.; Kiva, V. AIChE Journal 2005, 51, 1144-1157.
- (7) Alsop, L.; Cowley, A. R.; Dilworth, J. R.; Donnelly, P. S.; Peach, J. M.; Rider, J. T. *Inorg. Chim. Acta* **2005**, *358*, 2770-2780.
- (8) Machura, B.; Kruszynski, R.; Jaworska, M. *Polyhedron* **2005**, *24*, 419-426.
- (9) Bronfman, M.; Loyola, G.; Koenig, C. S. *Anal. Biochem.* **1998**, *255*, 252-256.
- (10) Lohaus, G.; Pennewiss, K.; Sattelmacher, B.; Hussmann, M.; Muehling, K. H. *Physiol. Plant.* **2001**, *111*, 457-465.
- (11) Wiig, H.; Aukland, K.; Tenstad, O. Am. J. Physiol. 2003, 284, H416-H424.
- (12) Glavin, D. P.; Bada, J. L. Anal. Chem 1998, 70, 3119-3122.
- (13) Glavin, D. P.; Schubert, M.; Bada, J. L. Anal. Chem 2002, 74, 6408-6412.
- (14) Goryunkov, A. A.; Kuvychko, I. V.; loffe, I. N.; Dick, D. L.; Sidorov, L. N.; Strauss, S. H.; Boltalina, O. V. *J. Fluorine Chem.* **2003**, *124*, 61-64.
- (15) Haitzer, M.; Aiken, G. R.; Ryan, J. N. *Environ. Sci. Technol.* **2002**, *36*, 3564-3570.
- (16) Johnson, M. T.; Komane, L. L.; N'Da, D. D.; Neuse, E. W. J. Appl. Polym. Sci. **2005**, *96*, 10-19.
- (17) Malygin, A.; Parakhnevitch, N.; Karpova, G. *Biochim. Biophys. Acta* **2005**, 1747, 93-97.
- (18) McHowat, J.; Jones, J. H.; Creer, M. H. *J. Chromatogr., B* **1997**, *702*, 21-32.

- (19) Kasche, V. J. Biochem. Biophys. Methods 2001, 49, 49-62.
- (20) Grancher, D.; Jaussaud, P.; Durix, A.; Berthod, A.; Fenet, B.; Moulard, Y.; Bonnaire, Y.; Bony, S. *J. Chromatogr., A* **2004**, *1059*, 73-81.
- (21) Mohsen, M. S.; Jaber, J. O.; Afonso, M. D. Desalination 2003, 157, 167.
- (22) Matsubara, Y.; Iwasaki, K.-i.; Nakajima, M.; Nabetani, H.; Nakao, S.-i. *Biosci. Biotech. Bioch.* **1996**, *60*, 421-428.
- (23) Hutson, T. Int. Dairy Fed. 1998, 9804, 88-92.
- (24) Vellenga, E.; Tragardh, G. Desalination 1998, 120, 211-220.
- (25) Wedian, F.; Atkinson, D. B. Environ. Sci. Technol. 2002, 36, 4152-4155.
- (26) Wedian, F.; Atkinson, D. B. Environ. Sci. Technol. 2003, 37, 4425-4428.
- (27) Goulas, A. K.; Grandison, A. S.; Rastall, R. A. *J. Sci. Food Agr.* **2003**, *83*, 675-680.
- (28) van Staden, J. F.; Hattingh, C. J. Anal. Chim. Acta 1995, 308, 222-230.
- (29) Shaposhnik, V. A.; Kesore, K. J. Membr. Sci. 1997, 136, 35-39.
- (30) Slesarenko, V. V. Desalination 2003, 158, 303-311.
- (31) Bazinet, L. Crit. Rev. Food Sci. Nutr. 2005, 45, 307-326.
- (32) Bohdziewicz, J.; Bodzek, M.; Wasik, E. Desalination 1999, 121, 139-147.
- (33) Krasemann, L.; Tieke, B. J. Membr. Sci. 1998, 150, 23-30.
- (34) Meier-Haack, J.; Lenk, W.; Lehmann, D.; Lunkwitz, K. *J. Membr. Sci.* **2001**, *184*, 233-243.
- (35) Toutianoush, A.; Tieke, B. *Mat. Sci. Eng. C* **2002**, *C22*, 459-463.
- (36) Pinnau, I.; Koros, W. J. *J. Appl. Polym. Sci.* **1991**, *43*, 1491-1502.
- (37) Pinnau, I.; Koros, W. J. *Ind. Eng. Chem. Res.* **1991**, *30*, 1837-1840.
- (38) Xiao, K. P.; Harris, J. J.; Park, A.; Martin, C. M.; Pradeep, V.; Bruening, M. L. *Langmuir* **2001**, *17*, 8236-8241.
- (39) Yaroshchuk, A.; Staude, E. Desalination 1992, 86, 115-134.

- (40) Bhattacharyya, D.; Williams, M. E.; Ray, R. J.; McCray, S. B., In *Membrane Handbook*; Ho W.S.W, Sirkar, K.K., Eds. Van Nostrand Reinhold: New York, 1992.
- (41) Baker, R. W. *Membrane Technology and Applications*; 2nd ed.; John Wiley: Chichester, England, **2004**.
- (42) Schafer, A. I.; Fane, A. G.; Waite, T. D. In *Nanofiltration: Principles and Applications*; 1st ed.; Waite, T. D., Ed.; Elsevier: Oxford, UK, **2005**.
- (43) Osmonics Filtration Spectrum, http://www.osmonics.com/library/zoom-spold.htm, Accessed 06-03-05
- (44) Liu, X.; Bruening, M. L. Chem. Mater. 2004, 16, 351-357.
- (45) Causserand, C.; Aimar, P.; Cravedi, J. P.; Singlande, E. *Water Res.* **2005**, 39, 1594-1600.
- (46) Boussahel, R.; Bouland, S.; Moussaoui, K. M.; Montiel, A. *Desalination* **2000**, *132*, 205-209.
- (47) Koyuncu, I. J. Chem. Technol. Biotechnol. 2003, 78, 1219-1224.
- (48) Kiefer, C. A.; Brinson, F.; Suratt, B. *Maximizing the Resources: Solutions for Pure and Plentiful Water, Membrane Technology Conference Proceedings, Atlanta, GA, United States, Mar. 2-5, 2003* **2003**, 325-334.
- (49) Krasemann, L.; Tieke, B. *Mat. Sci. Eng. C-Bio S* **1999**, *C8-C9*, 513-518.
- (50) Harris, J. J.; Stair, J. L.; Bruening, M. L. *Chem. Mater.* **2000**, *12*, 1941-1946.
- (51) Stair, J. L.; Harris, J. J.; Bruening, M. L. Chem. Mater. **2001**, *13*, 2641-2648.
- (52) Dai, J.; Jensen, A. W.; Mohanty, D. K.; Erndt, J.; Bruening, M. L. *Langmuir* **2001**. *17*. 931-937.
- (53) Stanton, B. W.; Harris, J. J.; Miller, M. D.; Bruening, M. L. *Langmuir* **2003**, *19*, 7038-7042.
- (54) Mulder, M. Basic Principles of Membrane Technology; 2nd ed.; Kluwer Academic Publishers: Dordrecht, The Netherlands, **1997**.
- (55) Bowen, W. R.; Welfoot, J. S. In *Nanofiltration: Principles and Applications*; 1st ed.; Waite, T. D., Ed.; Elsevier: Oxford, UK, **2005**.
- (56) Bowen, W. R.; Mukhtar, H. J. Membr. Sci. 1996, 112, 263-274.

- (57) Bowen, W. R.; Mohammad, A. W.; Hilal, N. *J. Membr. Sci.* **1997**, *126*, 91-105.
- (58) Siegel, J.; Suhling, K.; Leveque-Fort, S.; Webb, S. E. D.; Davis, D. M.; Phillips, D.; Sabharwal, Y.; French, P. M. W. Rev. Sci. Instrum. 2003, 74, 182-192.
- (59) Tedeschi, C.; Möhwald, H.; Kirstein, S. J. Am. Chem. Soc. **2001**, *123*, 954-960.
- (60) Vankelecom, I. F. J.; De Smet, K.; Gevers, L. E. M.; Jacobs, P. A. In *Nanofiltration: Principles and Applications*; 1st ed.; Waite, T. D., Ed.; Elsevier: Oxford, UK, **2005**.
- (61) Ahmad, A. L.; Ooi, B. S. J. Membr. Sci. 2005, 255, 67-77.
- (62) Song, Y.; Sun, P.; Henry, L. L.; Sun, B. J. Membr. Sci. 2005, 251, 67-79.
- (63) Kim, S. H.; Kwak, S.-Y.; Suzuki, T. *Environ. Sci. Technol.* **2005**, *39*, 1764-1770.
- (64) Kwak, S.-Y.; Kim, C. K.; Kim, J.-J. *J. Polym. Sci., Part B: Polym. Phys.* **1996**, *34*, 2201-2208.
- (65) Tomaschke, J. E., Amine monomers and their use in preparing interfacially synthesized polyamide membranes for reverse osmosis and nanofiltration, U.S. Patent 5,922,203, **1999**
- (66) Tomaschke, J. E., Interfacial polymerization of bipiperidine-polyamide membranes for reverse osmosis, nanofiltration, and seawater desalination, Eur. Pat. Appl. 1060785. **2000**
- (67) Loeb, S.; Sourirajan, S. Advances in Chemistry Series 1963, 38, 117-132.
- (68) Fan, S.-C.; Wang, Y.-C.; Li, C.-L.; Lee, K.-R.; Liaw, D.-J.; Huang, H.-P.; Lai, J.-Y. *J. Membr. Sci.* **2002**, *204*, 67-79.
- (69) Huang, J.; Cranford, R. J.; Matsuura, T.; Roy, C. *J. Membr. Sci.* **2004**, *241*, 187-196.
- (70) Kinzer, K. E.; Lloyd, D. R.; Gay, M. S.; Wightman, J. P.; Johnson, B. C.; McGrath, J. E. *J. Membr. Sci.* **1985**, 22, 1-29.
- (71) Tang, B.; Xu, T.; Gong, M.; Yang, W. J. Membr. Sci. 2005, 248, 119-125.
- (72) Liu, X.; Neoh, K. G.; Kang, E. T. Surf. Interface Anal. 2004, 36, 1037-1040.
- (73) Feng, C.; Shi, B.; Li, G.; Wu, Y. J. Membr. Sci. 2004, 237, 15-24.

- (74) Stephan, A. M.; Renganathan, N. G.; Gopukumar, S.; Dale, T. *Mater. Chem. Phys.* **2004**, *85*, 6-11.
- (75) Zhai, G.-Q.; Lei, Y.; Kang, E. T.; Neoh, K. G. Surf. Interface Anal. 2004, 36, 1048-1051.
- (76) Jeon, J.-D.; Cho, B.-W.; Kwak, S.-Y. *J. Power Sources* **2005**, *143*, 219-226.
- (77) Zhai, G.; Kang, E. T.; Neoh, K. G. *Macromolecules* **2004**, *37*, 7240-7249.
- (78) Lai, J. Y.; Chao, Y. C. J. Appl. Polym. Sci. 1990, 39, 2293-2303.
- (79) Byun, H. S.; Burford, R. P.; Fane, A. G. *J. Appl. Polym. Sci.* **1994**, *52*, 825-835.
- (80) Ulbricht, M.; Oechel, A.; Lehmann, C.; Tomaschewski, G.; Hicke, H.-G. *J. Appl. Polym. Sci.* **1995**, *55*, 1707-1723.
- (81) Ulbricht, M.; Schwarz, H.-H. J. Membr. Sci. 1997, 136, 25-33.
- (82) Frahn, J.; Malsch, G.; Schwarz, H.-H. *J. Mater. Proc. Tech.* **2003**, *143*-144, 277-280.
- (83) Hwang, T.-s.; Park, J.-w. Macromol. Res. 2003, 11, 495-500.
- (84) Hilal, N.; Kochkodan, V.; Al-Khatib, L.; Levadna, T. *Desalination* **2004**, *167*, 293-300.
- (85) Geismann, C.; Ulbricht, M. Macromol. Chem. Phys. 2005, 206, 268-281.
- (86) Ulbricht, M.; Yang, H. Chem. Mater. 2005, 17, 2622-2631.
- (87) Esumi, K.; Masuda, A.; Otsuka, H. *Langmuir* **1993**, *9*, 284-287.
- (88) Rignenbach, E.; Chauveteau, G.; Pefferkorn, E. Colloids Surf., A 1995, 99, 161-173.
- (89) Esumi, K.; Goino, M. Langmuir 1998, 14, 4466-4470.
- (90) Michaels, A. S.; Miekka, R. G. J. Phys. Chem. 1961, 65, 1765-1773.
- (91) Dauginet, L.; Duwez, A. S.; Legras, R.; Demoustier-Champagne, S. *Langmuir* **2001**, *17*, 3952-3957.
- (92) Murata, T.; Tanioka, A. J. Colloid Interface Sci. 1997, 192, 26-36.
- (93) Nystrom, M. J. Membr. Sci. 1989, 44, 183-196.

- (94) Lvov, Y.; Decher, G.; Möhwald, H. Langmuir 1993, 9, 481-486.
- (95) Decher, G.; Lvov, Y.; Schmitt, J. Thin Solid Films 1994, 244, 772-777.
- (96) Ferreira, M.; Cheung, J. H.; Rubner, M. F. *Thin Solid Films* **1994**, *244*, 806-809.
- (97) Keller, S. W.; Johnson, S. A.; Brigham, E. S.; Yonemoto, E. H.; Mallouk, T. E. J. Am. Chem. Soc. **1995**, *117*, 12879-12880.
- (98) Caruso, F.; Niikura, K.; Furlong, D. N.; Okahata, Y. *Langmuir* **1997**, *13*, 3427-3433.
- (99) Ageev, E. P.; Vikhoreva, G. A.; Gal'braikh, L. S.; Matushkina, N. N.; Chaika, E. M.; Jaminsky, I. V. *Vysokomol. Soedin., Ser. A Ser. B* **1998**, *40*, 1198-1204.
- (100) Cassier, T.; Lowack, K.; Decher, G. Supramol. Sci. 1998, 5, 309-315.
- (101) Kotov, N. A.; Magonov, S.; Tropsha, E. Chem. Mater. 1998, 10, 886-895.
- (102) Cho, J.; Caruso, F. *Macromolecules* **2003**, *36*, 2845-2851.
- (103) DeLongchamp, D. M.; Hammond, P. T. Langmuir 2004, 20, 5403-5411.
- (104) Zhang, H.; Wang, Z.; Zhang, Y.; Zhang, X. *Langmuir* **2004**, *20*, 9366-9370.
- (105) Mwaura, J. K.; Pinto, M. R.; Witker, D.; Ananthakrishnan, N.; Schanze, K. S.; Reynolds, J. R. *Langmuir*, ACS ASAP.
- (106) Decher, G. In *Multilayer Thin Films*; Schlenoff, J. B., Ed.; Wiley-VCH: Weinheim, **2003**.
- (107) Decher, G. Science 1997, 277, 1232-1237.
- (108) Decher, G.; Hong, J. D.; Schmitt, J. *Thin Solid Films* **1992**, *210/211*, 831-835.
- (109) Baur, J. W.; Rubner, M. F.; Reynolds, J. R.; Kim, S. *Langmuir* **1999**, *15*, 6460-6469.
- (110) Dubas, S. T.; Schlenoff, J. B. *Macromolecules* **1999**, *32*, 8153-8160.
- (111) Schoeler, B.; Kumaraswamy, G.; Caruso, F. *Macromolecules* **2002**, *35*, 889-897.
- (112) Ladam, G.; Schaad, P.; Voegel, J. C.; Schaaf, P.; Decher, G.; Cuisinier, F. *Langmuir* **2000**, *16*, 1249-1255.

- (113) Shiratori, S. S.; Rubner, M. F. *Macromolecules* **2000**, *33*, 4213-4219.
- (114) Yoo, D.; Shiratori, S. S.; Rubner, M. F. *Macromolecules* **1998**, *31*, 4309-4318.
- (115) Choi, J.; Rubner, M. F. *Macromolecules* 2005, 38, 116-124.
- (116) Lavalle, P.; Gergely, C.; Cuisinier, F. J. G.; Decher, G.; Schaaf, P.; Voegel, J. C.; Picart, C. *Macromolecules* **2002**, *35*, 4458-4465.
- (117) McAloney, R. A.; Sinyor, M.; Dudnik, V.; Goh, M. C. Langmuir **2001**, *17*, 6655-6663.
- (118) Richert, L.; Lavalle, P.; Payan, E.; Shu, X. Z.; Prestwich, G. D.; Stoltz, J.-F.; Schaaf, P.; Voegel, J.-C.; Picart, C. Langmuir 2004, 20, 448-458.
- (119) Lavalle, P.; Picart, C.; Mutterer, J.; Gergely, C.; Reiss, H.; Voegel, J.-C.; Senger, B.; Schaaf, P. *J. Phys. Chem. B* **2004**, *108*, 635-648.
- (120) Picart, C.; Lavalle, P.; Hubert, P.; Cuisinier, F. J. G.; Decher, G.; Schaaf, P.; Voegel, J. C. *Langmuir* **2001**, *17*, 7414-7424.
- (121) Kujawa, P.; Badia, A.; Winnik, F. M. *Polym. Mater. Sci. Eng.* **2004**, *90*, 192-193.
- (122) Picart, C.; Mutterer, J.; Richert, L.; Luo, Y.; Prestwich, G. D.; Schaaf, P.; Voegel, J. C.; Lavalle, P. *Proc. Natl. Acad. Sci. U. S. A.* **2002**, *99*, 12531-12535.
- (123) Jin, W.; Toutianoush, A.; Tieke, B. *Langmuir* **2003**, *19*, 2550-2553.
- (124) Lenk, W.; Meier-Haack, J. Desalination 2002, 148, 11-16.
- (125) Toutianoush, A.; Krasemann, L.; Tieke, B. Colloids Surf., A 2002, 198-200, 881-889.
- (126) Schwarz, H. H.; Malsch, G. J. Membr. Sci. 2005, 247, 143-152.
- (127) Sullivan, D. M.; Bruening, M. L. J. Membr. Sci. 2005, 248, 161-170.
- (128) Lajimi, R. H.; Ben Abdallah, A.; Ferjani, E.; Roudesli, M. S.; Deratani, A. Desalination 2004, 163, 193-202.
- (129) Sullivan, D. M.; Bruening, M. L. Chem. Mater. 2003, 15, 281-287.
- (130) Krasemann, L.; Tieke, B. Langmuir 2000, 16, 287-290.
- (131) Goulas, A. K.; Kapasakalidis, P. G.; Sinclair, H. R.; Rastall, R. A.; Grandison, A. S. *J. Membr. Sci.* **2002**, *209*, 321-335.

- (132) Hinkova, A.; Bubnik, Z.; Kadlec, P.; Pridal, J. Sep. Purif. Technol. 2002, 26, 101-110.
- (133) Wang, X.-L.; Zhang, C.; Ouyang, P. J. Membr. Sci. 2002, 204, 271-281.
- (134) Sukhorukov, G. B.; Schmitt, J.; Decher, G. Berichte der Bunsen-Gesellschaft 1996, 100, 948-953.
- (135) Harris, J. J.; Bruening, M. L. *Langmuir* **2000**, *16*, 2006-2013.
- (136) Kim, B.-S.; Vinogradova, O. I. J. Phys. Chem. B 2004, 108, 8161-8165.
- (137) Hiller, J. A.; Rubner, M. F. *Macromolecules* 2003, 36, 4078-4083.
- (138) Wong, J. E.; Rehfeldt, F.; Haenni, P.; Tanaka, M.; Klitzing, R. v. *Macromolecules* **2004**, *37*, 7285-7289.
- (139) Ruths, J.; Essler, F.; Decher, G.; Riegler, H. *Langmuir* **2000**, *16*, 8871-8878.
- (140) Carriere, D.; Krastev, R.; Schönhoff, M. Langmuir 2004, 20, 11465-11472.
- (141) Poptoshev, E.; Schoeler, B.; Caruso, F. Langmuir 2004, 20, 829-834.
- (142) Dubas, S. T.; Schlenoff, J. B. Langmuir 2001, 17, 7725-7727.
- (143) Tanchak, O. M.; Barrett, C. J. Chem. Mater. 2004, 16, 2734-2739.
- (144) Mendelsohn, J. D.; Yang, S. Y.; Hiller, J.; Hockbaum, A. I.; Rubner, M. F. *Biomacromolecules* **2003**, *4*, 96-106.
- (145) Burke, S. E.; Barrett, C. J. *Biomacromolecules* **2005**, *6*, 1419-1428.
- (146) Wang, L.; Schöenhoff, M.; Möhwald, H. *J. Phys. Chem. B* **2004**, *108*, 4767-4774.

Chapter 2

CONTROLLING THE NANOFILTRATION PROPERTIES OF MULTILAYER POLYELECTROLYTE MEMBRANES THROUGH VARIATION OF FILM COMPOSITION

SUMMARY

This chapter describes the use of a variety of polyelectrolyte multilayers (PEMs) as selective skins in composite membranes for nanofiltration (NF) and Deposition of PEMs occurs through simple alternating diffusion dialysis. adsorption of polycations and polyanions, and separations can be optimized by varying the constituent polyelectrolytes as well as deposition conditions. general, the use of polycations and polyanions with lower charge densities allows separation of larger analytes. Depending on the polyelectrolytes employed, PEM membranes can remove salt from sugar solutions, separate proteins, or allow size-selective passage of specific sugars. Additionally, because of the minimal thickness of PEMs, NF pure water fluxes through these membranes typically range from 1.5 to 3 m³/(m² day) at 4.8 bar. Specifically, to separate sugars, we employed poly(styrene sulfonate) (PSS)/poly(diallyldimethylammonium chloride) (PDADMAC) films, which allow 42% passage of glucose along with a 98% rejection of raffinose and a pure water flux of 2.4 m³/(m² day). PSS/PDADMAC membranes are also capable of separating NaCl and sucrose (selectivity of ~10), while high-flux hyaluronic acid/chitosan membranes (pure water flux of 5 m³/(m² day) at 4.8 bar) may prove useful in protein separations.

2.1 Introduction

Nanofiltration (NF) is an important membrane-based separation technique that is similar to reverse osmosis (RO), but the relatively high permeability of NF membranes allows high-flux separations at operating pressures that are much lower than those used in RO.¹⁻³ The economic advantages of lower operating pressures have recently led to applications of NF in several areas.⁴⁻¹² Water softening is probably the biggest NF operation, and plants have been designed to treat as much as 40 million gallons of water per day.¹³ Other NF applications include recovery of ammonium lactate from a fermentation solution,⁴ recycling of NaCl from textile dyeing wastewater,⁹ and reduction of the salinity of seawater for its use as a body washing solution.¹¹ Development of stable membranes with even higher fluxes and selectivities, as well as resistance to fouling could further expand the utility of NF.

This chapter examines the potential of a new class of NF membranes (polyelectrolyte multilayers) for the separation of different saccharides and isolation of sugar from salt solutions. Because of the industrial importance of such separations, several groups have investigated the performance of commercial membranes in this area. Wang et al. used NF45 membranes from Dow Chemical to separate glycerol and several saccharides and obtained rejections of 20%, 81%, 95%, and near 100% for glycerol, glucose, sucrose, and raffinose, respectively. Though this membrane could recover saccharides, the high glucose rejection would pose a problem for sugar separations, and pure water flux was only 0.5 m³/(m² day) at 4.8 bar. Wang also succeeded in

separating NaCl from sugar but reported a 0.01 M NaCl rejection of ~40%, which may lead to difficulties in recovering salt from a process stream.¹⁴ Similarly, Vellenga and Tragardh used a DS5 membrane from Desalination Systems to separate NaCl and sucrose, but NaCl rejection was above 60%.¹⁸ Another commercial membrane, the DS-5-DL from Osmonics, successfully separated glucose from higher saccharides, but it allowed a water flux of only ~1 m³/(m² day) at 5 bar.¹⁵ Hence, membranes with fluxes >1 m³/(m² day) at a pressure <5 bar and the ability to provide low (<40%) rejection of salts or glucose while rejecting larger saccharides should provide performance improvements over commercial systems. Of course, in addition to rejections and fluxes, fouling resistance and stability are vital to the application of any membrane.

To achieve high fluxes, separation membranes generally contain a dense, thin layer on a porous support. The "skin" layer provides selectivity, but its minimal thickness still allows high flux. In contrast, the porous support supplies mechanical stability while adding little resistance to mass transport. Several recent studies suggest that polyelectrolyte multilayer (PEM) films are promising candidates for "skin" layers in composite membranes. PEM films are attractive for this role because of their deposition procedure, which simply involves alternating adsorption of polycations and polyanions. This layer-by-layer technique affords control over thickness through variation of the number of adsorbed layers and allows formation of "skins" with thicknesses less than 50 nm. Of equal importance, a wide range of polyelectrolytes are capable of

forming PEM films,³²⁻³⁵ and judicious selection of constituent polyelectrolytes should permit tailoring of flux, selectivity, and possibly fouling rates.^{27,28,35-38}

In spite of the versatility of PEM films, NF studies of membranes containing these materials have thus far focused primarily poly(vinylamine)/poly(vinyl sulfate) and poly(styrene sulfonate)/poly(allylamine hydrochloride) (PSS/PAH) systems. Tieke and coworkers showed that 60-bilayer poly(vinylamine)/poly(vinyl sulfate) films exhibit sulfate rejections greater than 95%, but flux through these membranes was relatively low due to the large number of bilayers.²⁶ Our group examined 4.5-bilayer PSS/PAH films (the extra 0.5 bilayer indicates that PSS is the top layer in the film) deposited on porous alumina and also achieved 95% Na₂SO₄ rejection with appropriate deposition conditions.²⁷ Moreover, the use of 4.5-bilayer films affords fluxes that are comparable to or higher than those of state of the art commercial NF membranes. 3,27,28,39 More recently, Liu and Bruening examined NF of methanol, alycerol, glucose, and sucrose to probe the size-based selectivities of PSS/PAHcontaining membranes.²⁸ While these membranes show glucose/sucrose selectivities in excess of 100, the rejection of both sugars is large enough to preclude the use of PSS/PAH films for realistic saccharide separations.²⁸

Building on previous work, this chapter demonstrates the control over NF fluxes and rejections that is possible through varying constituent polyelectrolytes in PEM-containing membranes. In an effort to lower the rejection of glucose while still separating it from sucrose or raffinose. examined we PSS/poly(diallyldimethylammonium chloride) (PDADMAC) films because literature reports show that PSS/PDADMAC is much more permeable than PSS/PAH in pervaporation and diffusion dialysis (DD) applications.^{24,35} Optimization of PSS/PDADMAC films permits high-flux (>2 m³/(m² day)) glycerol/sucrose and glucose/raffinose separations that would not be possible with PSS/PAH. In stark contrast to PSS/PDADMAC and PSS/PAH, PEM films prepared from hyaluronic acid (HA) and chitosan allow essentially quantitative passage of glucose, sucrose, and raffinose along with a pure water flux of 5 m³/(m² day) at 4.8 bar. Even for myoglobin (M_W 17000), HA/chitosan membranes exhibit rejections <15%. These data are consistent with the mechanism of formation of HA/chitosan films which likely involves diffusion of chitosan throughout the film. 40 However, HA/chitosan films do show 97% rejection of bovine serum albumin (M_W 67000). Thus, the use of different polyelectrolytes should allow separation of molecules with molecular weights ranging from 100 to \sim 30,000 along with pure water fluxes from 2 to 5 m³/(m² day) at only 4.8 bar.

2.2 Experimental

Materials. Poly(styrene sulfonic acid) sodium salt (PSS, M_W 125000, Alfa Aesar), poly(diallyldimethylammonium chloride) (PDADMAC, M_W 100000-200000, 20 wt% in water, Aldrich), NaCl (CCl), glycerol (anhydrous, CCl), glucose (Aldrich), sucrose (Aldrich), raffinose (Aldrich), myoglobin (Horse, M_W 17000, Aldrich), bovine serum albumin (BSA, M_W 67000, Aldrich), hydrogenated dextran (M_W 4000 – 6000, Polysciences), chitosan ("medium molecular weight"

 $(M_W 190000-310000)$ based on viscosity measurements by Aldrich), 75-85% deacetylated, Aldrich), hyaluronic acid (HA, MW 1.5 x 10^6 - 1.8 x 10^6 , sodium salt, Fluka), and 3-mercaptopropanoic acid (MPA, Aldrich) were used as received. The porous alumina supports (0.02 μm Whatman Anodisc filters) were UV/O₃ cleaned with the filtrate side up (Boekel UV-Clean model 135500) for 15 min before film deposition. Deionized water (Milli-Q, 18.2 MΩ cm) was used for membrane rinsing and preparation of polyelectrolyte solutions.

Film Deposition. A UV/O₃-cleaned bare alumina support was oriented in an O-ring holder so that only the feed side of the alumina contacted the polyelectrolyte solutions. PSS/PDADMAC deposition started with immersion of the support in an aqueous solution containing 0.02 M PSS in 0.1 or 0.5 M NaCl for 3 min (molarities of polyelectrolytes are given with respect to the repeating unit). The alumina support was rinsed with deionized water for 1 min before exposure to 0.02 M PDADMAC in 0.1 or 0.5 M NaCl for 3 min, followed by another water rinse for 1 min. This process was repeated until the target number of bilayers was produced. To make PSS/chitosan films, the substrate was immersed in 0.02 M PSS in 0.5 M NaCl for 3 min and then 0.005 M chitosan at pH 2.2 for 5 minutes, with 1 min water rinses after deposition of each polyelectrolyte. Hyaluronic acid (HA) and chitosan films were prepared using a literature procedure. 40 Briefly, we exposed the alumina support to alternating solutions of 1 mg/mL HA and chitosan in 0.15 M NaCl adjusted to pH 5 with 0.1 M acetic acid with water rinsing between each deposition step.

Film Thickness Determinations. Ellipsometric thickness determinations (J.A. Woollam model M-44 rotating analyzer ellipsometer) for PSS/PDADMAC films were performed under ambient conditions (40-55% relative humidity) on Alcoated Si wafers (200 nm Al on Si(100) wafers) using a previously reported procedure. Formation of polyelectrolyte films on Al wafers took place under the same conditions as on alumina supports, and reported uncertainties in thicknesses are the standard deviations of measurements on at least three substrates. To estimate thicknesses of films on porous alumina, images of membrane cross sections were obtained with a Hitachi S4700 II field-emission scanning electron microscope (SEM). Prior to imaging, membranes were fractured under liquid nitrogen and sputter-coated (Pelco model SC-7 auto sputter coater) on both sides with 5 nm of gold.

Transport Studies. DD through polyelectrolyte films was studied using a home-built apparatus with a membrane surface area of 2.3 cm² that was described previously.²⁸ For sugar separations, the permeate side of the dialysis cell was filled with deionized water, while the composition of the feed solution varied slightly with the membrane type in order to achieve detectable amounts of sugar in the receiving phase. Feed solutions contained 0.001 M glycerol, glucose, sucrose and raffinose when using bare alumina supports and alumina coated with 3- and 4-bilayer PSS/PDADMAC films deposited from 0.1 M NaCl, as well as 4- and 5-bilayer films deposited from 0.5 M NaCl. For all other PSS/PDADMAC films, the feed solution contained 0.005 M glycerol, glucose, and sucrose and 0.015 M raffinose. For sucrose/NaCl separations, the feed was 0.01

M NaCl, 0.001 M sucrose when using bare alumina supports and alumina coated with 3- and 4-bilayer PSS/PDADMAC films deposited from 0.1 M NaCl and 4- and 5-bilayer PSS/PDADMAC films deposited from 0.5 M NaCl. For all other PSS/PDADMAC films, the feed solution was 0.01 M NaCl, 0.005 M sucrose.

A 2-mL sample was taken from the permeate dialysis cell every 10 minutes, and an equal volume was withdrawn from the feed side to ensure that differing fluid levels on each side of the membrane would not contribute to flux. To determine NaCl concentration, a conductivity measurement (Oakton CON 100 or Orion 115 conductivity meters) was taken at the same time as sampling, and the feed cell conductivity was also measured after completion of the dialysis. Conductivities were converted to concentrations using a calibration curve. The sugar and glycerol concentrations were determined by liquid chromatography (Dionex, DX-600, CarboPac PA-10 column, 100 mM NaOH mobile phase) coupled with integrated amperometric detection (Dionex, ED-50). Flux values were normalized by dividing them by the concentration of the probe molecule in the feed at the end of the experiment. Both myoglobin and dextran were also detected via integrated amperometric detection using the Dionex DX-600. Bovine serum albumin was detected by UV absorption using a Perkin Elmer, Lambda 40 spectrophotometer set to 198 nm.

NF was performed at a pressure of 4.8 bar²⁷ with the cross-flow apparatus shown in Figures 2.1 and 2.2. Despite the bench scale of this apparatus, it possesses the same components found in nearly all cross-flow NF units.

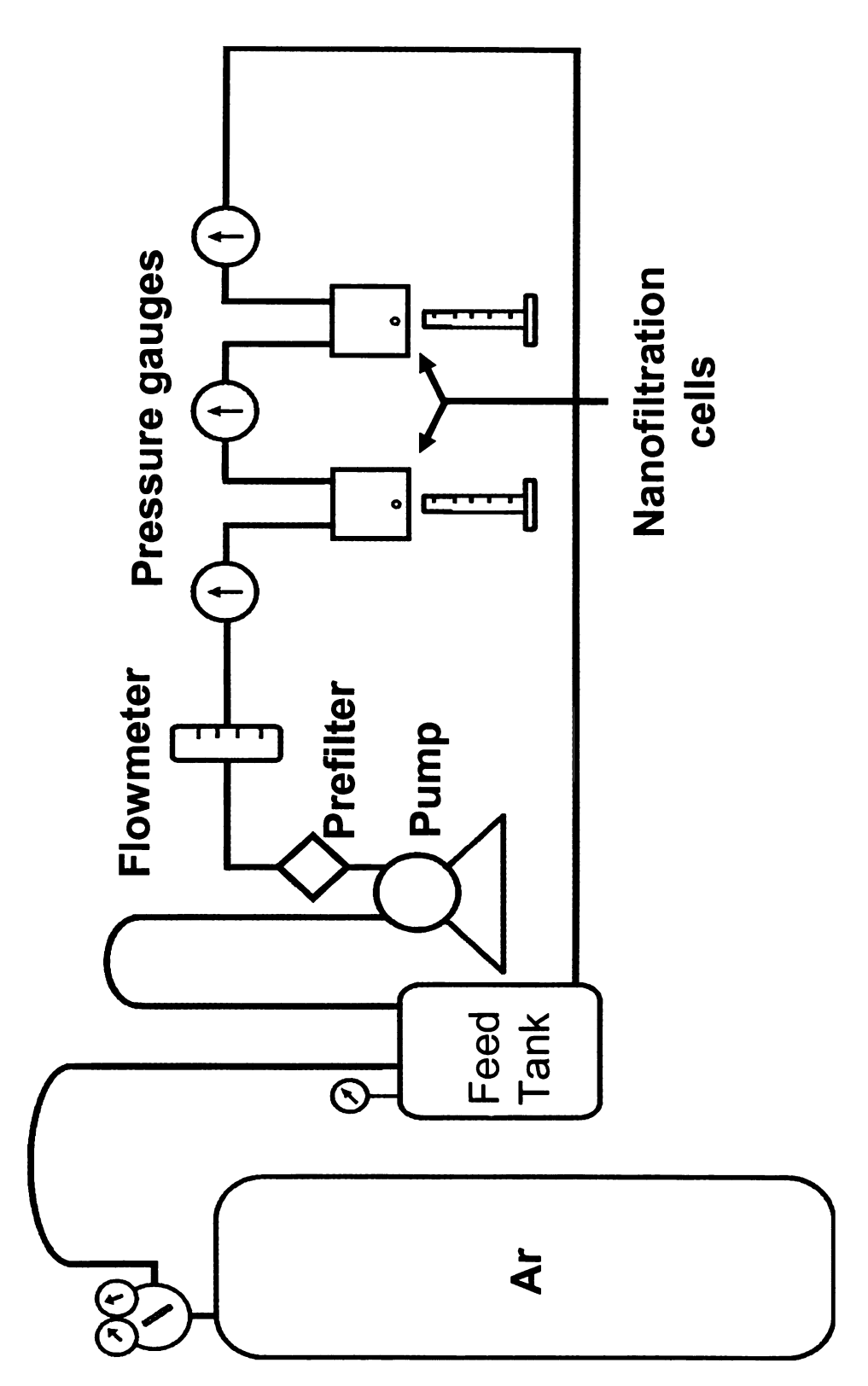


Figure 2.1: Schematic showing the NF unit used in this dissertation. This figure is adapted from Stanton et al. 27

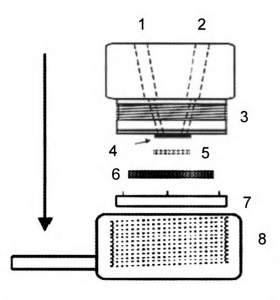


Figure 2.2: Schematic diagram of a "nanofiltration cell" from Figure 2.1 showing the assembly of the cell components. From top to bottom: (1) and (2) are the inlet and outlet ports, (3) are the threads, (4) is the rubber O-ring, (5) is the membrane, (6) is the stainless steel frit that the membrane is placed on, (7) is the cap that holds the frit, and (8) is the bottom part of the cell that screws into the threads (3). This figure is adapted from Stanton et al.²⁷ The arrow indicates flow direction through the cell.

Pressure is applied from a tank of Ar, and the pump provides the cross-flow. A flow meter ensures that the cross-flow rate is 18 mL/min, which is ~100 times the permeate flow rate and sufficient to minimize concentration polarization, ²⁷ and the pressure gauges verify that there is minimal pressure drop between membranes ordered in series. Flow passes parallel to the membrane surface (membrane surface area 1.5 cm²) while solution that passes through the membrane exits the system where it is collected for analysis.

The feed solution for NF of sugars contained 0.001 M glycerol, glucose, sucrose, and raffinose. Salt/sugar NF separations employed a feed solution containing 0.01 M NaCl and 0.001 M sucrose. After an 18 h equilibration time, four samples were collected for times ranging from 15 to 40 min each, depending on the flux through the membrane, and the feed was sampled at the conclusion of the experiment. Solution analysis occurred as described above for DD. Flux measurements reported are for pure water passage through the membranes. When sugars or salts were present, the solution flux decreased by 5-25% for PSS/PDADMAC and PSS/chitosan films. All reported transport results are the average of experiments with at least 3 different membranes.

2.3 Results and Discussion

To examine how polyelectrolyte structure affects separation properties, we investigated three polyelectrolyte systems: PSS/PDADMAC, PSS/chitosan, and hyaluronic acid (HA)/chitosan. (Figure 2.3 shows polyelectrolyte structures.)

The polyelectrolytes in these films have a wide range of charge densities, which

Figure 2.3: Structures of polyelectrolytes used in this study.

should lead to varying degrees of ionic cross-linking. Based on previous ion-dialysis and pervaporation studies by Tieke and coworkers, ^{24,35} films with high densities of ionic cross-links should resist swelling and provide high NF rejections and selectivities. In contrast, lower cross-linking densities should result in swollen membranes capable of separating larger analytes. Below, we briefly discuss film characterization and then present separations that employ a series of hydrophilic molecules (Table 2.1) to probe size-based selectivities in each of the PEM systems. We most fully studied PSS/PDADMAC, as this is one of the prototypical polyelectrolyte pairs. Additionally, we examined separation of NaCl from sucrose to illustrate a potential application of PEM membranes.

Table 2.1: Molecular weights, aqueous diffusion coefficients (D), and Stokes' radii (r_s) of the neutral molecules used in transport studies.⁴²⁻⁴⁴

Solute	Molecular Weight (g/mol)	D (10 ⁻⁹ m ² s ⁻¹)	r _s (nm)
Glycerol	92	0.95	0.26
Glucose	180	0.69	0.36
Sucrose	342	0.52	0.47
Raffinose	504	0.42	0.56

Film Characterization

To determine approximate film thicknesses, we initially deposited PEMs on Al-coated Si wafers. The aluminum oxide that forms on the surface of the coated wafers should be similar to the chemical structure of the porous alumina supports used in NF and DD. In accord with literature results, ellipsometric studies of PSS/PDADMAC films showed that thickness increases approximately linearly with the number of bilayers deposited (see Table 2.2 for thickness values). 45,46

Cross-sectional SEM images corroborate ellipsometric thickness Figure 2.4a shows the SEM image of a 5-bilayer measurements. PSS/PDADMAC film (deposited from 0.5 M NaCl) on alumina. The thickness of the film in the figure is ~30 nm, which is in good agreement with the ellipsometric thickness of 34 nm (Table 2.2). SEM-determined thicknesses of 8.5-bilayer HA/chitosan films (~40 nm) also agree well with ellipsometric results (38 ± 6 nm). The agreement between ellipsometric data and SEM images suggests that there is little effect of the SEM vacuum on film thickness. However, thicknesses of films in water may be substantially higher than in air.47,48 The deposition conditions we employed for PSS/chitosan films (pH 2.2 for chitosan) corroded the Al-coated wafers, precluding the use of ellipsometry, but the SEM-determined thicknesses of 4 and 4.5-bilayer films were ~35 and ~45 nm, respectively. In addition, top-down SEM images such as the one shown in Figure 2.4b were taken for each type of membrane. These images demonstrate that all of the polyelectrolyte films used in this study are thick enough to cover the 20-nm pores

Table 2.2: Flux and selectivity values for DD of glycerol, glucose, sucrose, and raffinose through porous alumina coated with various PSS/PDADMAC films deposited from 0.5 M NaCl.

		Norma	Normalized Flux ^a (nmol cm ⁻² s ⁻¹ M ⁻¹)	(nmol cm	² s ⁻¹ M ⁻¹)		Selectivity ^b	
Bilayers PSS/PDADMAC	Film Thickness ^c Glycerol Glucose Sucrose (nm)	Glycerol	Glucose	Sucrose	Raffinose	Glycerol/ Glucose	Glucose/ Sucrose	Glucose/ Raffinose
0 (Bare Alumina)	N/A	230±20	180±20	140±20	120±10	1.32±0.04	1.32±0.04 1.24±0.02 1.42±0.05	1.42±0.05
3.5	17.3±0.5	120±20	70±10	7±2	0.4±0.1	1.75±0.06	10±2	200±60
4	21±1	200±10	150±10	120±10	6 + 56	1.35 ± 0.03	1.30±0.03	1.57±0.07
4.5	25±1	160±30	90 ±10	7±2	0.3±0.1	1.78±0.06	13±3	400 ±100
ß	34±1	186±3	140±10	110±10	88±8	1.3±0.1	1.35 ± 0.04	1.6±0.1
5.5	39±2	100±30	60±10	8±1	0.4±0.1	1.64±0.07	8±3	200±100

^aFlux was normalized by dividing by the source-phase concentration.

^bDD selectivities are defined as the ratio of the flux values for individual solutes.

^cEllipsometric thickness of films deposited on the oxide layer of sputtered aluminum measured at ambient conditions.

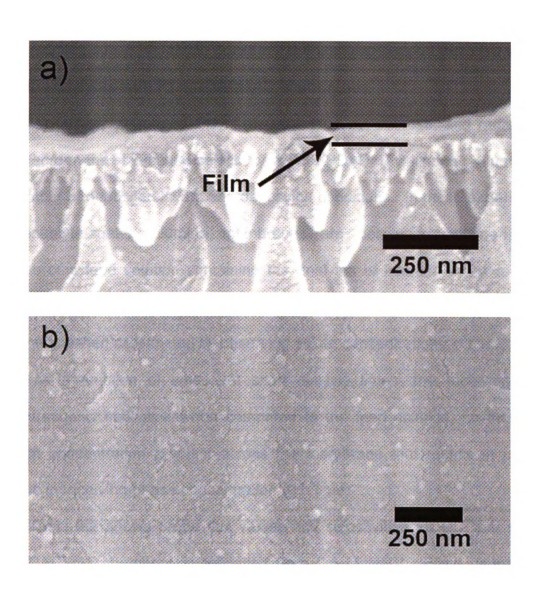


Figure 2.4: SEM images of porous alumina coated with polyelectrolyte films. (a) cross section of a ~30 nm thick, 5-bilayer PSS/PDADMAC film deposited from 0.5 M NaCl. (b) top-down view of a 4.5-bilayer PSS/chitosan film.

on the alumina substrate, as the pores in the underlying support were not visible.

Diffusion Dialysis with PSS/PDADMAC Membranes

We initially performed DD of glycerol, glucose, sucrose, and raffinose to rapidly screen the size-based selectivity of PSS/PDADMAC films as a function of the number of deposited layers and deposition conditions. In these experiments, polyelectrolyte-coated alumina membranes are positioned between equal volumes of a feed solution containing the analytes of interest and a receiving phase that is initially deionized water. The rate of transport across the membrane is then determined by observing solute concentrations in the receiving phase as a function of time. At short dialysis times, the receiving-phase concentration is negligible when compared to the feed solution, so there is a constant concentration gradient across the membrane that results in a linear increase in receiving-phase concentration with time.

Table 2.2 shows probe flux values and selectivities for DD with several PSS/PDADMAC membranes deposited from 0.5 M NaCl. Films capped with PSS (3.5, 4.5, and 5.5 bilayers) allow much lower fluxes of sucrose and raffinose than films capped with PDADMAC, and this results in a ~100-fold greater glucose/raffinose selectivity and a ~10-fold greater glucose/sucrose selectivity for the PSS-terminated films. The fluxes of glycerol and glucose are high and much less affected by the choice of capping layer. In fact, glycerol and glucose fluxes through PDADMAC-capped films are only 20% less than those through bare alumina, even with film thicknesses as high as 34 nm. The lower selectivity of

films terminated in PDADMAC suggests that these coatings are more swollen than those capped with PSS. This is consistent with swelling studies detailed in Chapter 3 of this dissertation as well as NMR studies that indicate that water molecules are more mobile when PSS/PDADMAC films terminate with PDADMAC rather than PSS.⁴⁹

When we deposited PSS-capped films from 0.1 M NaCl, we observed flux and selectivity values similar to those of the PSS-capped systems deposited from 0.5 M NaCl. The decrease in glucose/sucrose and glucose/raffinose selectivity due to PDADMAC capping was not as dramatic for films prepared from 0.1 M NaCl, but selectivities did decrease by a factor of 2 to 4 with PDADMAC as the outer layer. Salt concentration in deposition solutions probably has more effect on PDADMAC-capped films than PSS-capped systems because swelling is much larger in the former case. DD data for films deposited from 0.1 M NaCl are available in Table 2.3.

Nanofiltration with PSS/PDADMAC Membranes

Table 2.4 contains percent rejection values, selectivities, and water fluxes from NF experiments with several PSS/PDADMAC membranes and feed solutions containing glycerol, glucose, sucrose, and raffinose. Percent rejection, R, is defined by Equation (2.1) where C_{perm} and C_{feed} are the solute concentrations in the permeate and feed, respectively. Selectivity for solute A over B is defined by Equation (2.2), which can conveniently be expressed in terms of rejections as shown. Percent rejection and selectivity were determined after allowing the system to equilibrate for 18 h to achieve steady-state permeate

Table 2.3: Flux and selectivity values for diffusion dialysis of glycerol, glucose, sucrose, and raffinose through bare porous alumina and alumina coated with various PSS/PDADMAC films deposited from 0.1 M NaCl.

		Norma	Normalized Flux ^a (nmol*cm ⁻² s ⁻¹ M ⁻¹)	(nmol*cm	⁻² s ⁻¹ M ⁻¹)		Selectivity ^b	
Bilayers Film Film PSS/PDADMAC Thickness ^c Glycerol Glucose Sucrose Raffinose (nm)	Film Thickness ^c (nm)	Glycerol	Glucose	Sucrose	Raffinose	Glycerol/ Glucose	Glucose/ Sucrose	Glucose/ Raffinose
0 (Bare Alumina)	N/A	230±20	180±20	140±20	120±10	1.32±0.04	1.32±0.04 1.24±0.02 1.42±0.05	1.42±0.05
ß	12.4±0.7	144±6	90∓5	25±3	2.7±0.5	1.61±0.03	3.7±0.3	34±5
5.5	14.3±0.5	156±5	90±4	11±2	0.5±0.3	1.73±0.03	8±2	200±100
	16.0±0.5	150±10	90±10	24±2	1.9±0.1	1.63±0.05	3.7±0.2	46±8
6.5	17.9±0.5	130±10	72±3	9±1	0.4±0.1	1.74±0.08	8±1	190±60
7	20.7±0.7	139±7	87±6	20±3	1.4±0.3	1.6±0.1	4.5±0.4	64±9

^aFlux was normalized by dividing by the source-phase concentration.

^bDiffusion dialysis selectivities are defined as the ratio of the flux values for individual solutes.

^cEllipsometric thickness of films deposited on the oxide layer of sputtered aluminum measured at ambient conditions.

Table 2.4: Rejections, water fluxes, and selectivities from nanofiltration of a series of neutral molecules using porous alumina coated with a variety of PEM films.

				Reject	Rejection (%)			Selectivity	
Film Type	Bilayers	Pure Water Flux³ (m³/(m² day))	Glycerol	Glycerol Glucose Sucrose		Raffinose	Glycerol/ Glucose	Glucose/ Sucrose	Glucose/ Raffinose
PSS/PDADMAC	3.5	2.4±0.5	12±5	58±6	95.5±0.7	98±1	1.9±0.5	8±2	°09±09
Deposited from	4	2.5±0.7	3±5	17±4	28±9	36±8	1.15±0.04	1.2 ± 0.2	1.3 ±0.1
O.5 M NACI	4.5	2.1±0.3	18±4	64±6	97.2±0.9	98.9±0.7	2.3±0.3	14±4	50±50°
	5.5	1.6±0.2	16±6	28±7	85±3	99.0±0.5	2.0±0.3	9 1 3	50±20
PSS/Chit	4	2.3±0.4	6∓6	33±3	80±4	93±3	1.4±0.1	3.7±0.6	15±8
	4.5	1.5±0.3	4±8	46±8	89±2	97±1	1.7±0.3	6±1	19±5

^aNF was run at 4.8 bar.

^cExperimental values for glucose/raffinose selectivity were: 21, 41, and 106

^bExperimental values for glucose/raffinose selectivity were: 14, 17, 37, 82, and 150

$$R = \left(1 - \frac{C_{perm}}{C_{feed}}\right) \times 100\% \tag{2.1}$$

Selectivity =
$$\frac{C_{A,perm}}{C_{A,feed}} \frac{C_{B,feed}}{C_{B,perm}} = \frac{100\% - R_A}{100\% - R_B}$$
(2.2)

concentrations, and the feed volume was sufficient that its concentration varied only slightly during the experiment.

NF selectivities of PSS/PDADMAC films are similar to those found in DD, with the exception of glucose/raffinose, which is 3- to 8-fold lower in NF with PSS-capped films. The lower glucose/raffinose selectivity may reflect the fact that transport in NF occurs primarily by convection, rather than diffusion. Concentration polarization could also reduce the selectivity in NF, but higher cross-flow rates did not change the NF results, suggesting that diffusion layers are not a major issue. The agreement between DD and NF selectivities for glucose/sucrose and the high sucrose rejections also suggest that the effect of concentration polarization is minimal. In any case, the NF glucose/raffinose selectivity of ~50 is still sufficient for high quality separations.

There are large uncertainties in the glucose/raffinose selectivities in both NF and DD experiments. This error could be sourced from small differences in the structure of individual membranes, as changes in pore size will strongly affect selectivities when highly rejected species are involved. Slight variations in rinsing pattern or in polyelectrolyte deposition conditions could result in pore size irregularity. These inconsistencies in membrane manufacturing could be mitigated by employing a "dipping robot" or other automated mechanical device to make the films, removing human error from this part of the experiment. It is

also possible that unseen defects in the alumina support translate to areas where the PEM film does not cover the pores completely. Depositing additional PEM bilayers may mitigate these effects.

The percent rejection values reinforce the fact that PDADMAC-capped films are more open than PSS-capped systems. The 4-bilayer films deposited from 0.5 M NaCl exhibited a raffinose rejection of 36%, while PSS-capped films, regardless of deposition conditions, had raffinose rejections ranging from 98-In spite of the fact that films terminated with PDADMAC show low rejections, water flux through these films is essentially the same as that through comparable films terminated with PSS. Perhaps this is a reflection of the already high water fluxes with these systems. Typical fluxes through commercial NF membranes are about 50% of the fluxes through PSS/PDADMAC.^{3,39} Membranes deposited from 0.1 M NaCl perform similarly to membranes prepared from 0.5 M NaCl, except that the glucose/sucrose and glucose/raffinose selectivities of PDADMAC-capped films are 3- and 5-fold higher for films deposited from 0.1 M NaCl (Table 2.5). This trend is consistent with DD data. Additionally, pure water fluxes are greater for films deposited from 0.1 M NaCl, probably because these coatings are half as thick as corresponding films deposited from 0.5 M NaCl.

The NF data in Table 2.4 demonstrate both the potential and the limitations of PSS/PDADMAC films capped with PSS for the separation of small molecules. Glycerol rejection is less than 20% for all films and, thus, high glycerol recoveries can be achieved. In contrast, sucrose and raffinose

Table 2.5: Rejections, water fluxes, and selectivities from nanofiltration of a series of neutral molecules using porous alumina coated with PSS/PDADMAC films deposited from 0.1 M NaCl.

			Reject	Rejection (%)			Selectivity	
Film Bilayers	Pure Water Flux ^a (m³/(m² day))	Glycerol	Glycerol Glucose	Sucrose	Raffinose	Glycerol/ Glucose	Glucose/ Sucrose	Glucose/ Raffinose
5	3.3±0.8	14±6	44±5	85±2	91.3±0.8	91.3±0.8 1.54±0.09 3.7±0.3	3.7±0.3	6.5±0.5
5.5	2.6±0.5	16±3	9∓89	96±2	98.8±0.6	2.0±0.2	10±2	31±8
6.5	2.3±0.4	8±5	53±5	95.6±0.8	99.0±0.4	2.0±0.2	11±1	60±30
0.0	Z.3IU.4	CHO	CICC	93.010.0		Z.UIU.2		

^aNF was run at 4.8 bar.

rejections are greater than 95%, so separation of glycerol from molecules larger than sucrose is possible, but recovery of sucrose from solutions containing even larger molecules is not. In the case of glucose, selectivity over raffinose (~50) is impressive, and selectivity over sucrose is as high as 14, but the ~60% rejection of glucose may prohibit practical separations. To achieve higher recoveries (lower rejections) of glucose, we investigated the polyelectrolyte systems described below.

Nanofiltration with PSS/Chitosan Membranes

Chitosan, the deacetylated form of the natural polymer chitin (Figure 2.3), contains free amine groups and can therefore serve as a polycation in PEM films. Because the charge density in chitosan is slightly lower than in PDADMAC, we thought that PSS/chitosan films would have fewer ionic cross-links and, hence, show lower rejections than PSS-capped PSS/PDADMAC. (PDADMAC and chitosan contain one charge per 9 and 11 non-hydrogen atoms, respectively.) For PSS-terminated films, there is a lower rejection of all molecules by PSS/chitosan than by PSS/PDADMAC (Table 2.4), but the difference between the two types of films is not large. For PSS/chitosan films terminated with chitosan (4 bilayers), glucose rejection is only 33%, so these films could allow relatively high glucose recoveries in glucose/raffinose separations. In spite of lower rejections, water fluxes through PSS/chitosan membranes are similar to or slightly lower than those through PSS/PDADMAC films deposited from 0.5 M NaCl, suggesting that the relatively high thickness of PSS/chitosan films (~40 nm) may restrict flux.

Nanofiltration with chitosan/hyaluronic acid films

We also performed NF experiments with 8.5-bilayer hyaluronic acid (HA)/chitosan polyelectrolyte membranes. This polyelectrolyte system is intriguing because a number of literature reports show that HA/chitosan films grow exponentially with the number of deposited layers using the conditions we employed. Our ellipsometric measurements also confirmed exponential growth as film thickness increased from ~40 to ~80 nm on going from an 8.5-bilayer to a 10.5-bilayer film. Such rapid increases in thickness occur because polycations can diffuse readily through HA-containing films, and thus, these films should be highly permeable to small analytes. Although HA/chitosan films are known to be somewhat heterogeneous, top-down SEM images of 4.5 and 8.5-bilayer films indicate that deposition of 8.5 bilayers is more than sufficient to completely cover the porous supports.

The pure water flux through 8.5-bilayer HA/chitosan membranes is 5.2±0.6 m³/(m² day), about twice that through PSS/PDADMAC and PSS/chitosan films. Along with a high water flux, the films show minimal rejections <12% of any of the previously mentioned neutral molecules. To probe the molecular weight cutoff (MWCO, molecular weight at which rejection reaches 90%) of these membranes, we performed NF with much larger solutes. The rejections of 4000-6000 MW hydrogenated dextran (0.5 g/L) and myoglobin (125 mg/L, M_W 17000) were still less than 15%, but rejection of bovine serum albumin (250 mg/L, M_W 67000) was 97%, indicating that the molecular weight cutoff (MWCO) for these HA/chitosan membranes is between 17000 and 67000. Although HA/chitosan

films are much too permeable for small molecule separations, they might prove useful in fractionating proteins. We should note that when performing NF with myoglobin, the solution flux through HA/chitosan membranes decreased by 80%, and when using BSA the flux decreased by 90%. Protein adsorption likely reduces the flux through the membranes.

Salt-sugar separations- Diffusion Dialysis

Salt/sugar separations are important for recovering the NaCl used to regenerate ion-exchange columns.⁵³ To quickly screen a large number of films for such separations, we examined DD with source-phase solutions containing NaCl and sucrose. Our ultimate goal is to maximize the flux of the NaCl through the membrane while rejecting the neutral sucrose. Figure 2.5 shows how NaCl flux and NaCl/sucrose selectivity vary with the number of bilayers for PSS/PDADMAC films deposited from 0.5 M NaCl. Again, there is an obvious dependence of membrane performance on the top layer composition, and PDADMAC-terminated films (4- and 5-bilayers) show selectivities similar to that of a bare alumina support. The 3.5- and 4.5-bilayer systems gave a NaCl/Sucrose selectivity of 40, 16 times better than the bare alumina value of 2.5 and an improvement of 60% over films deposited from 0.1 M NaCl (see Figure 2.6 for data for films deposited from 0.1 M NaCl). The 5.5 bilayer PSS/PDADMAC film deposited from 0.5 M NaCl suffered from lower NaCl fluxes, which reduced selectivity.

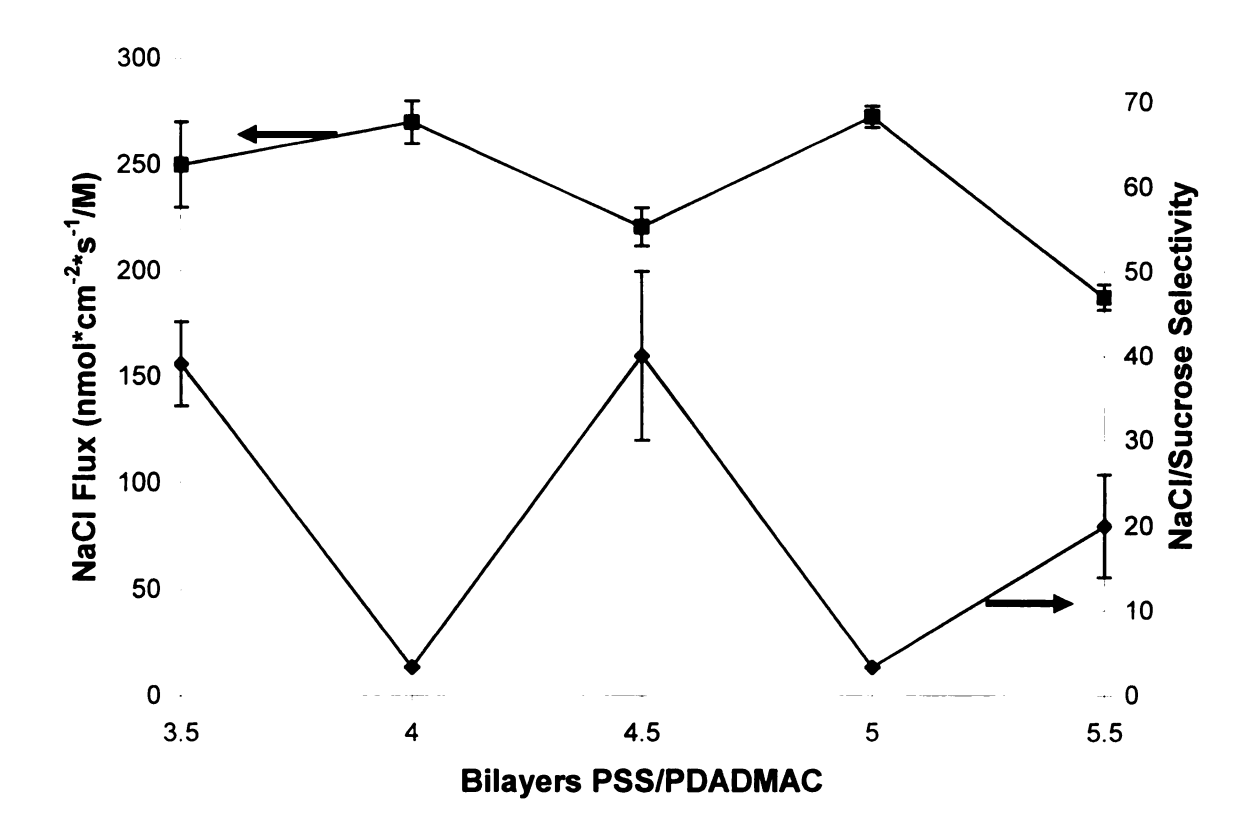


Figure 2.5: NaCl flux and NaCl/Sucrose selectivity from DD through porous alumina coated with PSS/PDADMAC films deposited from 0.5 M NaCl. The arrows indicate which y-axis pertains to each data set. Flux was normalized by dividing by the source-phase concentration.

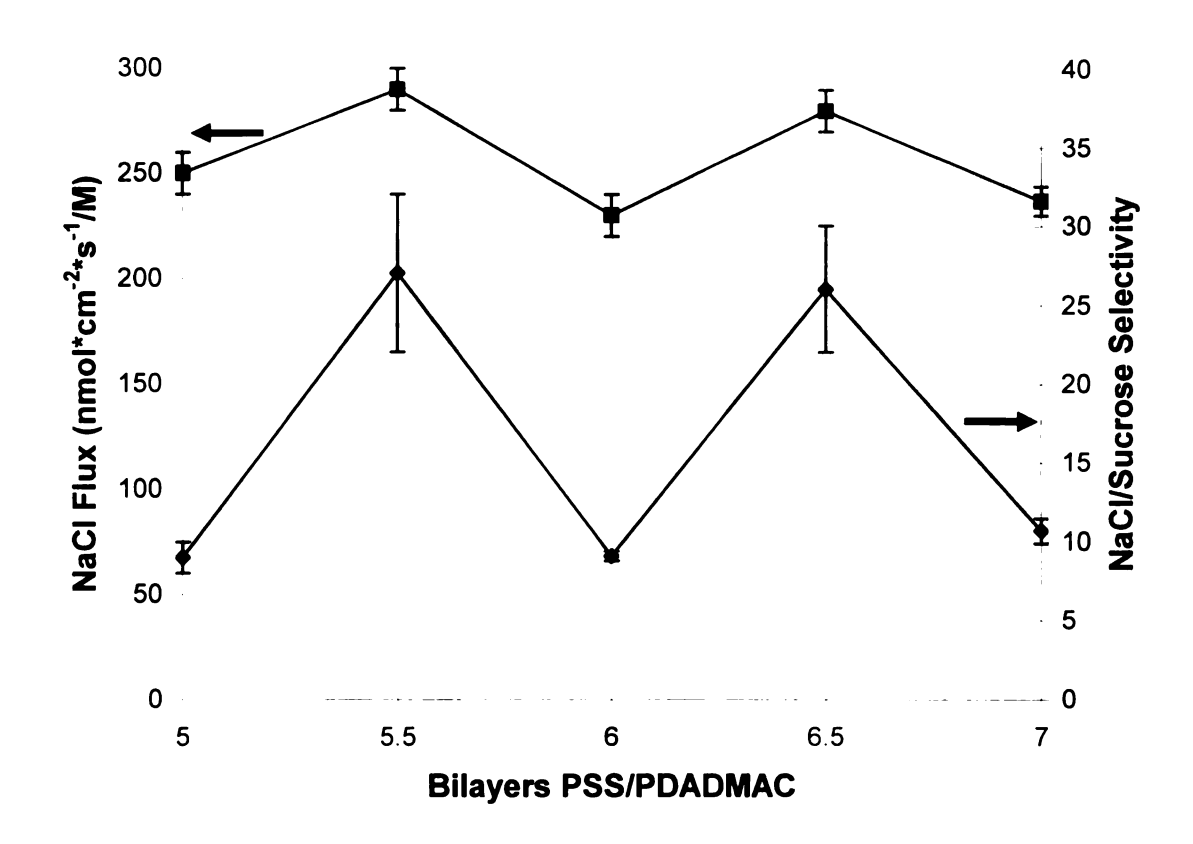


Figure 2.6: NaCl flux and NaCl/Sucrose selectivity from diffusion dialysis through porous alumina coated with PSS/PDADMAC films deposited from 0.1 M NaCl. The arrows indicate which y-axis pertains to each data set. Flux was normalized by dividing by the source-phase concentration.

Salt-sugar separations- Nanofiltration

Table 2.6 shows the percent rejection, water flux, and selectivity for NF of a NaCl/sucrose solution using PSS/PDADMAC films. The results show trends similar to those seen with DD. Films capped with PDADMAC and deposited from 0.5 M NaCl were so open that they provided a NaCl/sucrose selectivity of only 1.3, which is too low to attempt any reasonable separation. In contrast, the selectivity of 10, NaCl rejection of 30%, and water flux of 2.4 m³/(m² day) at 4.8 bar for the 3.5-bilayer PSS/PDADMAC films deposited from 0.5 M NaCl may be attractive for NaCl/sucrose separations. PSS-terminated films deposited from 0.1 M NaCl show even lower NaCl rejections along with high flux and >90% sucrose rejections, and such films are even more attractive for salt/sugar separations.

Salt-sugar separations are complicated by charge-exclusion of cations or anions. Because most cations and anions are relatively small, salt rejection is likely to be influenced more by surface charge than bulk film density. Decreasing surface charge by lowering the salt concentration in deposition solutions appears to be one way to reduce NaCl rejections.⁵⁴

Comparison of PEM Systems

All of the rejection data suggest that the use of polyelectrolytes with high charge densities results in heavily ionically cross-linked PEM membranes that exhibit high rejections of neutral molecules. Glycerol, glucose, and sucrose PSS/PAH²⁸>PSS/PDADMAC order rejections decrease in the >PSS/chitosan>HA/chitosan, which is decreasing order also the

Table 2.6: Rejections, water fluxes, and selectivities from nanofiltration of sucrose and NaCl by porous alumina coated with PSS/PDADMAC films.

		_	Rejection (%)		Selectivity
Film Type	Bilayers	Pure Water Flux ^a (m ³ /(m ² day))	NaCl	Sucrose	NaCl/ Sucrose
PSS/PDADMAC Deposited from 0.5 M NaCl	3.5	2.4±0.5	28±4	92.5±0.8	10±1
	4	2.5±0.7	14±5	32±4	1.27±0.07
	4.5	2.1±0.3	40±4	93.8±0.8	10±1
	5.5	1.6±0.2	41±3	92±2	7±2
PSS/PDADMAC Deposited from 0.1 M NaCl	5	3.3±0.8	21±2	81±4	4.3±0.7
	5.5	2.6±0.5	20±2	94±1	15±5
	6.5	2.3±0.4	22±2	91±1	9±1

^aNF was run at 4.8 bar.

polyelectrolyte charge densities. Previous DD data for poly(acrylic acid)/PAH films suggest that this system would have higher rejections than even PSS/PAH,²⁸ further confirming the trend of rejection versus polyelectrolyte charge density. This chapter demonstrates the utilization of this trend to prepare polyelectrolytes capable of separating molecules with different size ranges. For example, the high rejections of PSS/PAH are not practical for sugar separation, but the use of PSS/PDADMAC may be. In the case of protein separations, HA/chitosan may prove useful while the other polyelectrolyte systems we have tested would not.

Although the PEM films presented in this chapter are quite attractive for sugar, salt/sugar, and even protein separations, many issues in the utilization of polyelectrolyte membranes for practical separations must still be addressed. Commercially employed NF membranes are often spiral-wound cartridges, where the membrane is wrapped with a flow spacer in a cylindrical configuration. This allows a high degree of membrane surface area to be confined in a small volume. Unfortunately, the PEMs in this dissertation are deposited on alumina, which is not compatible with spiral-wound technology. To counter this problem, recent research has focused on exploring NF with PEMs deposited on polymeric membrane supports. 56

Questions about the effects of both extreme solution conditions and fouling on PEMs also need to be answered. The highly charged surface of PEMs could attract oppositely charged species that may affix to the film, obstructing the pores over time (fouling). Additionally, since electrostatic interactions bind the

film together, exposure to high ionic strength and pH extremes may decompose the film, reducing performance. Long term fouling and stability studies are both important steps that must be performed before PEM assemblies are scaled up to the industrial level.

2.4 Conclusions

Variation of the constituent polyelectrolytes in PEM membranes allows tailoring of NF properties. Rejection of neutral molecules increases with an increasing charge density on the polyelectrolytes that constitute the PEM membrane, and this effect is large enough to allow synthesis of polyelectrolyte membranes with MWCOs ranging from 100 (PSS/PAH) to >20,000 (HA/chitosan). Moreover, the minimal thickness of polyelectrolyte membranes allows NF to occur at fluxes of more than 2 m³/(m² day). DD and NF data with PSS/PDADMAC membranes also demonstrate that rejection, flux, and selectivity strongly depend on deposition conditions and which polyelectrolyte terminates the membrane.

2.5 Acknowledgment

We thank the Division of Chemical Sciences in the Office of Basic Energy Sciences of the Department of Energy for financial support of this work. We also thank Pall Corporation for financial support.

2.6 Works Cited

- (1) Yaroshchuk, A.; Staude, E. *Desalination* **1992**, *86*, 115-134.
- (2) Bohdziewicz, J.; Bodzek, M.; Wasik, E. Desalination 1999, 121, 139-147.
- (3) Bhattacharyya, D., et al, In Membrane Handbook; Ho W.S.W, Sirkar, K.K., Eds.; Van Nostrand Reinhold; New York, 1992.
- (4) Kang, S. H.; Chang, Y. K.; Chang, H. N. *Biotechnol. Progr.* **2004**, *20*, 764-770.
- (5) Aydogan, N.; Gurkan, T.; Yilmaz, L. Separ. Sci. Technol. 2004, 39, 1059-1072.
- (6) Li, S.-L.; Li, C.; Liu, Y.-S.; Wang, X.-L.; Cao, Z.-A. *J. Membr. Sci.* **2003**, 222, 191-201.
- (7) Van der Bruggen, B.; Daems, B.; Wilms, D.; Vandecasteele, C. Sep. Purif. Technol. 2001, 22/23, 519-528.
- (8) Akbari, A.; Remigy, J. C.; Aptel, P. *Chem. Eng. Process.* **2002**, *41*, 601-609.
- (9) Koyuncu, I.; Topacik, D.; Yuksel, E. Sep. Purif. Technol. 2004, 36, 77-85.
- (10) Sungpet, A.; Jiraratananon, R.; Luangsowan, P. *Desalination* **2004**, *160*, 75-81.
- (11) Pontie, M.; Diawara, C.; Rumeau, M.; Aureau, D.; Hemmery, P. *Desalination* **2003**, *158*, 277-280.
- (12) Favre-Reguillon, A.; Lebuzit, G.; Foos, J.; Guy, A.; Draye, M.; Lemaire, M. *Ind. Eng. Chem. Res.* **2003**, *42*, 5900-5904.
- (13) Kiefer, C. A.; Brinson, F.; Suratt, B. *Maximizing the Resources: Solutions for Pure and Plentiful Water, Membrane Technology Conference Proceedings, Atlanta, GA, United States, Mar. 2-5, 2003* **2003**, 325-334.
- (14) Wang, X.-L.; Zhang, C.; Ouyang, P. J. Membr. Sci. 2002, 204, 271-281.
- (15) Goulas, A. K.; Kapasakalidis, P. G.; Sinclair, H. R.; Rastall, R. A.; Grandison, A. S. *J. Membr. Sci.* **2002**, *209*, 321-335.
- (16) Goulas, A. K.; Grandison, A. S.; Rastall, R. A. *J. Sci. Food Agr.* **2003**, *83*, 675-680.
- (17) Gyura, J.; Seres, Z.; Vatai, G.; Molnar, E. B. *Desalination* **2002**, *148*, 49-56.

- (18) Vellenga, E.; Tragardh, G. *Desalination* **1998**, *120*, 211-220.
- (19) Literature value for water flux is reported as a function of pressure. This value is based on the same pressure used in our experiments, 70 psi.
- (20) Stroeve, P.; Vasquez, V.; Coelho, M. A. N.; Rabolt, J. F. *Thin Solid Films* **1996**, *284-285*, 708-712.
- (21) Levaesalmi, J.-M.; McCarthy, T. J. *Macromolecules* **1997**, *30*, 1752-1757.
- (22) Kotov, N. A.; Magonov, S.; Tropsha, E. Chem. Mater. 1998, 10, 886-895.
- (23) Schlenoff, J. B.; Ly, H.; Li, M. J. Am. Chem. Soc. 1998, 120, 7626-7634.
- (24) Krasemann, L.; Tieke, B. Langmuir 2000, 16, 287-290.
- (25) Dubas, S. T.; Farhat, T. R.; Schlenoff, J. B. *J. Am. Chem. Soc.* **2001**, *123*, 5368-5369.
- (26) Jin, W.; Toutianoush, A.; Tieke, B. *Langmuir* **2003**, *19*, 2550-2553.
- (27) Stanton, B. W.; Harris, J. J.; Miller, M. D.; Bruening, M. L. *Langmuir* **2003**, *19*, 7038-7042.
- (28) Liu, X.; Bruening, M. L. Chem. Mater. 2004, 16, 351-357.
- (29) Meier-Haack, J.; Lenk, W.; Lehmann, D.; Lunkwitz, K. *J. Membr. Sci.* **2001**, *184*, 233-243.
- (30) Decher, G. Science 1997, 277, 1232-1237.
- (31) Harris, J. J.; Stair, J. L.; Bruening, M. L. *Chem. Mater.* **2000**, *12*, 1941-1946.
- (32) Lvov, Y.; Ariga, K.; Ichinose, I.; Kunitake, T. *J. Am. Chem. Soc.* **1995**, *117*, 6117-6123.
- (33) Liu, R. C. W.; Morishima, Y.; Winnik, F. M. *Macromolecules* **2001**, *34*, 9117-9124.
- (34) Hollman, A. M.; Bhattacharyya, D. Langmuir 2004, 20, 5418-5424.
- (35) Krasemann, L.; Tieke, B. *Mat. Sci. Eng. C-Bio S* **1999**, *C8-C9*, 513-518.
- (36) Thierry, B.; Winnik, F. M.; Merhi, Y.; Silver, J.; Tabrizian, M. *Biomacromolecules* **2003**, *4*, 1564-1571.
- (37) Berg, M. C.; Yang, S. Y.; Hammond, P. T.; Rubner, M. F. *Langmuir* **2004**, *20*, 1362-1368.

- (38) Carroll, T.; Booker, N. A.; Meier-Haack, J. J. Membr. Sci. 2002, 203, 3-13.
- (39) Hutchinson, R. A.; Beuermann, S.; Paquet, D. A., Jr.; McMinn, J. H.; Jackson, C. *Macromolecules* **1998**, *31*, 1542-1547.
- (40) Richert, L.; Lavalle, P.; Payan, E.; Shu, X. Z.; Prestwich, G. D.; Stoltz, J.-F.; Schaaf, P.; Voegel, J.-C.; Picart, C. Langmuir 2004, 20, 448-458.
- (41) Harris, J. J.; Bruening, M. L. *Langmuir* **2000**, *16*, 2006-2013.
- (42) Derlacki, Z. J.; Easteal, A. J.; Edge, A. V. J.; Woolf, L. A.; Roksandic, Z. *J. Phys. Chem.* **1985**, *89*, 5318-5322.
- (43) Creeth, J. M.; Woolf, L. A. J. Phys. Chem. 1963, 67, 2777-2780.
- (44) Boyle, M. D. P.; Gee, A. P.; Borsos, T. J. Immunol. 1979, 123, 77-82.
- (45) Lavalle, P.; Gergely, C.; Cuisinier, F. J. G.; Decher, G.; Schaaf, P.; Voegel, J. C.; Picart, C. *Macromolecules* **2002**, *35*, 4458-4465.
- (46) Ramsden, J. J.; Lvov, Y. M.; Decher, G. *Thin Solid Films* **1995**, *254*, 246-251.
- (47) Tanchak, O. M.; Barrett, C. J. Chem. Mater. 2004, 16, 2734-2739.
- (48) Hiller, J. A.; Rubner, M. F. *Macromolecules* 2003, 36, 4078-4083.
- (49) McCormick, M.; Smith, R. N.; Graf, R.; Barrett, C. J.; Reven, L.; Spiess, H. W. *Macromolecules* **2003**, *36*, 3616-3625.
- (50) Lavalle, P.; Picart, C.; Mutterer, J.; Gergely, C.; Reiss, H.; Voegel, J.-C.; Senger, B.; Schaaf, P. *J. Phys. Chem. B* **2004**, *108*, 635-648.
- (51) Picart, C.; Lavalle, P.; Hubert, P.; Cuisinier, F. J. G.; Decher, G.; Schaaf, P.; Voegel, J. C. *Langmuir* **2001**, *17*, 7414-7424.
- (52) Kujawa, P.; Badia, A.; Winnik, F. M. *Polym. Mater. Sci. Eng.* **2004**, *90*, 192-193.
- (53) Hinkova, A.; Bubnik, Z.; Kadlec, P.; Pridal, J. Sep. Purif. Technol. 2002, 26, 101-110.
- (54) Dubas, S. T.; Schlenoff, J. B. *Macromolecules* **1999**, *32*, 8153-8160.
- (55) Baker, R. W. *Membrane Technology and Applications*; 2nd ed.; John Wiley: Chichester, England, **2004**.
- (56) Malaisamy, R.; Bruening, M. L. Langmuir 2005, Accepted for Publication.

Chapter 3

CORRELATION OF THE SWELLING AND PERMEABILITY OF POLYELECTROLYTE MULTILAYER FILMS

SUMMARY

Alternating adsorption of polycations and polyanions on porous supports yields a variety of size-selective membranes whose swelling and transport properties depend on constituent polyelectrolytes, capping layer choice (polycation or polyanion), and deposition conditions. This chapter shows that in aqueous experiments, ellipsometrically determined swelling percentages correlate well with nanofiltration (NF) rejections and diffusion dialysis fluxes. For example, hyaluronic acid (HA)/chitosan films swell 4 times more than poly(styrene sulfonate) (PSS)/poly(allylamine hydrochloride) coatings, and in NF experiments, the HA/chitosan membranes permit a 250-fold greater fractional passage of sucrose. In general, films prepared from polyelectrolytes with a high charge density show low swelling and slow solute transport, presumably because of a high degree of ionic cross-linking. In the case of PSS/poly(diallyldimethylammonium chloride) (PDADMAC), PDADMAC-capped films can swell 4-fold more than their PSS-terminated counterparts, and as would be expected, alucose and sucrose transport rates in diffusion dialysis are about 1.7- and 17fold more, respectively, when these films end in PDADMAC. Polyelectrolyte multilayers also exhibit wide-ranging swelling properties in ethanol, but transport rates do not correlate with ethanol uptake. In this solvent, the density of ionic cross-links and film hydrophobicity likely exert opposite effects on swelling, which could complicate the correlation between swelling and transport.

3.1 Introduction

Polyelectrolyte multilayers (PEMs) are attractive as selective films in pervaporation, 1-6 (NF).⁷⁻¹¹ applications such as nanofiltration and encapsulation. 12-21 Their synthesis, which simply involves alternating adsorption of polycations and polyanions, 22 yields ultra-thin (<50 nm) coatings capable of allowing high fluxes. 9,11,23 Additionally, many materials can be used to form PEMs, ^{2,24-26} and judicious selection of component polyelectrolytes and deposition conditions results in films with a wide range of permeation properties.^{2,8,9,11,25,27,28} In the above applications, PEMs are in contact with solvent, reducing the relevance of physiochemical measurements in the "dry" state. understand the permeability of polyelectrolyte films, this chapter aims at correlating transport through PEMs with their swelling in both aqueous and ethanolic solutions.

Several groups have already examined the swelling of individual PEMs in solvents. Neutron reflectometry studies suggest that poly(styrene sulfonate) (PSS)/protonated poly(allylamine) (PAH) film swelling is a function of the capping layer, as films capped with PAH swell 25% less than those capped with PSS (40% versus 30% D₂O as a function of capping layer).²⁹ Wong et al. observed the same outer-layer dependence for PSS/PAH films when they performed ellipsometric swelling experiments in 99% relative humidity.³⁰ Harris and

Bruening found that immersion of [PSS/PAH]₁₀ films in pH 3.2- and 6.3-buffered water solutions results in a thickness increase of 40% relative to ambient humidity conditions, while exposure of these films to pH 10 buffers yields even greater swelling followed by film delamination.31 Other studies showed that PSS/PAH swelling is affected by deposition pH and ionic strength as well as swellant pH. 32,33 Though most swelling research has been performed on PSS/PAH films, 29-36 Schlenoff and Dubas demonstrated that water uptake in poly(acrylic acid) (PAA)/poly(diallyldimethylammonium chloride) (PDADMAC), PSS/PDADAMC, and PSS/PAH films is a strong function of the swellant ionic strength and that PAA/PDADMAC and PSS/PDADMAC films swell more in water than PSS/PAH coatings.³⁷ Two recent papers showed that the swelling of PAA/PAH films depends on both deposition conditions and pretreatments. 38,39 Burke and Barrett also found that in some cases, PAH/hyaluronic acid (HA) films are capable of 800% swelling. Excepting Schlenoff and Dubas' work. 37 however, there have been no systematic studies of how "dry" versus waterswollen PEM thicknesses differ with variables such as constituent polyelectrolytes and capping-layer choice.

In contrast, several studies show that the permeability of PEMs varies dramatically with their composition. Tieke and coworkers found that transport rates in pervaporation and diffusion dialysis (DD) through PEMs generally decrease as the charge density in the film increases.² Presumably, greater charge density on the polyelectrolytes results in more ionic cross-linking, less swelling, and lower permeabilities.^{2,8,9,11} As not all prospective applications of

PEMs are in water, swelling in other solvents is important as well. PEM swelling should depend on both the solvent and the hydrophobicity of the polyelectrolytes. Poptoshev et al. demonstrated that exposure of poly(ethyleneimine) (PEI)/PSS/PAH films to a solution of >40% ethanol in water collapses these films to essentially their dry thickness,³⁶ but another study suggests that thicker PSS/PAH films undergo only a 5% thickness reduction when immersed in ethanol rather than water.⁴¹ Regardless, the permeability of solutes through PEMs will likely be significantly different in ethanol than in water.

Few publications link polyelectrolyte swelling and transport. 31,41-44 and many specialize in PEM capsules⁴¹ or materials formed by precipitation of polyanion/polycation complexes, 42,44 rather than layer-by-layer adsorption. In this work, we attempt to directly correlate swelling with permeability data for three PEM systems: PSS/PAH, PSS/PDADMAC, and HA/chitosan. These systems were selected in part because they exhibit a wide range of transport properties. as reported previously. 9,11 For example HA/chitosan membranes have a molecular weight cutoff (MWCO, solute molecular weight required to achieve 90% rejection in NF) of >17,000, while PSS/PAH films have a MWCO of 200. 9,11 Consistent with these transport data, this work shows that the percent swelling of HA/chitosan films in water is 4-fold greater than that for PSS/PAH. Remarkably, similarly striking differences in swelling and transport properties occur on going from a PSS-capped to a PDADMAC-capped PSS/PDADMAC film. Below, we examine swelling and transport as a function of ionic strength, capping layer composition, and swelling solvent.

3.2 Experimental

Materials. Poly(styrene sulfonic acid) sodium salt (M_W 125000, Alfa Aesar), poly(diallyldimethylammonium chloride) (M_W 100000-200000, 20 wt% in water, Aldrich), poly(allylamine hydrochloride) (M_W 70000, Aldrich), chitosan ("medium molecular weight" (M_W 190000-310000 based on viscosity measurements by Aldrich), 75-85% deacetylated, Aldrich), hyaluronic acid (M_W 1500000-1800000, sodium salt, Fluka), polyethyleneimine (M_W 25000, Aldrich), NaCl (CCl), glycerol (anhydrous, CCl), glucose (Aldrich), sucrose (Aldrich), raffinose (Aldrich), hydrogen peroxide (30%, Jade Scientific), sulfuric acid (concentrated, CCl) and ethanol (Pharmco) were used as received. Deionized water (Milli-Q, 18.2 MΩ cm) was used for membrane rinsing, preparation of polyelectrolyte solutions, and aqueous swelling experiments.

Film Deposition. For swelling experiments, films were prepared on pieces of silicon wafers (Si(100), Silicon Quest International) that were first cleaned in a 3:1 solution of concentrated sulfuric acid and hydrogen peroxide. (Caution! This solution reacts violently with organic compounds and should be stored in slightly open containers!) Following copious rinsing with water, the wafers were dried in a stream of N₂ and then cleaned with UV/O₃ (Boekel UV-Clean model 135500) for 15 minutes. The cleaned silicon was immersed in 1 mg/mL PEI at pH 9 for 15 minutes to establish a dense, positively charged layer, and films were then built on this precursor layer. For NF and DD experiments, porous alumina supports (0.02 μm Whatman Anodisc filters) were also UV/O₃ cleaned for 15 minutes, but because these supports are positively

charged below pH 9,⁴⁶ no precursor PEI layer was necessary. The cleaned alumina membranes were subsequently placed in an o-ring holder so that the concentrate side of the alumina membrane contacted the deposition solution.

Synthesis of PSS/PDADMAC films began with a 3-min immersion of the substrate in an aqueous solution containing 0.02 M PSS (concentrations of polyelectrolytes are given with respect to the repeat unit) and 0.1 M or 0.5 M NaCl. The substrate was then rinsed with deionized water for 1 min and dipped in a 0.02 M solution of PDADMAC in 0.1 M or 0.5 M NaCl for 3 min. The sample was then rinsed again with deionized water for 1 min, and this entire process was repeated until the desired number of bilayers was deposited. PSS/PAH films were deposited using the same polyelectrolyte concentrations (no pH adjustment) and deposition times, except that films were only deposited from 0.5 M NaCl. HA/chitosan films were deposited using 5 min immersions of the PEl-coated silicon slides or bare alumina supports in pH 5 solutions containing 0.15 M NaCl and 1 mg/mL polyelectrolyte, with 1 min rinses with 0.15 M NaCl at pH 5 after polycation and polyanion adsorption. Films were rinsed with pure water and dried with N₂ only after all layers were deposited.

Ellipsometry. Ellipsometric thicknesses of the SiO₂ layers on Si wafers were first determined assuming literature values for the refractive indices of Si and SiO₂ at the 44 wavelengths of the ellipsometer (J.A. Woollam model M-44 rotating analyzer ellipsometer, 75° angle of incidence) between 414.0 nm and 736.1 nm. After coating of these wafers, film thicknesses under nitrogen (<5% relative humidity (RH)), water, or ethanol were obtained using a home-built cell

with glass windows. The ellipsometric thicknesses and refractive indices of each type of film were determined at three different points per wafer on three different wafers, and the reported results are the averages and standard deviations of these values. Film thicknesses were also obtained in 55% RH (ambient) for comparison to AFM data. Optical constants of water as a function of wavelength were calculated using the Cauchy equation in coordination with constants in the literature. For ethanol, literature optical constants were interpolated to obtain data at the ellipsometer wavelengths, but due to limited ethanol literature data, fitting of ellipsometric measurements in this solvent was performed only between 476.5 nm and 632.8 nm. Swelling percentages were subsequently determined using Equation 3.1.

Percent Swelling =
$$\frac{\text{Swollen Thickness - Dry Thickness}}{\text{Dry Thickness}}*100\%$$
 (3.1)

Atomic Force Microscopy. AFM experiments (Digital Instruments Dimension 3100, Nanoscope III controller in Tapping Mode, TappingMode™ etched silicon probe tip, spring constant 20-100 N/m) were performed to validate the 'dry' ellipsometric PEM thicknesses. Thicknesses were determined by scratching a film-coated Si wafer with Techni-Tool™ tweezers and scanning a 3 x 25 µm area over the scratch to produce an average line scan. A 'step height' measurement subtracted the average height of the bare silicon wafer from the average height of the film on top of the wafer. Three PEM-coated wafers were each scanned three times (in different places) for every type of film examined in this study. The RMS roughness values were equal to or less than the standard deviation of the thickness measurements for all coatings except 4.5-bilayer

PSS/PDADMAC films deposited from 0.5 M NaCl, which had an RMS roughness of 11% of the film thickness. Due to experimental constraints, the AFM thicknesses were measured at 54% RH and are compared to ellipsometric thicknesses measured at 55% RH.

Transport Experiments. Film permeation properties were investigated by DD and cross-flow NF experiments, some of which were reported previously.9 New data presented here include all DD in ethanol, aqueous dialysis with the PSS/PAH and HA/chitosan systems, and NF data for PSS/PAH. dialysis was performed using a glass apparatus in which the membrane separated a source phase from a receiving phase that was initially deionized water or pure ethanol.^{9,11} In water, source-phase solutions for all PSS/PAH films. PDADMAC-capped PSS/PDADMAC films deposited from 0.5 M NaCl, and HA/chitosan films contained 5 mM glycerol, glucose, sucrose, and raffinose, while DD solutions for PSS/PDADMAC films deposited from 0.1 M NaCl and PSS-capped PSS/PDADMAC films deposited from 0.5 M NaCl contained 5 mM glycerol, glucose, and sucrose and 15 mM raffinose. For ethanol-based diffusion dialysis, the feed contained only 140 µM glucose, sucrose, and raffinose because of the low solubility of these compounds. Because glycerol was not present in all solutions (it co-elutes with ethanol during analysis), its transport rates are not reported. When present, glycerol was always the fastest transporting solute. Samples were collected every 10-30 minutes and subsequently analyzed by liquid chromatography (Dionex, DX-600, CarboPac PA-10 column, 100 mM NaOH mobile phase) with integrated amperometric detection (Dionex, ED-50).

Nanofiltration experiments occurred at a pressure of 4.8 bar (70 psi), and feed solutions were flowed across the membrane at a rate of 18 mL/min.^{8,9,11} NF rejection is defined by Equation 3.2, where R is the percent solute rejection and C_{perm} and C_{feed} are the concentrations of the solute in the permeate and the feed, respectively. The NF feed solutions contained 1 mM glycerol, glucose, sucrose, and raffinose for PSS/PDADMAC as well as HA/chitosan films, and 1 mM glycerol and glucose with 5 mM sucrose and raffinose for PSS/PAH films. The system was equilibrated for 18 h before permeate samples were acquired.

$$R = \left(1 - \frac{C_{perm}}{C_{feed}}\right) \times 100\%$$
 (3.2)

3.3 Results and Discussion

Swelling. Ellipsometry, which involves the measurement of the ratios of the complex reflection coefficients for p- and s-polarized light, served as the primary tool for ascertaining the extent of film swelling. From the phase difference, Δ , and the ratio of amplitudes, $\tan \Psi$, of the two reflection coefficients, one can calculate film thickness and refractive index using a model that sums the many individual reflections in the system (Figure 3.1). In the particular case of coatings on Si wafers, this model includes both film and SiO_2 layers on the substrate, so oxide layer thicknesses were determined prior to deposition of films. To examine the reliability of ellipsometric data, we calculated how the ellipsometric parameters Δ and Ψ vary with coating refractive index and thickness in nitrogen, water, and ethanol. Figures 3.2, 3.3 and 3.4 show examples of simulations where the film is immersed in water, nitrogen (<5% relative humidity), and ethanol. With a possible error of 0.3° in Δ and Ψ due to

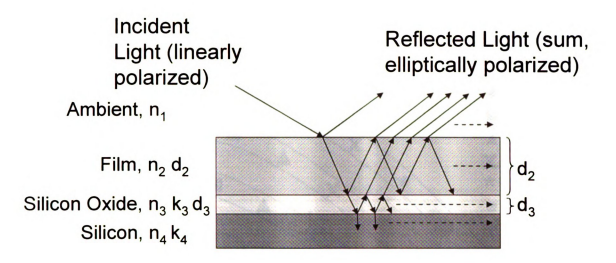


Figure 3.1: Diagram depicting the model of light reflection used to fit ellipsometric data. The n and k terms describe the real and imaginary parts of the complex refractive indices, while d represents the layer thickness. The layers are not drawn to scale.

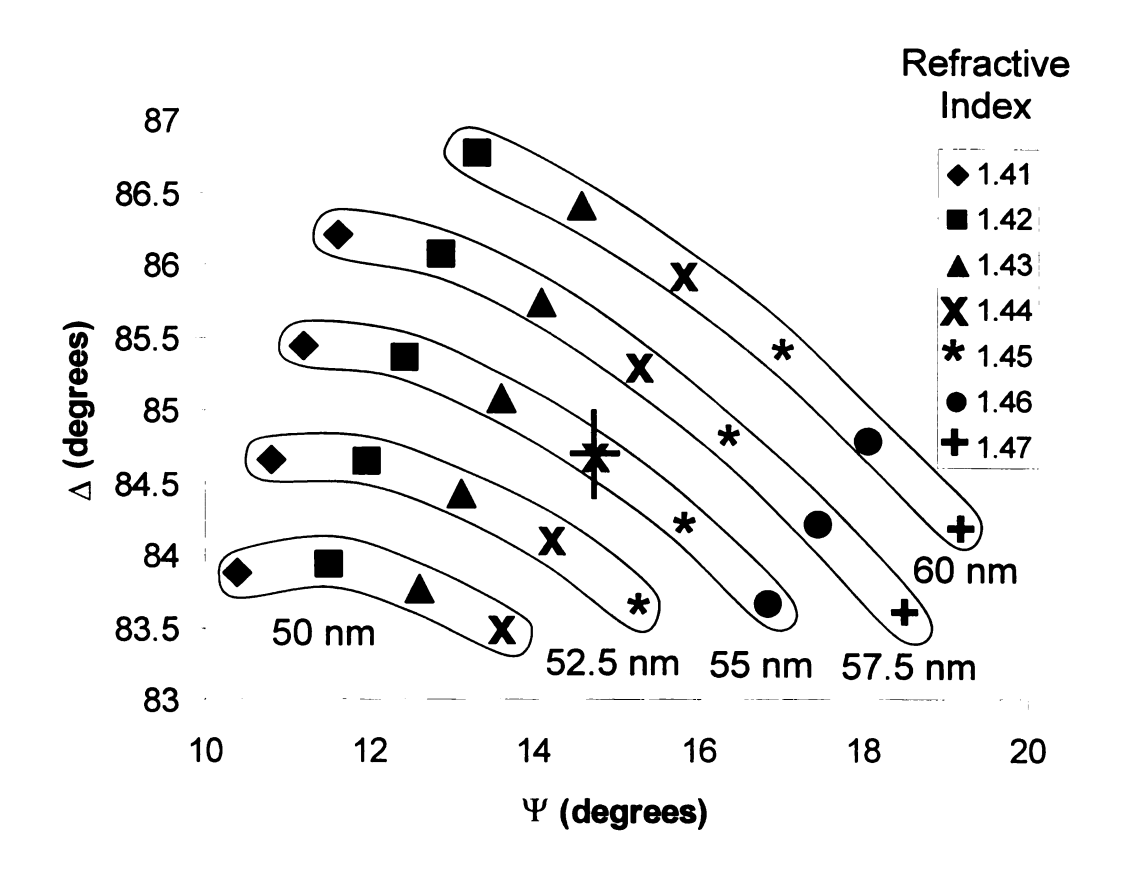


Figure 3.2: Calculated Ψ and Δ values for a Si/SiO₂/film system (water as the ambient medium and a 2.0 nm silicon oxide layer) as a function of the refractive index and thickness of the film. The simulation was performed at a wavelength of 450.5 nm where the optical constants are: water - n=1.3395, silicon oxide - n=1.4644, k=0, and silicon - n=4.7108, and k=0.0963. The point with a thickness of 55 nm and a refractive index of 1.44 represents a 9.5-bilayer PSS/PDADAMC film deposited from 0.1 M NaCl, and the black lines through that point show the \pm 0.3° uncertainty in Ψ and Δ measurements. Enclosed data points correspond to identical thicknesses at different refractive indices.

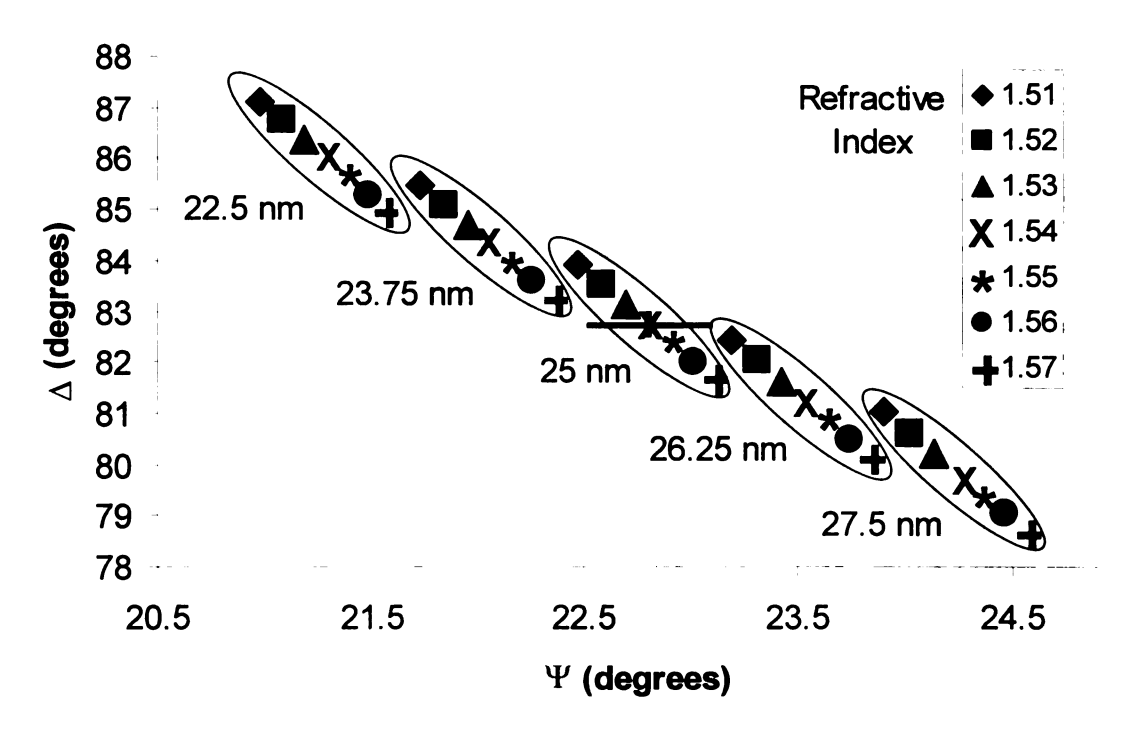


Figure 3.3: Calculated Ψ and Δ values for the system depicted in Figure 3.1 (nitrogen with <5% relative humidity as the ambient medium and a 2.0 nm silicon oxide layer) as a function of the refractive index, n_2 , and thickness, d_2 , of the film. The simulation was performed at a wavelength of 450.5 nm where the optical constants are n_1 =1.000, n_3 =1.4644, k_3 =0, n_4 =4.7108, and k_4 = 0.0963. The point with a thickness of 25 nm and a refractive index of 1.54 represents a 9.5-bilayer PSS/PDADAMC film deposited from 0.1 M NaCl, and the black lines through that point show the $\pm 0.3^\circ$ uncertainty in Ψ and Δ measurements. Enclosed data points correspond to identical thicknesses at different refractive indices.

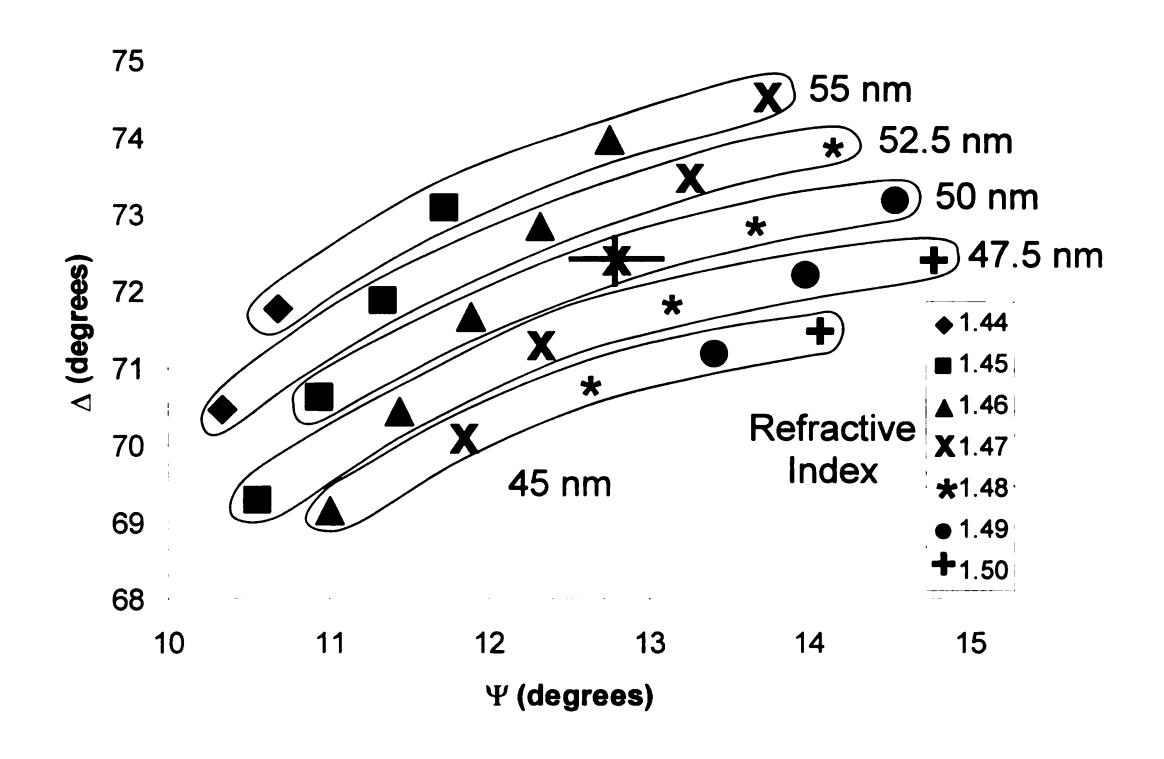


Figure 3.4: Calculated Ψ and Δ values for the system depicted in Figure 3.1 (ethanol as the ambient medium and a 2.0 nm silicon oxide layer) as a function of the refractive index, n_2 , and thickness, d_2 , of the film. The simulation was performed at a wavelength of 480.2 nm where the optical constants are n_1 =1.3645, n_3 =1.4636, k_3 =0, n_4 =4.412, and k_4 = 0.0629. The point with a thickness of 50 nm and a refractive index of 1.47 represents a 9.5-bilayer PSS/PDADAMC film deposited from 0.1 M NaCl, and the black lines through that point show the $\pm 0.3^\circ$ uncertainty in Ψ and Δ measurements. Enclosed data points correspond to identical thicknesses at different refractive indices.

both window effects and measurement uncertainty, the simulations show that film thicknesses and refractive indices can be determined to at least $\pm 5\%$ and ± 0.01 , respectively, in both water and ethanol. For "dry" films, thicknesses and refractive indices can be determined to $\pm 5\%$ and ± 0.04 , respectively.

To further validate the ellipsometric results, we determined PEM thicknesses using atomic force microscopy (AFM) images of intentionally scratched PEM-coated Si wafers. A typical AFM image can be found in Figure 3.5. AFM-derived thicknesses for PSS/PDADMAC deposited from 0.1 M NaCl, [PSS/PDADMAC]₄PSS deposited from 0.5 M NaCl, and HA/chitosan films were consistently 10-15% greater than the ellipsometric thicknesses acquired at a similar relative humidity. AFM-derived thicknesses for [PSS/PDADMAC]4 deposited from 0.5 M NaCl and PSS/PAH films were not significantly different from ellipsometrically determined thicknesses. The positive deviation of AFM thicknesses from ellipsometric thicknesses has been reported before⁵⁰ and could result from scratching of the underlying SiO₂ layer or deposition of the removed material on the nearby film. In any case, the ellipsometric measurements are validated by the reasonable agreement between ellipsometric and AFM methods. One assumption in most ellipsometric thickness determinations is that films are smooth and uniform. The RMS roughness values of PSS/PAH, PSS/PDADMAC, and HA/chitosan films were always less than 15% of film thickness.

Table 3.1 shows the ellipsometric thicknesses of PSS/PAH, PSS/PDADMAC, and HA/chitosan films under nitrogen (<5% RH), water, and ethanol (See Figures 3.6, 3.7, and 3.8 for some typical experimental and fitting

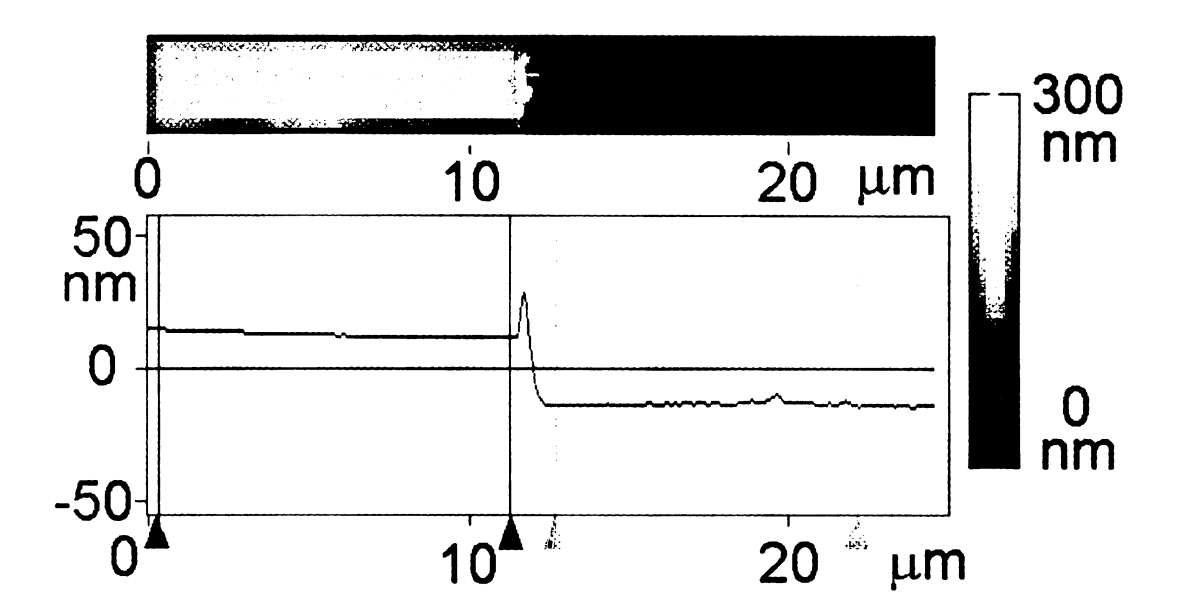


Figure 3.5: A 3 x 25 μ m AFM topographical image and the derived average line scan for thickness analysis of a [PSS/PDADMAC]₁₀ film deposited from 0.1 M NaCl. The region between the two black arrows on the left determines the average film + wafer height, and the area between the two dark grey arrows on the right determines the height of the scratched Si wafer. The average PEM thickness for this particular scan is 28.3 nm.

Table 3.1: Ellipsometric thicknesses of PEMs under nitrogen (<5% RH), water, or ethanol, and percent swelling in the two solvents.

Film Type	Dry Film Thickness (nm)	Film Thickness in H ₂ O (nm)	Percent Swelling in H ₂ O	Film Thickness in Ethanol (nm)	Percent Swelling in Ethanol
[HA/Chitosan] ₈	24±4	118±9	390±50	55±1	130±20
[HA/Chitosan] ₇ HA	24±3	118±6	390±40	55±3	130±20
[PSS/PDADMAC]₄ from 0.5 M NaCl	20±1	95±9	380±60	30±1	54±10
[PSS/PDADMAC]₄PSS from 0.5 M NaCl	24.4±0.4	50±2	106±9	33±2	37±8
[PSS/PDADMAC] ₁₀ from 0.1 M NaCl	24.7±0.9	57±1	129±7	52±1	110±7
[PSS/PDADMAC]₀PSS from 0.1 M NaCl	24±1	54±1	124±8	51.2±0.5	112±5
[PSS/PAH] ₁₀	25.2±0.7	51±1	101±6	49±2	94±8
[PSS/PAH] ₉ PSS	25.1±0.5	49±2	95±9	49±3	96±13

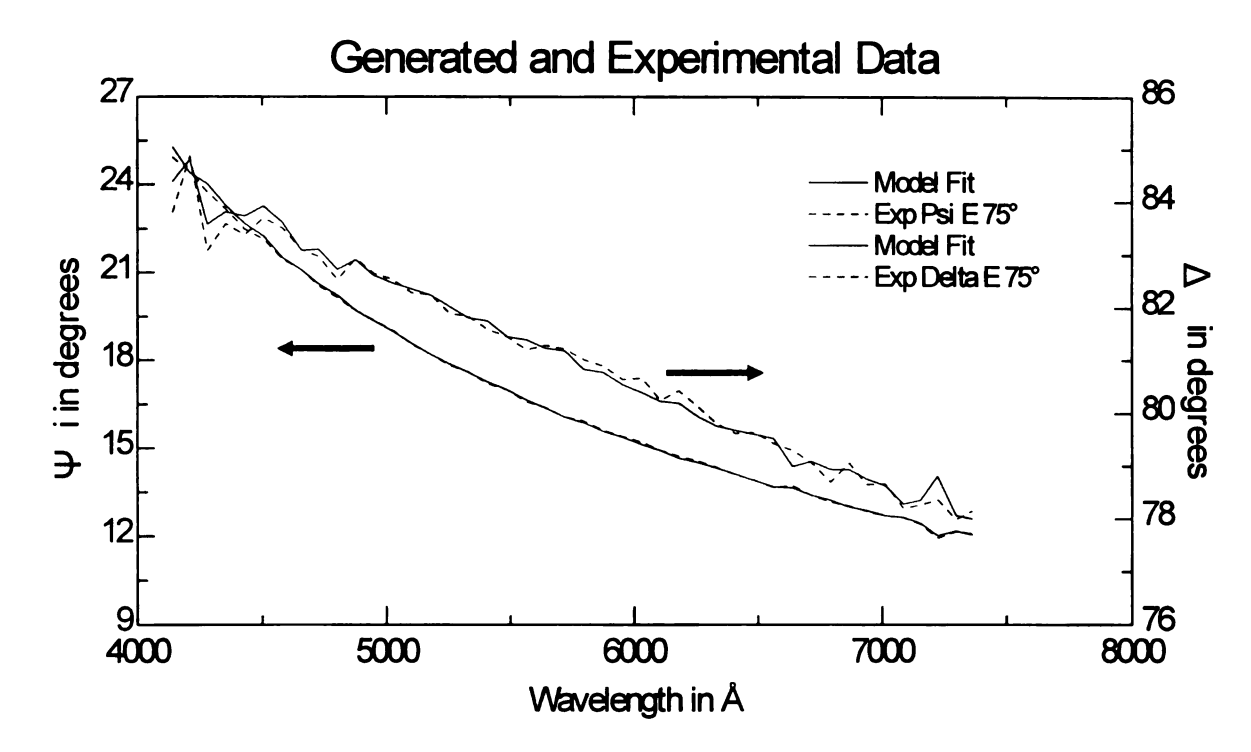


Figure 3.6: The experimental (dashed line) and generated (fit, solid line) Ψ and Δ ellipsometric data for a dry (under <5% RH nitrogen) 10-bilayer PSS/PDADMAC film deposited from 0.1 M NaCl. This fit corresponds to a film that is 24 nm thick and has a refractive index of 1.541 at 450.5 nm.

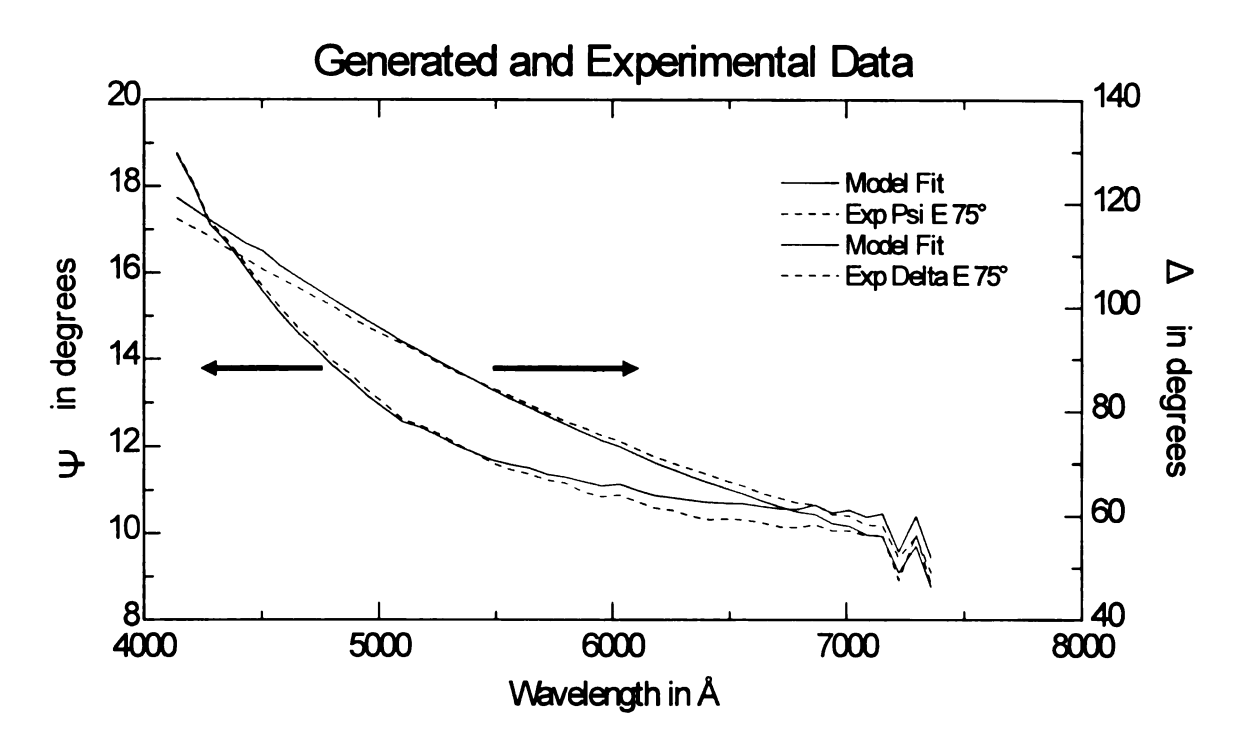


Figure 3.7: The experimental (dashed line) and generated (fit, solid line) Ψ and Δ ellipsometric data for a water-submerged 8-bilayer HA/chitosan film. This fit corresponds to a film that is 124 nm thick and has a refractive index of 1.389 at 450.5 nm.

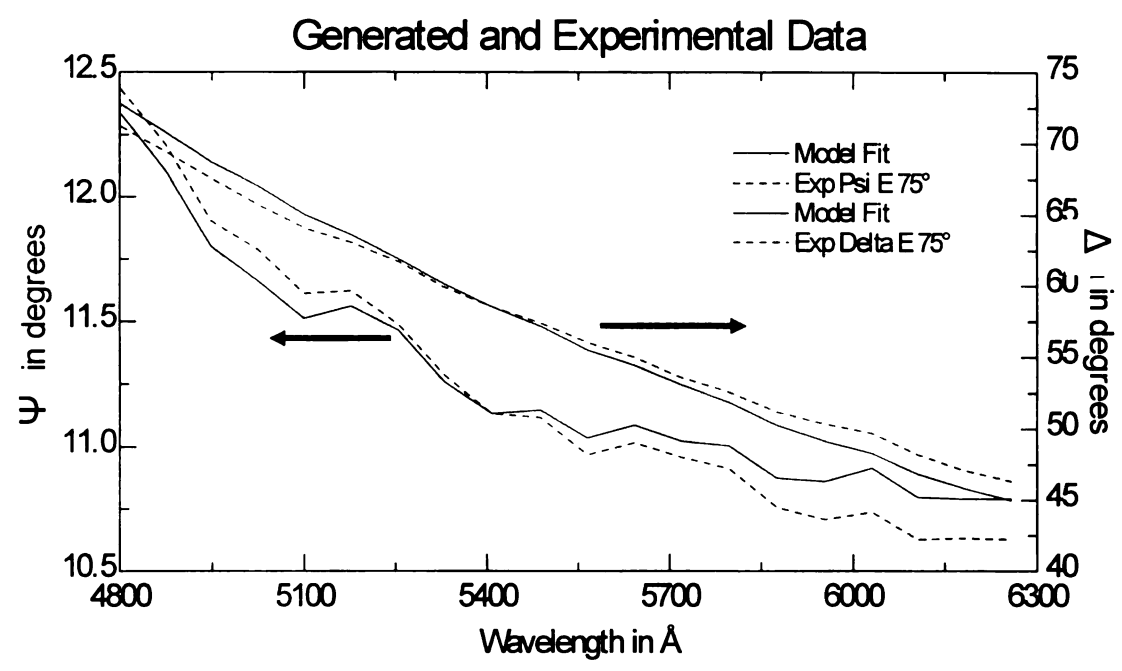


Figure 3.8: The experimental (dashed line) and generated (fit, solid line) Ψ and Δ ellipsometric data for an ethanol-submerged 9.5-bilayer PSS/PDADMAC film deposited from 0.1 M NaCl. This fit corresponds to a film that is 52 nm thick and has a refractive index of 1.453 at 480.2 nm.

data for "dry," water-submerged, and ethanol-submerged films). The number of bilayers in these films was chosen such that all coatings would have similar thicknesses. There are clear variations in percent swelling as a function of both the constituent polyelectrolytes and the swelling solvent. Figure 3.9, which presents the structures of the constituent polyelectrolytes, shows that chitosan, PDADMAC, and PAH contain one positive charge per 11, 9, and 4 non-hydrogen atoms, respectively. In the case of the polyanions, PSS contains one negative charge per 12 non-hydrogen atoms, while HA has only one charge per 26 nonhydrogen atoms. Thus, if swelling increases with decreasing charge density on the polyelectrolytes (due to a lower density of ionic cross-links), HA/chitosan should swell much more than PSS/PDADMAC, which should swell more than PSS/PAH, and this is generally the case in water, though swelling in ethanol is complicated by other factors. The especially low charge density on HA and chitosan results in films that are nearly 80% water. In accord with such a high water content, refractive indices at 603.1 nm for swollen [HA/chitosan]₇HA films are only 1.382. (At the same wavelength, dry [HA/chitosan], HA films have a refractive index of 1.53, while the refractive index of water is 1.333.) For all types of water-swollen or ethanol-swollen films, the refractive index is essentially a linear combination of the refractive indices of water and the dry film, as described by Equation 3.3 where T_{sf} and T_{df} are the thickness of the swollen film and the dry film, respectively, and n_{sf}, n_{df}, and n_s are the refractive indices of the swollen film, the dry film, and the swelling solvent (ethanol or water), respectively.

Figure 3.9: Structures of the polyelectrolytes used in this work.

Estimations of n_{sf} calculated with Equation 3.3 vary from ellipsometrically determined n_{sf} values by less than 1.5% in water and less than 3% in ethanol.

$$T_{sf} n_{sf} = (T_{sf} - T_{df}) n_{s} + T_{df} n_{df}$$
 (3.3)

In most cases, the difference in swelling between films terminated with a polycation and a polyanion is not statistically significant. This is consistent with previous studies that suggest that although water uptake can depend on the composition of the terminating layer in PSS/PAH films, 29,30,51 the solvent fraction in PAH-capped films is only 25% less than in PSS-capped films (40% versus 30% water as a function of capping layer). 29,30 PSS/PDADMAC films deposited from 0.5 M NaCl are a notable exception to the phenomenon of capping layer choice not affecting swelling. The water uptake in [PSS/PDADMAC] films prepared in 0.5 M NaCl is almost 4-fold greater than that in the corresponding [PSS/PDADMAC]4PSS films. We speculate that this occurs because the PDADMAC penetrates the entire film and disrupts ionic cross-linking. This is similar to the explanation for the rapid, exponential (as a function of the number of adsorption steps) growth of some PEMs. 52,53 Indeed, we observed that PSS/PDADMAC films grown in >0.3 M NaCl do show exponential growth, while films grown in 0.1 M NaCl do not.⁵⁴ Consistent with PDADMAC penetrating the entire film, Smith et al. used ¹³C solid-state NMR to show that PDADMAC is more mobile than PSS in PSS/PDADMAC films.⁵⁵ This high mobility was attributed to the low glass transition temperature of PDADMAC, which is below room temperature when there is >20% water content. 55,56 McCormick et al. also reported an increase in both water and PDADMAC mobility in PSS/PDADMAC films when PDADMAC is the top layer.⁵⁷

Interestingly, in ethanol, there is only a small difference between the swelling of [PSS/PDADMAC]4 and [PSS/PDADMAC]4PSS prepared in 0.5 M NaCl (54 versus 37%), and the swelling of both of these films is only 1/3 to 1/2 of that for corresponding coatings prepared in 0.1 M NaCl. Films deposited from 0.1 M NaCl likely swell more in ethanol because they contain fewer ion-exchange sites and are less hydrophilic than films deposited from 0.5 M NaCl. The hydrophilic, non-polyelectrolyte-paired (ion-exchange) charged groups in PSS/PDADMAC films deposited from 0.5 M NaCl likely make them less susceptible to swelling in ethanol.³⁷ Moreover, ethanol may not lower the glass transition temperature of PDADMAC the same way that water does, which could decrease chain mobility and reduce swelling. NMR studies of PEMs in ethanol could reveal if the lack of swelling in PSS/PDADMAC deposited from 0.5 M NaCl correlates with a lack of PDADMAC mobility.⁵⁷ HA/chitosan films also swell less in ethanol than in water, and this likely reflects the fact that ethanol is a poorer solvent for these hydrophilic polymers. Additionally, increased ion pairing (crosslinking) may occur in the presence of ethanol. In the case of films that are already heavily cross-linked in water (PSS/PAH and PSS/PDADMAC deposited from 0.1 M NaCl), swelling is similar in ethanol and water.

Below, we compare swelling and transport results. For HA/Chitosan and PSS/PDADMAC deposited from 0.5 M NaCl, films used in transport and swelling experiments had essentially the same number of bilayers, but in the case of

PSS/PDADMAC deposited from 0.1 M NaCl and PSS/PAH, more bilayers were used in ellipsometric than in transport studies. This was necessary because ellipsometric measurements require relatively thick films for accurate refractive index and thickness determinations, but overly thick films severely retard flux in transport experiments. PSS/PDADMAC deposited from 0.1 M NaCl and PSS/PAH are less permeable than the other systems, so the minimal thickness required for accurate transport experiments with these films was not sufficient for ellipsometric thickness determinations in solvents. A previous study showed that the permeability of PSS/PDADMAC is constant after the deposition of 5 to 6 bilayers, 58 so we expect that the swelling of 9.5 and 10-bilayer films should still be relevant to transport through 5 and 5.5-bilayer systems. Our previous NF studies also indicated that solute rejections by PSS/PDADMAC films deposited from 0.1 M NaCl did not change on going from 5.5 to 6.5 bilayer films. 9

Transport Experiments in Water. Large changes in swelling by water correlate well with both NF and DD data. Table 3.2 shows that the rejections of glucose, sucrose, and raffinose in NF generally increase as film swelling decreases, as would be expected. Highly swollen [HA/chitosan]₈HA films show essentially no rejection of any of the sugars, while the least swelling system, PSS/PAH, rejects >99.6% of sucrose. DD data (Table 3.3) confirm the trends seen in NF. With the possible exception of the comparison of PSS/PAH films with PSS-capped PSS/PDADMAC deposited from 0.5 M NaCl (the swelling is similar between the films), fluxes of glucose, sucrose, and raffinose all increase with increasing film swelling, even though the more swollen HA/chitosan and

Table 3.2: Percent rejection in nanofiltration of glucose, sucrose, and raffinose dissolved in water. PSS/PDADMAC and HA/chitosan data are from Chapter 2.9

The swelling values are from analogous films (Table 3.1).

Percent Rejection

Film Type	Percent Swelling in Water	Glucose	Sucrose	Raffinose
[HA/Chitosan] ₈ HA	390±40	<12%	<12%	<12%
[PSS/PDADMAC]₄ from 0.5 M NaCl	380±60	17±4	28±9	36±8
[PSS/PDADMAC]₄PSS from 0.5 M NaCl	106±9	64±6	97.2±0.9	98.9±0.7
[PSS/PDADMAC]₅ from 0.1 M NaCl	129±7	44±5	85±2	91.3±0.8
[PSS/PDADMAC]₅PSS from 0.1 M NaCl	124±8	58±6	96±2	98.8±0.6
[PSS/PAH]₅	101±6	91.3±0.6	99.6±0.1	99.8±0.1
[PSS/PAH]₅PSS	95±9	88±1	99.70±0.09	99.90±0.07

Table 3.3: Fluxes in diffusion dialysis of glucose, sucrose, and raffinose (dissolved in water) through porous alumina coated with various polyelectrolyte films. The bare alumina and PSS/PDADMAC data are from Chapter 2.9 All film thicknesses were measured in a <5% RH nitrogen atmosphere except for that of [HA/chitosan]₈HA, which is an estimate based upon the thickness of 8-bilayer HA/chitosan films.

Normalized Flux^a (nmol cm⁻² s⁻¹ M⁻¹)

Film Type	Film Thickness (nm)	Percent Swelling in H ₂ O ^b	Glucose	Sucrose	Raffinose
Bare Alumina	N/A	N/A	180±20	140±20	120±10
[HA/Chitosan] ₈ HA	~25	390±40	180±30	140±20	110±20
[HA/Chitosan] ₈	24±4	390±50	180±20	131±9	110±10
[PSS/PDADMAC] ₄ from 0.5 M NaCl	20±1	380±60	150±10	120±10	95±9
[PSS/PDADMAC]₄PSS from 0.5 M NaCl	24.4±0.4	106±9	90±10	7±2	0.3±0.1
[PSS/PDADMAC] ₆ from 0.1 M NaCl	15±1	129±7	90±10	24±2	1.9±0.1
[PSS/PDADMAC]₅PSS from 0.1 M NaCl	12±1	124±8	90±4	11±2	0.5±0.3
[PSS/PAH] ₅	12.5±0.6	101±6	43±3	1.2±0.4	0.6±0.4
[PSS/PAH]₅PSS	13.1±0.4	95±9	56±9	1.1±0.7	0.5±0.5

^aFluxes were normalized by dividing by the source-phase concentration at the end of the experiment.

bValues are taken from Table 3.1 and were measured with films that in some cases had different thicknesses than those used here.

PSS/PDADAMC films prepared in 0.5 M NaCl are about 1.5 to 2-fold thicker than the other films. Fluxes through both HA-terminated and chitosan-terminated HA/chitosan films are essentially the same as those through bare alumina. This is not surprising considering the low (<12%) rejection of sugars in NF and the rapid passage of molecules as large as myoglobin through HA/chitosan films.⁹

For the PSS/PDADMAC systems, the transport data demonstrate that variations in film permeability can occur upon changing the top layer in the film from a polycation to a polyanion. On going from PDADMAC-capped to PSScapped PSS/PDADMAC films made in 0.5 M NaCl, sucrose rejection in NF increases from 28 to 97%, and fluxes in DD decrease by factors of 1.7, 17, and 300 for glucose, sucrose, and raffinose, respectively. This correlates well with the almost 4-fold decrease in swelling that occurs upon addition of a PSS capping layer. A similar, though smaller, effect occurs for PSS/PDADMAC films prepared in 0.1 M NaCl, but in this instance the differences in the rejections and fluxes exhibited by PSS-terminated and PDADMAC-terminated films are larger than what one might expect, given the insignificant differences in their water uptake. Other factors such as polymer intermingling and chain mobility probably affect the permeability of these films. As discussed earlier, NMR experiments by McCormick and Smith indicate that the PDADMAC portions of PSS/PDADMAC films are more mobile when the entire film is terminated end in PDADMAC. 55,57

The aqueous NF and DD data show that PEMs can exhibit extraordinarily diverse permeability properties ranging from nearly complete rejection to nearly complete passage of sugar molecules, depending on polyelectrolyte type, top-

layer choice, and deposition conditions.^{9,11} However, many processes are incompatible with water, and aqueous data may not describe PEM behavior in organic solvents.⁴¹ Thus, we investigated diffusion dialysis through PSS/PAH, PSS/PDADAMC, and HA/chitosan films in ethanol.

Diffusion dialysis in ethanol. Table 3.1 shows that there is significantly less swelling of PEMs in ethanol than in water, particularly for the highly swollen films [HA/chitosan]₈, [HA/chitosan]₇HA, and [PSS/PDADMAC]₈ prepared in 0.5 M Still, there is a significant variation in ethanol swelling among the NaCl. polyelectrolyte systems, ranging from 37% for [PSS/PDADMAC]₄PSS deposited from 0.5 M NaCl to 130% for HA/chitosan films. Nevertheless, DD data in ethanol exhibit minimal correlation between fluxes and film swelling (Table 3.4). For example, polycation-capped [PSS/PDADMAC]₄ films swell slightly more in ethanol than [PSS/PDADMAC] PSS films (both prepared in 0.5 M NaCl), and glucose, sucrose, and raffinose DD fluxes through [PSS/PDADMAC]₅PSS and [PSS/PDADMAC]₅ films differ by factors of 2, 6, and 4, respectively. However, the more highly swollen PSS/PAH and PSS/PDADMAC films deposited from 0.1 M NaCl exhibit less sugar flux than either of the less swollen PSS/PDADMAC films deposited from higher ionic strength. Moreover, fluxes through [HA/chitosan]₈ films are 70-75% lower than those through [PSS/PDADMAC]₅ deposited from 0.5 M NaCl, even though the HA/chitosan swells over twice as much, and the thicknesses of these films differ by only 15%.

Table 3.4: Fluxes in diffusion dialysis of 140 μ M glucose, sucrose, and raffinose in ethanol through porous alumina coated with various polyelectrolyte films. All film thicknesses were measured in a <5% RH nitrogen atmosphere except for that of [HA/chitosan]₈HA, which is an estimate based upon the thickness of 8-bilayer HA/chitosan films.

Normalized Flux^a (nmol cm⁻² s⁻¹ M⁻¹)

Film Type	Film Thickness (nm)	Percent Swelling in Ethanol ^b	Glucose	Sucrose	Raffinose
Bare Alumina	N/A	N/A	210±20	180±40	190±20
[HA/Chitosan] ₈ HA	~25	130±20	100±30	40±20	30±10
[HA/Chitosan] ₈	24±4	130±20	40±20	30±20	30±20
[PSS/PDADMAC]₅ from 0.5 M NaCl	27.3±0.9	54±10	150±10	110±10	100±20
[PSS/PDADMAC]₅PSS from 0.5 M NaCl	31.8±0.6	37±8	74±6	19±2	28±2
[PSS/PDADMAC] ₆ from 0.1 M NaCl	15±1	110±7	50±10	<4 ^c	<4 ^c
[PSS/PDADMAC] ₅ PSS from 0.1 M NaCl	12±1	112±5	40±10	<4 ^c	<4 ^c
[PSS/PAH] ₅	12.5±0.6	94±8	13.1±0.1	<4 ^c	<4°
[PSS/PAH]₅PSS	13.1±0.4	96±13	10.4±0.1	<4 ^c	<4 ^c

^aFluxes were normalized by dividing by the source-phase concentration at the end of the experiment.

bValues are taken from Table 3.1 and were measured with films that in some cases had different thicknesses than those used here.

^cLower limits of measurable, normalized flux are higher in ethanol than in water because of limited sugar solubility in ethanol.

In contrast to PSS/PDADMAC prepared in 0.5 M NaCl, HA/chitosan films show significant (2-fold) *decreases* in glucose fluxes in ethanol when the outer layer of the film is a polycation rather than a polyanion (Table 3.4). Again, however, these trends do not correlate with swelling, as the solvent uptake of both types of films does not depend significantly on the composition of the top layer. PSS/PAH films deposited from 0.5 M NaCl show a slightly higher glucose flux when capped by the polycation, but the differences in swelling are negligible. We think that the ethanol swelling reflects a tradeoff between ionic cross-linking and film hydrophilicity. Highly cross-linked films may be more hydrophobic and soluble in ethanol, and this may oppose the reduction of swelling due to ionic cross-links, even though cross-linking could slow transport by limiting chain mobility. In contrast, such an effect would amplify decreases in aqueous swelling that result from ionic cross-linking, and in that case, we do see a strong correlation between swelling and flux.

3.4 Conclusions

Swelling of PEMs in water increases as the density of charge on constituent polyelectrolytes decreases, and increased water uptake generally leads to decreased sugar rejections in NF and higher solute fluxes in diffusion dialysis. Presumably, higher swelling occurs when fewer ionic cross-links and/or many hydrophilic ion-exchange sites are present in the film. With PSS/PDADMAC films prepared in 0.5 M NaCl, water uptake can vary 4-fold

depending on whether the capping layer is a polycation or a polyanion, and the higher water content leads to minimal sugar rejections in NF. Solvent uptake is generally smaller with ethanol than water, and there is no clear correlation between ethanolic DD data and swelling.

3.5 Acknowledgements

We thank the Department of Energy Office of Basic Energy Sciences for financial support of this work. We also thank Dr. Baokang Bi of Michigan State University for his assistance in the AFM studies.

3.6 Works Cited

- (1) Krasemann, L.; Tieke, B. *J. Membr. Sci.* **1998**, *150*, 23-30.
- (2) Krasemann, L.; Tieke, B. *Mat. Sci. Eng. C-Bio S* **1999**, *C8-C9*, 513-518.
- (3) Toutianoush, A.; Tieke, B. Mat. Sci. Eng. C 2002, C22, 459-463.
- (4) Lenk, W.; Meier-Haack, J. Desalination 2002, 148, 11-16.
- (5) Sullivan, D. M.; Bruening, M. L. J. Membr. Sci. 2005, 248, 161-170.
- (6) Schwarz, H. H.; Malsch, G. J. Membr. Sci. 2005, 247, 143-152.
- (7) Jin, W.; Toutianoush, A.; Tieke, B. *Langmuir* **2003**, *19*, 2550-2553.
- (8) Stanton, B. W.; Harris, J. J.; Miller, M. D.; Bruening, M. L. *Langmuir* **2003**, *19*, 7038-7042.
- (9) Miller, M. D.; Bruening, M. L. Langmuir 2004, 20, 11545-11551.
- (10) Lajimi, R. H.; Ben Abdallah, A.; Ferjani, E.; Roudesli, M. S.; Deratani, A. *Desalination* **2004**, *163*, 193-202.
- (11) Liu, X.; Bruening, M. L. Chem. Mater. 2004, 16, 351-357.
- (12) Donath, E.; Sukhorukov, G. B.; Caruso, F.; Davis, S. A.; Möhwald, H. *Angew. Chem., Int. Ed.* **1998**, *37*, 2202-2205.
- (13) Caruso, F.; Trau, D.; Möhwald, H.; Renneberg, R. *Langmuir* **2000**, *16*, 1485-1488.
- (14) Diaspro, A.; Silvano, D.; Krol, S.; Cavalleri, O.; Gliozzi, A. *Langmuir* **2002**, *18*, 5047-5050.
- (15) Trau, D.; Yang, W.; Seydack, M.; Caruso, F.; Yu, N.-T.; Renneberg, R. *Anal. Chem.* **2002**, *74*, 5480-5486.
- (16) Yu, A.; Caruso, F. Anal. Chem. 2003, 75, 3031-3037.
- (17) Kidambi, S.; Dai, J.; Li, J.; Bruening, M. L. *J. Am. Chem. Soc.* **2004**, *126*, 2658-2659.
- (18) Shchukin, D. G.; Shutava, T.; Shchukina, E.; Sukhorukov, G. B.; Lvov, Y. M. *Chem. Mat.* **2004**, *16*, 3446-3451.
- (19) Pargaonkar, N.; Lvov, Y. M.; Li, N.; Steenekamp, J. H.; de Villiers, M. M. *Pharm. Res.* **2005**, *22*, 826-835.

- (20) Zahr, A. S.; de Villiers, M.; Pishko, M. V. Langmuir 2005, 21, 403-410.
- (21) Zhu, H.; McShane, M. J. Langmuir 2005, 21, 424-430.
- (22) Decher, G. Science 1997, 277, 1232-1237.
- (23) Harris, J. J.; Stair, J. L.; Bruening, M. L. *Chem. Mater.* **2000**, *12*, 1941-1946.
- (24) Lvov, Y.; Ariga, K.; Ichinose, I.; Kunitake, T. *J. Am. Chem. Soc.* **1995**, *117*, 6117-6123.
- (25) Hollman, A. M.; Bhattacharyya, D. Langmuir 2004, 20, 5418-5424.
- (26) Caruso, F.; Niikura, K.; Furlong, D. N.; Okahata, Y. *Langmuir* **1997**, *13*, 3427-3433.
- (27) Garza, J. M.; Schaaf, P.; Muller, S.; Ball, V.; Stoltz, J.-F.; Voegel, J.-C.; Lavalle, P. *Langmuir* **2004**, *20*, 7298-7302.
- (28) Rivin, D.; Meermeier, G.; Schneider, N. S.; Vishnyakov, A.; Neimark, A. V. *J. Phys. Chem. B* **2004**, *108*, 8900-8909.
- (29) Carriere, D.; Krastev, R.; Schoenhoff, M. *Langmuir* **2004**, *20*, 11465-11472.
- (30) Wong, J. E.; Rehfeldt, F.; Haenni, P.; Tanaka, M.; Klitzing, R. v. *Macromolecules* **2004**, *37*, 7285-7289.
- (31) Harris, J. J.; Bruening, M. L. *Langmuir* **2000**, *16*, 2006-2013.
- (32) Hiller, J. A.; Rubner, M. F. *Macromolecules* **2003**, *36*, 4078-4083.
- (33) Sukhorukov, G. B.; Schmitt, J.; Decher, G. Berichte der Bunsen-Gesellschaft 1996, 100, 948-953.
- (34) Kim, B.-S.; Vinogradova, O. I. J. Phys. Chem. B 2004, 108, 8161-8165.
- (35) Ruths, J.; Essler, F.; Decher, G.; Riegler, H. *Langmuir* **2000**, *16*, 8871-8878.
- (36) Poptoshev, E.; Schoeler, B.; Caruso, F. Langmuir 2004, 20, 829-834.
- (37) Dubas, S. T.; Schlenoff, J. B. Langmuir 2001, 17, 7725-7727.
- (38) Mendelsohn, J. D.; Yang, S. Y.; Hiller, J.; Hockbaum, A. I.; Rubner, M. F. *Biomacromolecules* **2003**, *4*, 96-106.
- (39) Tanchak, O. M.; Barrett, C. J. Chem. Mater. 2004, 16, 2734-2739.

- (40) Burke, S. E.; Barrett, C. J. Biomacromolecules 2005, 6, 1419-1428.
- (41) Kim, B.-S.; Lebedeva, O. V.; Koynov, K.; Gong, H.; Glasser, G.; Lieberwirth, I.; Vinogradova, O. I. *Macromolecules* **2005**, *38*, 5214-5222.
- (42) Cardenas, A.; Argueelles-Monal, W.; Goycoolea, F. M.; Higuera-Ciapara, I.; Peniche, C. *Macromol. Biosci.* **2003**, *3*, 535-539.
- (43) Burke, S. E.; Barrett, C. J. *Macromolecules* 2004, 37, 5375-5384.
- (44) Kim, S. J.; Lee, K. J.; Kim, S. I. J. Appl. Polym. Sci. 2004, 93, 1097-1101.
- (45) Tedeschi, C.; Möhwald, H.; Kirstein, S. J. Am. Chem. Soc. **2001**, *123*, 954-960.
- (46) Rezwan, K.; Meier, L. P.; Gauckler, L. J. Langmuir 2005, 21, 3493-3497.
- (47) Schiebener, P.; Straub, J.; Sengers, J. M. H. L.; Gallagher, J. S. *J. Phys. Chem. Ref. Data* **1990**, *19*, 677-717.
- (48) Harvey, A. H.; Gallagher, J. S.; Sengers, J. M. H. L. *J. Phys. Chem. Ref. Data* **1998**, *27*, 761-774.
- (49) Moreels, E.; De Greef, C.; Finsy, R. Appl. Opt. 1984, 23, 3010-3013.
- (50) Porcel, C. H.; Izquierdo, A.; Ball, V.; Decher, G.; Voegel, J. C.; Schaaf, P. *Langmuir* **2005**, *21*, 800-802.
- (51) Schwarz, B.; Schönhoff, M. *Langmuir* **2002**, *18*, 2964-2966.
- (52) Lavalle, P.; Picart, C.; Mutterer, J.; Gergely, C.; Reiss, H.; Voegel, J.-C.; Senger, B.; Schaaf, P. *J. Phys. Chem. B* **2004**, *108*, 635-648.
- (53) Picart, C.; Mutterer, J.; Richert, L.; Luo, Y.; Prestwich, G. D.; Schaaf, P.; Voegel, J. C.; Lavalle, P. *Proc. Natl. Acad. Sci. U. S. A.* 2002, 99, 12531-12535.
- (54) McAloney, R. A.; Sinyor, M.; Dudnik, V.; Goh, M. C. *Langmuir* **2001**, *17*, 6655-6663.
- (55) Smith, R. N.; Reven, L.; Barrett, C. J. *Macromolecules* **2003**, *36*, 1876-1881.
- (56) Yeo, S. C.; Eisenberg, A. J. J. Macromol. Sci., Phys. 1977, B13, 441.
- (57) McCormick, M.; Smith, R. N.; Graf, R.; Barrett, C. J.; Reven, L.; Spiess, H. W. *Macromolecules* **2003**, *36*, 3616-3625.
- (58) Farhat, T. R.; Schlenoff, J. B. *Langmuir* **2001**, *17*, 1184-1192.

Chapter 4

MODIFIED POLYELECTROLYTE MULTILAYER FILMS FOR ENHANCED NANOFILTRATION OF NEUTRAL AND CHARGED MOLECULES

SUMMARY

Polyelectrolyte multilayer films are promising materials for nanofiltration (NF) membranes because their minimal thickness affords high flux, and control over film composition allows tailoring of solute rejections. This chapter describes two modifications that attempt to improve fluxes and selectivities through these films. The first alteration involves hybrid multilayer polyelectrolyte membranes composed of poly(styrene sulfonate) (PSS)/protonated poly(allylamine) (PAH) bilayers deposited on PSS/poly(diallyldimethylammonium chloride) (PDADMAC) "gutter layers." Ideally, these films would combine the high permeability of PSS/PDADMAC films with the selectivity of PSS/PAH, leading to higher NF solution fluxes than pure PSS/PAH films. A more successful modification is the deposition of the final layer of PSS/PAH assemblies from high ionic strength solutions ([PSS/PAH]₄PSS*). This alters the film structure, enhancing both NF solution fluxes and recoveries while maintaining the high selectivities of pure Both types of modified films exhibit NaCl/sucrose NF PSS/PAH films. selectivities at least ten-fold greater than those of pure PSS/PDADMAC membranes, though only [PSS/PAH]₄PSS* films allows fluxes superior to pure PSS/PAH films. These systems also exhibit glucose/sucrose selectivities that are twice those of pure PSS/PDADMAC films and glucose recoveries that are almost double those of pure PSS/PAH assemblies. Additionally, both [PSS/PDADMAC]_m[PSS/PAH]_nPSS* and [PSS/PAH]₄PSS* films can reject multivalent salts from solutions containing butanetriol while maintaining fluxes greater than those of commercial NF membranes. Such separations could prove valuable in the purification of butanetriol, which is a precursor to a high explosive, produced by fermentation.

4.1 Introduction

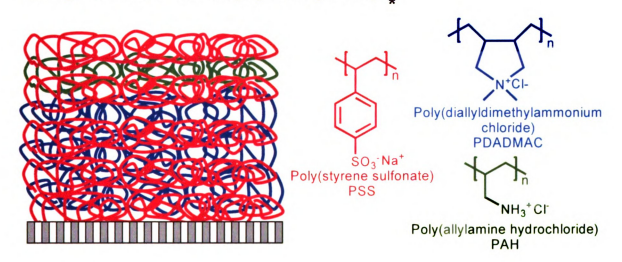
Alternating adsorption of polycations and polyanions on porous supports is an attractive method for forming the skins of composite membranes because it can yield extremely thin (<50 nm), defect-free layers.¹⁻³ The minimal thickness of these coatings results in high fluxes, and careful selection of constituent polyelectrolytes or deposition parameters such as salt concentration allows tuning of permselectivity.⁴⁻⁸ Recently, several studies examined the use of multilayer polyelectrolyte films in encapsulation,⁹⁻¹⁴ nanofiltration (NF),^{3,5-7,15} pervaporation,¹⁶⁻²³ and gas separations.^{4,24,25}

Within the realm of NF alone, polyelectrolyte-modified porous substrates are capable of separating ions, ^{3,5,15} sugars and other small neutral molecules, ^{6,7} and even proteins. ⁶ Jin et al. demonstrated that polyvinylamine/polyvinylsulfate films can achieve 94% rejection of NaCl at 40 bar, although fluxes through those films were low because they contained 60 bilayers. ³ Much thinner (4.5 bilayers) poly(styrene sulfonate) (PSS)/poly(allylamine hydrochloride) (PAH) films can separate chloride and sulfate with a selectivity of 33 and a solution flux of 1.8

m³/(m² day) at a pressure of only 4.8 bar.^{5,26} [PSS/PAH]₆PSS films also exhibit glucose/sucrose selectivities as high as 150, but low glucose recoveries limit the applicability of these membranes in sugar separations.⁷ As shown in chapter 2, simply changing the polycation employed to form such films from PAH to poly(diallyldimethylammonium chloride) (PDADMAC) results in a 4-10 fold increase in glucose recovery and a flux of more than 2 m³/(m² day), albeit with lower glucose/sucrose selectivities (~15).^{6,7} Additionally, PSS/PDADMAC films can separate NaCl from sucrose with a selectivity of 10.^{6,27} Though these results are impressive first steps, greater selectivities matched with higher glucose or NaCl passages and high fluxes are desirable for practical separations such as the refining of oligosaccharides in corn syrup or the recovery of brine from sugar decolorization processes.^{28,29}

This chapter describes attempts to improve the NF solution flux and selectivity of polyelectrolyte multilayer (PEM) membranes through two structure modifications. The first involves hybrid films, i.e., PEMs that contain regions with different polyelectrolyte pairs as shown in Figure 4.1. Specifically, selective PSS/PAH layers are deposited on top of PSS/PDADMAC "gutter layers". A previous report stated that the NF flux through 30 nm-thick (at ambient conditions) PSS/PAH films is about 0.9 m³/(m² day),7 while the solution flux through 30 nm PSS/PDADMAC films deposited from 0.5 M NaCl is 1.5-1.9 m³/(m² day). The PSS/PDADMAC portion of the film is presumably more permeable than PSS/PAH, as the lower charge density on PDADMAC than on PAH results in fewer ionic cross-links and more swelling. (As shown in

Figure 4.1: Schematic illustration of the concept of hybrid polyelectrolyte membranes containing PSS, PDADMAC, and PAH deposited onto a porous alumina support. The color-coded chemical structures of the individual polyelectrolytes are also shown. (The porous support is actually several orders of magnitude thicker than the polyelectrolyte film.)



^{*}Images in this dissertation are presented in color.

Figure 4.1, PAH has 4 non-hydrogen atoms per unit charge, while PDADMAC has 9). We hypothesized that a hybrid film would be advantageous because a few PSS/PDADMAC bilayers would allow for coverage of a porous support with fewer PSS/PAH bilayers than if PSS/PAH were used alone – producing films with high flux and high selectivity.

A few recent papers demonstrated the formation of hybrid polyelectrolyte films. 34-37 Garza et al. showed that deposition of PSS/PAH between hyaluronic acid/poly(L-lysine) bilayers results in a film with highly permeable compartments separated by relatively impermeable PSS/PAH barriers. 37 We previously employed membranes consisting of either poly(acrylic acid)/PAH layers or poly(pyromellitic dianhydride-phenylenediamine)/PAH layers on top of PSS/PAH films to enhance selectivity between Cl⁻ and SO₄²⁻ in diffusion dialysis. However, this study represents the first investigation of the potential benefits of hybrid films in a practical separation technique such as nanofiltration.

The second film modification described here entails a slight change in the deposition of recently described PSS/PAH films.⁷ Previously, the PSS layers of [PSS/PAH]₆PSS films were deposited from pH 2.1 0.5 M MnCl₂, and the films exhibited a molecular weight cutoff (MWCO, the molecular weight at which 90% of a solute is rejected) of about 100 g/mol, as glycerol (M_w of 92) was ~90% rejected. However, this chapter shows that depositing the final PSS layer of a PSS/PAH film from 2.5 M MnCl₂ at a pH of 2.1 (these films are referred to as [PSS/PAH]₄PSS* films from this point on) results in a higher MWCO (>200 g/mol) while still maintaining high SO₄²⁻ rejection (>96%). Previously, the use of high

ionic strength solutions for depositing PSS capping layers enhanced SO₄²-rejection,⁵ but this chapter shows that it can also be advantageous for obtaining higher passage of small, neutral molecules. NF solution fluxes through [PSS/PAH]₄PSS* membranes rival those through PSS/PDADMAC films,⁶ and are about twice the flux through commercial NF membranes.^{38,39} The positive effect of high ionic strength during deposition likely results from film rearrangement, as several studies showed that PEMs can rearrange, sometimes dramatically, in response to changes in ionic strength or pH.^{32,40}

This chapter shows that the hybrid and modified [PSS/PAH]₄PSS* films yield double to triple the glucose/sucrose selectivity and at least ten times the NaCl/sucrose selectivity of pure PSS/PDADMAC films. Additionally, solution fluxes with these films are comparable to those through PSS/PDADMAC membranes (2 m³/(m² day) at 4.8 bar), though only [PSS/PAH]₄PSS* films possess statistically enhanced flux compared to pure PSS/PAH films. Also, both membrane systems remove sulfate and phosphate anions from a 1,2,4-butanetriol (BT) solution while maintaining a high (>60%) recovery of BT. Such separations may be relevant to the production of BT from renewable feedstocks, 41 which is important because BT is a precursor for the high explosive 1,2,4-butanetriol trinitrate.

4.2 Experimental

Materials. Poly(styrene sulfonic acid) sodium salt (PSS, M_w 125000, Alfa Aesar), poly(diallyldimethylammonium chloride) (PDADMAC, M_w 100000-200000,

20 wt. % in water, Aldrich), poly(allylamine hydrochloride) (PAH, M_w 70000, Aldrich), polyethyleneimine (M_w 25000, Aldrich), MnCl₂ (Acros), NaBr (Spectrum), NaCl (CCl), Na₂SO₄ (CCl), 1,2,4-butanetriol (Aldrich), glycerol (anhydrous, CCl), glucose (Aldrich), sucrose (Aldrich), and raffinose (Aldrich) were used as received. Deionized water (Milli-Q, 18.2 MΩcm) was used for membrane rinsing and preparation of polyelectrolyte solutions.

Film Preparation. For swelling experiments, [PSS/PDADMAC]₄PSS* films (Film 1 from Table 4.1) were prepared on pieces of silicon wafers (Si(100), Silicon Quest International) that were first cleaned with UV/O₃ (Boekel UV-Clean model 135500) for 15 minutes. The cleaned silicon was immersed in 1 mg/mL polyethyleneimine at pH 9 for 15 minutes to establish a dense, positively charged layer, and films were then built on this precursor layer.

Porous alumina substrates (0.02 µm Whatman Anodisc filters) were initially cleaned with UV/O₃ for 15 min and then placed concentrate-side up in an O-ring holder to limit film deposition to the feed side of the membrane. To make hybrid films, the alumina supports were first exposed to an aqueous solution of 0.02 M PSS in 0.1 or 0.5 M NaCl for 3 minutes and rinsed with deionized water for 1 minute. (Polymer concentrations are always given with respect to the repeating unit.) Next, the samples were exposed to a 0.02 M PDADMAC solution in 0.1 M or 0.5 M NaCl for 3 min and rinsed again. This process was repeated until the desired number of bilayers for the gutter-layer was formed. To form the selective capping layer(s), the PDADMAC-terminated films were

Table 4.1: Rejections, solution fluxes, and selectivities from nanofiltration of a series of neutral molecules using porous 0.5 M NaCl was used in deposition of the alumina coated with a variety of multilayer polyelectrolyte films.6.7 PSS/PDADMAC layers. Films are given numbers to aid in discussion.

				Rejec	Rejection (%)			Selectivity	
Film	Film Type	Solution Flux ^a (m ³ /(m ² day))	Glycerol	Glucose	Sucrose	Raffinose	Glycerol/ Glucose	Glucose/ Sucrose	Glucose/ Raffinose
—	[PSS/PDADMAC] ₄ PSS*	1.3±0.3	40±30	57±9	88±4	93±5	1.4±0.4	4±2	10±10
2	[PSS/PDADMAC]₄ PSS ^b	2.0±0.3	18±4	64±6	97.2±0.9	98.9±0.7	2.3±0.3	14±4	50±50°
ო	[PSS/PDADMAC] ₃ [PSS/PAH]PSS*	2.0±0.2	10±20	64±9	98.2±0.5	99.2±0.5	2.7±0.7	20±5	70±50
4	[PSS/PDADMAC] ₃ [PSS/PAH] ₂ PSS*	1.8±0.2	10±10	77±4	99.2±0.2	99.6±0.2	4.0±0.7	30±7	70±40
Ω	[PSS/PAH]4PSS*	2.2±0.2	18±6	76±2	99.4±0.1	6.66<	3.4±0.3	43±9	>250
ဖ	[PSS/PAH] ₄ PSS	1.7±0.2	28±7	87±1	99.6±0.4	6.66<	5.6±0.4	50±20	>160

^aNF was run at 4.8 bar.

^bData are from Chapter 2 (PSS/PDADMAC).⁶
^cSelectivities of three different membranes were: 21, 41, and 106.
^{*}Final layer of PSS was deposited from pH 2.1 2.5 M MnCl₂.

exposed to an aqueous solution of pH 2.1 0.02 M PSS in 0.5 M MnCl₂ for 2 minutes, rinsed with deionized water for 1 minute, immersed in a solution of pH 2.3 0.02 M PAH with 0.5 M NaBr for 5 minutes, and again rinsed with water. This procedure was repeated as necessary to form more capping bilayers. The final PSS layer of the PSS/PAH capping layers was deposited from 2.5 M MnCl₂ at pH 2.1 instead of 0.5 M MnCl₂ at pH 2.1 (thus, these films are designated [PSS/PDADMAC]_m[PSS/PAH]_nPSS*). Deposition of [PSS/PAH]₄PSS* films utilized the same procedure as the synthesis of capping PSS/PAH layers of hybrid films. The final PSS layer was again deposited from 2.5 M MnCl₂ at pH 2.1 for 2 minutes, followed by a final rinse.

Ellipsometry. Ellipsometric thicknesses of the SiO₂ layers on Si wafers were first determined assuming literature values for the refractive indices of Si and SiO₂ at the 44 wavelengths of the ellipsometer (J.A. Woollam model M-44 rotating analyzer ellipsometer, 75° angle of incidence) between 414.0 nm and 736.1 nm. After coating of these wafers, film thicknesses were obtained either in ambient conditions (40% relative humidity (RH)), or under water using a homebuilt cell with glass windows for swelling experiments. The ellipsometric thicknesses and refractive indices of [PSS/PDADMAC]₄PSS* (Film 1) films were determined at three different points per wafer on three different wafers, and the reported results are the average and standard deviation of these values. Optical constants of water as a function of wavelength were calculated using the Cauchy equation in coordination with constants in the literature.^{42,43}

Nanofiltration. NF was performed as previously reported (see Chapter 2).⁵⁻⁷ The feed for sugar/NaCl separation experiments with hybrid, [PSS/PAH]₄PSS*, and [PSS/PAH]₄PSS films contained 1 mM glycerol and glucose, 5 mM sucrose and raffinose, and 10 mM NaCl. For sugar separations with PSS/PDADAMAC films, the feed contained 1 mM glycerol, glucose, sucrose, and raffinose. For salt/sugar separations with pure PSS/PDADMAC the feed was 1 mM sucrose and 10 mM NaCl, and for BT/salt separations, the feed was either 1 mM BT and 2.5 mM Na₂SO₄ or 1 mM BT and 21.5 mM K₂HPO₄. The pH of the BT/phosphate solution was adjusted to 7 or 8 by addition of 1 M HCl.

For all experiments, the feed was passed over the membrane at 18 mL/min, and the system was pressurized to 4.8 bar (70 psi). After 18 h of equilibration time, membrane permeate was acquired for intervals of 15-30 minutes. Glycerol, glucose, sucrose, raffinose, and BT concentrations were determined via chromatography (Dionex, DX-600, CarbonPac PA-10 column, mobile phase: 0.1 M NaOH at 1.0 mL/min) coupled with pulsed amperometric detection (Dionex, ED-50). Single salts in solution (i.e. Na₂SO₄/BT separations) were analyzed with conductivity measurements (Orion model 115).

Equation 4.1 defines solute rejection, where C_{feed} is the concentration of the solute in the feed, C_{perm} is the concentration of the solute in the permeate, and R is the percent rejection of the solute. Equation 4.2 describes the membrane selectivity between two different solutes, where R_A is the percent rejection of solute A, and R_B is the percent rejection of solute B.

$$R = \left(1 - \frac{C_{perm}}{C_{feed}}\right) \times 100\% \tag{4.1}$$

Selectivity =
$$\frac{C_{A,perm}}{C_{A,feed}} \frac{C_{B,feed}}{C_{B,perm}} = \frac{100\% - R_A}{100\% - R_B}$$
(4.2)

4.3 Results and Discussion

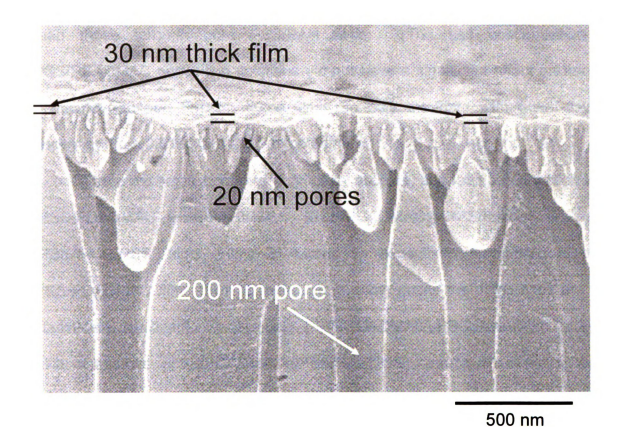
This section first presents the enhancement in selectivity that hybrid [PSS/PDADMAC]_m/[PSS/PAH]_nPSS* and [PSS/PAH]₄PSS* membranes provide in NF of small neutral molecules such as sugars. Subsequent results show that these films are very promising for NaCl/sucrose separations, and finally, we examine the performance of such films in a specific potential application, removal of salts from a solution containing BT.

Sugar Separations

Figure 4.2 shows a scanning electron microscope (SEM) image of a [PSS/PDADMAC]₃[PSS/PAH]PSS* film deposited on an alumina support. The 20 nm-diameter surface pores and 200 nm-diameter bulk pores of the alumina as well as the 30 nm-thick polyelectrolyte skin layer are clearly visible. The image suggests that hybrid films fully cover underlying pores without filling them, and the high rejections of raffinose and sucrose in Table 4.1 are indicative of a film with very few defects.

Consistent with a size-exclusion mechanism, Table 4.1 shows that PSS/PAH membranes (Film 6) show larger rejections of glucose, sucrose, and raffinose than do the lower charge density pure PSS/PDADMAC films (Film 2). Our goal in using hybrid and [PSS/PAH]₄PSS* films to separate neutral

Figure 4.2: Cross-sectional SEM image of a [PSS/PDADMAC]₃[PSS/PAH]PSS* film deposited on porous alumina. The final PSS layer was deposited from 2.5 M MnCl₂.⁴⁴



molecules was to create a membrane that had the high rejections of pure PSS/PAH films along with the high fluxes typical of pure PSS/PDADMAC membranes. The data in Table 4.1 illustrate that [PSS/PAH]₄PSS* films barely achieve this goal, but not hybrid films, as their fluxes are not statistically greater than those through pure PSS/PAH films. (The salt concentration in PSS/PDADMAC deposition solutions did not have a significant effect on neutral molecule transport through these films, so only the data with gutter layers deposited from 0.5 M NaCl are presented here.)

There are small increases in glucose, sucrose, and raffinose rejection with [PSS/PDADMAC]₃[PSS/PAH]PSS*, [PSS/PDADMAC]₃-[PSS/PAH]₂PSS*, and [PSS/PAH]₄PSS* films (Films 3, 4, and 5, respectively) compared to pure PSS/PDADMAC films (Film 2), although in some cases the differences are not statistically significant. For example, [PSS/PDADMAC]₄PSS films (Film 2) reject 97% of sucrose, [PSS/PDADMAC]₃[PSS/PAH]PSS* membranes (Film 3) reject 98% of sucrose, and [PSS/PDADMAC]₃[PSS/PAH]₂PSS* as well as [PSS/PAH]₄PSS* assemblies (Films 4 and 5, respectively) reject 99% of sucrose. Beneficially, [PSS/PAH]₄PSS* films with 99+% sucrose rejection exhibit glucose rejections of only 76%, leading to glucose/sucrose selectivities 3-times greater than pure PSS/PDADMAC assemblies. Note that glucose rejection through [PSS/PAH]₄PSS* membranes (Film 5) is about 11% lower compared to typical PSS/PAH films (Film 6), almost doubling glucose recovery. [PSS/PAH]₄PSS* films also show increased raffinose rejection relative to PSS/PDADMAC films

(Film 2), resulting in glucose/raffinose selectivities in excess of 250. Glycerol rejection is below 30% for all modified films.

Notably, the solution fluxes through hybrid films (Films 3 and 4) are essentially unaffected by the addition of a second PSS/PAH capping layer. The PSS/PDADMAC films with no capping layers (Film 2) have a solution flux of 2 m³/(m² day), and the hybrid films show at most a 10% loss in flux. Though the sucrose rejection increases due to capping layers, the cumulative transport resistance due to both PSS/PDADMAC and the additional PSS/PAH layers reduces the flux to the point that it is indistinguishable from pure [PSS/PAH]₄PSS films. Thus, the benefit of hybrid films over pure PSS/PAH films in sugar separations is limited to a slight increase in glucose recovery (compare films 3 and 5).

Considering the above results, we wondered if just depositing a single layer of PSS from 2.5 M MnCl₂ on top of a gutter layer is enough to create these improved selectivities compared to pure PSS/PDADMAC films. We deposited 4 bilayers of PSS/PDADMAC from 0.5 M NaCl and then capped the films with a single layer of PSS from 2.5 M MnCl₂ at pH 2.1 (Film 1, [PSS/PDADMAC]₄PSS*). Ellipsometry experiments suggest that increasing the ionic strength of the final PSS deposition solution significantly alters the composition of the film. As shown previously, depositing the final PSS layer on top of a 4-bilayer PSS/PDADMAC membrane (assembled in 0.5 M NaCl) from 0.5 M NaCl results in only a 20% thickness increase (Chapter 2, Table 2.2).⁶ Surprisingly, when that PSS final layer is added from 2.5 M MnCl₂ instead, film thicknesses double from 21.6±0.6

nm to 44±3 nm. Ellipsometric swelling experiments suggest that [PSS/PDADMAC]₄PSS* films (Film 1) swell almost 5 times as much in water as 4.5-bilayer PSS/PDADMAC assemblies where every layer is deposited from 0.5 M NaCl (Film 2). (Film 1 swells 380±70% while a version of Film 2 with more bilayers swells 106±9%, see Chapter 3 Table 3.1.⁴⁵)

In conjunction with this high swelling, the NF results for [PSS/PDADMAC]₄PSS* from Table 4.1 (Film 1) depict lower rejections for all sugar molecules. Interestingly, though initial solution fluxes through these films were extremely high (>5 m³/(m² day)), after 18 h of operation their flux was 35% less than [PSS/PDADMAC]₄PSS films deposited from 0.5 M NaCl (Film 2). These films likely undergo significant compaction under pressure. Apparently, PAH plays a critical role in establishing a hybrid system.

Salt-Sugar Separations

The data in Table 4.1, in conjunction with previous research, ^{5,6} suggest that modified films should allow passage of NaCl while retaining sucrose and raffinose, which would be ideal for an application like salt recovery from ion-exchange regeneration wastes. ²⁷ Table 4.2 shows the flux and rejection data in NF of solutions containing NaCl and sucrose by modified films as well as pure PSS/PAH and PSS/PDADMAC membranes. In the case of the pure films, [PSS/PAH]₄PSS (Film 6) shows a higher sucrose rejection than [PSS/PDADMAC]₄PSS (Film 2), but the latter films exhibit slightly less NaCl rejection that might allow better salt recovery. Both types of modified films exhibit less salt rejection than PSS/PAH films and higher selectivities than

Table 4.2: Rejections, solution fluxes, and selectivities from nanofiltration of sucrose and NaCl by porous alumina coated with a variety of PEM films arranged in order of increasing NaCl/sucrose selectivity. 0.5 M NaCl was used in deposition of the PSS/PDADMAC layers. Films are numbered to aid in discussion.

Film	Film Type	Solution Flux ^a (m ³ /(m ² day))	NaCl Rejection (%)	Sucrose Rejection (%)	NaCl/ Sucrose Selectivity
1	[PSS/PDADMAC] ₄ PSS*	1.3±0.3	32±4	88±4	6±3
2	[PSS/PDADMAC] ₄ PSS ^b	2.0±0.3	40±4	93.8±0.8	10±1
3	[PSS/PDADMAC] ₃ [PSS/PAH]PSS*	2.0±0.2	24±2	98.2±0.5	40±10
4	[PSS/PDADMAC] ₃ [PSS/PAH] ₂ PSS*	1.8±0.2	23±3	99.2±0.2	100±20
5	[PSS/PAH] ₄ PSS*	2.2±0.2	29±3	99. 4± 0.1	130±30
6	[PSS/PAH] ₄ PSS	1.7±0.2	50±9	99.6±0.4	170±70

^aNF was run at 4.8 bar.

^bThese PSS/PDADMAC data are from Chapter 2.⁶

^{*}Final layer of PSS was deposited from pH 2.1 2.5 M MnCl₂.

PSS/PDADMAC films, as [PSS/PDADMAC]₃[PSS/PAH]₂PSS* and [PSS/PAH]₄PSS* (Films 4 and 5, respectively) show a NaCl rejection of only 25-30% and a NaCl/sucrose selectivity of 100 or more. The high NaCl passage makes them more attractive than [PSS/PAH]₄PSS for NaCl-sugar separations. Selectivity increases 2.5-fold on going from [PSS/PDADMAC]₃[PSS/PAH]PSS* to [PSS/PDADMAC]₃[PSS/PAH]₂PSS* (Films 3 and 4, respectively). For all modified films, flux is ~2 m³/(m² day), about twice the flux through commercial NF membranes.^{38,39} The remarkable flux, NaCl/sucrose selectivity, and NaCl recovery possible with these films make them attractive for salt recovery applications.

Removal of sulfate and phosphate salts from solutions containing butanetriol

The final application explored here involves purification of BT from solutions containing sulfate and phosphate salts. This separation is relevant to collection of BT from a fermentation broth⁴¹ in which magnesium sulfate, sulfuric acid and potassium phosphate are added for pH adjustment but are contaminants of the end product. Frost and coworkers recently showed that production of this explosive precursor from renewable feedstocks may be preferable to the current synthetic method involving the reduction of esterified D,L-malic acid.⁴¹ In this separation, instead of rejecting an organic molecule and allowing salt to pass as described above, we want to design a film to reject divalent salts and allow a small organic molecule (BT) to pass.

Table 4.3 shows the rejections, solution fluxes, and BT/sulfate selectivities for a variety of PEM films. Pure PSS/PAH films were not explored for this application as previous data show that divalent anions are less than 60% rejected with these assemblies.⁵ Initial experiments with 4.5-bilayer membranes of PSS/PDADMAC deposited from 0.5 M NaCl (Film 2) showed high fluxes and low BT rejection (2.3 m³/(m² day) and 20%, respectively), but, unfortunately, only 75% sulfate rejection. Deposition of the terminating PSS layer from 2.5 M MnCl₂ at pH 2.1 (instead of 0.5 M NaCl) (Film 1) gave a significantly lower flux of 1.5 m³/(m² day), the same BT rejection, and 91% sulfate rejection. The higher sulfate rejection was encouraging, but previous reports using PSS/PAH films with terminating PSS layers deposited from 2.5 M MnCl₂ suggested that modified films would lead to considerably higher sulfate rejection.⁵

The sulfate rejection with [PSS/PDADMAC]₃[PSS/PAH]PSS* films (Film 3) was 96% while the BT rejection was 40%, and fluxes were an adequate 1.45 m³/(m² day). [PSS/PAH]₄PSS* films (Film 5) produced nearly identical rejection data, but with surprisingly higher fluxes than the hybrid film systems. Previous data suggest that gutter layer thickness does affect flux (solution flux through [PSS/PDADMAC]₅[PSS/PAH]PSS* films is only 33% that of [PSS/PDADMAC]₂[PSS/PAH]PSS* assemblies),⁴⁴ but thinner PSS/PDADMAC gutter layers may not cover the alumina pores completely, which could lead to sulfate leakage.

Table 4.3: Rejections, solution fluxes, and selectivities from nanofiltration of BT and sodium sulfate using porous alumina coated with a variety of PEM films. All PSS/PDADMAC layers were deposited from 0.5 M NaCl unless indicated otherwise. Films are numbered to aid in discussion.

Film	Film Type	Solution Flux ^a (m ³ /(m ² day))	BT Rejection (%)	Sulfate Rejection (%)	BT/Sulfate Selectivity
1	[PSS/PDADMAC] ₄ PSS*	1.5±0.5	20±20	91±4	12±7
2	[PSS/PDADMAC] ₄ PSS	2.3±0.3	20±10	75±4	3.4±0.9
3	[PSS/PDADMAC] ₃ [PSS/PAH]PSS*	1.45±0.07	40±20	96.2±0.9	20±10
5	[PSS/PAH] ₄ PSS*	2.4±0.3	30±10	96.5±0.8	22±6

^aNF was run at 4.8 bar.

^{*}Final layer of PSS was deposited from pH 2.1 2.5 M MnCl₂

A second aspect of this separation, removal of phosphate salts, was more difficult. Because phosphate is a trivalent base, its charge is a function of pH, and ion-exclusion separations can be challenging. Schlenoff and coworkers previously reported that control over pH can have a dramatic effect on the transport of weak acids.⁴⁶ Initial work with PEM films and pH 7 solutions resulted in only 50% rejection of the total phosphate species because at pH 7 the phosphate is roughly half HPO₄²⁻ and half H₂PO₄⁻.

Table 4.4 shows the phosphate rejection, BT rejection, and solution flux for hybrid and [PSS/PAH]₄PSS* films after adjusting the solution pH to 8. At this point the phosphate is approximately 90% HPO₄², and rejection is about 90% with hybrid films. Similar phosphate rejections were observed for [PSS/PDADMAC]3[PSS/PAH]PSS* and [PSS/PDADMAC]₃[PSS/PAH]₂PSS* membranes (Films 3 and 4), and the flux was 1.6-1.7 m³/(m² day) for both films. [PSS/PAH]₄PSS* films (Film 5) also exhibit low BT rejection, but unfortunately they reject 15% less phosphate than hybrid films. The lower phosphate rejection of [PSS/PAH]₄PSS* films could result from slow film decomposition at pH 8, as individual [PSS/PAH]₄PSS* membranes with higher flux possessed lower phosphate rejection. For example, a membrane with an average flux of 1.9 m³/(m² day) exhibited a phosphate rejection of 86%, while a film with an average flux of 2.4 m³/(m² day) possessed a 69% phosphate rejection. The gutter layers may supply additional stability to the hybrid systems, as the PSS/PDADMAC layers are composed of strong polyelectrolytes and thus are pH tolerant. Separations at even higher pH values where nearly all phosphate

Table 4.4: Rejections, solution fluxes, and selectivities from nanofiltration of BT and potassium phosphate at pH 8 using porous alumina coated with PEM films.

All PSS/PDADMAC layers were deposited from 0.5 M NaCl. Films are numbered to aid in discussion.

Film	Film Type	Solution Flux ^a (m ³ /(m ² day))	BT Rejection (%)	Phosphate Rejection (%)	BT/ Phosphate Selectivity
3	[PSS/PDADMAC] ₃ [PSS/PAH]PSS*	1.7±0.2	30±10	89±1	7±1
4	[PSS/PDADMAC] ₃ [PSS/PAH] ₂ PSS*	1.6±0.1	10±10	90±1	9±1
5	[PSS/PAH] ₄ PSS*	2.0±0.4	32±8	75±11	4±2

^aNF was run at 4.8 bar.

^{*}Final layer of PSS was deposited from pH 2.1 2.5 M MnCl₂

species would be highly charged are challenging, as complete decomposition of the PEMs or dissolution of the alumina support may occur.

The best choice of PEM for the removal of sulfate and/or phosphate from a BT solution depends on a number of factors. If sulfate anions are the contaminant of interest, then [PSS/PAH]₄PSS* assemblies are the best choice, as they possess higher fluxes than hybrid films (Table 4.3). However, if removal of phosphate is paramount, then hybrid films would be better choices, as they reject the most phosphate. A case where both salts are present is more problematic. If high fluxes are more critical than permeate quality, then [PSS/PAH]₄PSS* films would suffice. However, if flux was not as important as obtaining low permeate salt concentrations, then hybrid films are superior as they reject 96% of sulfate and 90% of phosphate anions while rejecting only 40% of BT.

4.4 Conclusion

This chapter describes two types of modified films that attempt to improve NF fluxes and selectivities in three diverse, model applications. In both sugar and sugar/salt separations, PSS/PAH films where the terminating PSS layer is deposited from 2.5 M MnCl₂ exhibit greater fluxes than pure PSS/PAH films while maintaining similar selectivities. Hybrid films, where selective PSS/PAH layers are deposited on presumably more permeable PSS/PDADMAC, are capable of higher selectivities than pure PSS/PDADMAC films, but the fluxes are not statistically greater than those through pure PSS/PAH films. In the purification of

BT, both types of modified films exhibit BT/sulfate selectivities of twenty, though [PSS/PAH]₄PSS* membranes have higher fluxes. However, in BT/phosphate separations, hybrid films show double the selectivity of [PSS/PAH]₄PSS* films, as the latter is likely not as tolerant of the slightly basic pH. Overall, hybrid films are better suited to remove salts from BT/salt solutions, while [PSS/PAH]₄PSS* assemblies excel at sugar and sugar/salt separations.

4.5 Acknowledgements

We thank the Division of Chemical Sciences in the Office of Basic Energy Sciences of the Department of Energy for financial support of this work.

4.6 Works Cited

- (1) Decher, G. Science 1997, 277, 1232-1237.
- (2) Harris, J. J.; Stair, J. L.; Bruening, M. L. *Chem. Mater.* **2000**, *12*, 1941-1946.
- (3) Jin, W.; Toutianoush, A.; Tieke, B. *Langmuir* **2003**, *19*, 2550-2553.
- (4) Krasemann, L.; Tieke, B. *Mat. Sci. Eng. C-Bio S* **1999**, *C8-C9*, 513-518.
- (5) Stanton, B. W.; Harris, J. J.; Miller, M. D.; Bruening, M. L. *Langmuir* **2003**, *19*, 7038-7042.
- (6) Miller, M. D.; Bruening, M. L. Langmuir 2004, 20, 11545-11551.
- (7) Liu, X.; Bruening, M. L. *Chem. Mater.* **2004**, *16*, 351-357.
- (8) Hollman, A. M.; Bhattacharyya, D. *Langmuir* **2004**, *20*, 5418-5424.
- (9) Donath, E.; Sukhorukov, G. B.; Caruso, F.; Davis, S. A.; Möhwald, H. *Angew. Chem., Int. Ed.* **1998**, *37*, 2202-2205.
- (10) Caruso, F.; Trau, D.; Möhwald, H.; Renneberg, R. *Langmuir* **2000**, *16*, 1485-1488.
- (11) Diaspro, A.; Silvano, D.; Krol, S.; Cavalleri, O.; Gliozzi, A. *Langmuir* **2002**, *18*, 5047-5050.
- (12) Trau, D.; Yang, W.; Seydack, M.; Caruso, F.; Yu, N.-T.; Renneberg, R. *Anal. Chem.* **2002**, *74*, 5480-5486.
- (13) Yu, A.; Caruso, F. Anal. Chem. 2003, 75, 3031-3037.
- (14) Shchukin, D. G.; Shutava, T.; Shchukina, E.; Sukhorukov, G. B.; Lvov, Y. M. *Chem. Mater.* **2004**, *16*, 3446-3451.
- (15) Lajimi, R. H.; Ben Abdallah, A.; Ferjani, E.; Roudesli, M. S.; Deratani, A. *Desalination* **2004**, *163*, 193-202.
- (16) Krasemann, L.; Tieke, B. *J. Membr. Sci.* **1998**, *150*, 23-30.
- (17) Krasemann, L.; Toutianoush, A.; Tieke, B. *J. Membr. Sci.* **2001**, *181*, 221-228.
- (18) Meier-Haack, J.; Lenk, W.; Lehmann, D.; Lunkwitz, K. *J. Membr. Sci.* **2001**, *184*, 233-243.
- (19) Toutianoush, A.; Tieke, B. Mat. Sci. Eng. C 2002, C22, 459-463.

- (20) Lenk, W.; Meier-Haack, J. Desalination 2002, 148, 11-16.
- (21) Budd, P. M.; Ricardo, N. M. P. S.; Jafar, J. J.; Stephenson, B.; Hughes, R. *Ind. Eng. Chem. Res.* **2004**, *43*, 1863-1867.
- (22) Sullivan, D. M.; Bruening, M. L. J. Membr. Sci. 2005, 248, 161-170.
- (23) Schwarz, H. H.; Malsch, G. J. Membr. Sci. 2005, 247, 143-152.
- (24) Quinn, R. J. Membr. Sci. 1998, 139, 97-102.
- (25) Sullivan, D. M.; Bruening, M. L. Chem. Mater. 2003, 15, 281-287.
- (26) Dai, J.; Jensen, A. W.; Mohanty, D. K.; Erndt, J.; Bruening, M. L. *Langmuir* **2001**, *17*, 931-937.
- (27) Hinkova, A.; Bubnik, Z.; Kadlec, P.; Pridal, J. Sep. Purif. Technol. 2002, 26, 101-110.
- (28) Gyura, J.; Seres, Z.; Vatai, G.; Molnar, E. B. *Desalination* **2002**, *148*, 49-56.
- (29) Goulas, A. K.; Grandison, A. S.; Rastall, R. A. *J. Sci. Food Agr.* **2003**, *83*, 675-680.
- (30) This estimate is based upon the flux of sugar solutions through 4.5-bilayer and 5.5-bilayer PSS/PDADMAC films deposited from 0.5 M NaCl. These films have thicknesses of 25 and 35 nm under ambient conditions, respectively, according to Table 2.2 in Chapter 2. However, the data in this chapter suggest that hybrid films have no flux advantage over the thinner 4.5-bilayer PSS/PAH films. This is because 4.5-bilayer PSS/PAH films have almost double the flux of previously reported 6.5-bilayer assembiles..
- (31) Krasemann, L.; Tieke, B. Chem. Eng. Technol. 2000, 23, 211-213.
- (32) Dubas, S. T.; Schlenoff, J. B. *Langmuir* **2001**, *17*, 7725-7727.
- (33) Miller, M. D.; Bruening, M. L. Chem. Mater., Submitted for Publication.
- (34) Stair, J. L.; Harris, J. J.; Bruening, M. L. *Chem. Mater.* **2001**, *13*, 2641-2648.
- (35) Sullivan, D. M.; Bruening, M. L. *J. Am. Chem. Soc.* **2001**, *123*, 11805-11806.
- (36) Kharlampieva, E.; Sukhishvili, S. A. Langmuir 2004, 20, 10712-10717.

- (37) Garza, J. M.; Schaaf, P.; Muller, S.; Ball, V.; Stoltz, J.-F.; Voegel, J.-C.; Lavalle, P. *Langmuir* **2004**, *20*, 7298-7302.
- (38) Bhattacharyya, D., et al, In Membrane Handbook; Ho W.S.W, Sirkar, K.K., Eds.; Van Nostrand Reinhold; New York, 1992.
- (39) Hutchinson, R. A.; Beuermann, S.; Paquet, D. A., Jr.; McMinn, J. H.; Jackson, C. *Macromolecules* **1998**, *31*, 1542-1547.
- (40) Mendelsohn, J. D.; Barrett, C. J.; Chan, V. V.; Pal, A. J.; Mayes, A. M.; Rubner, M. F. *Langmuir* **2000**, *16*, 5017-5023.
- (41) Niu, W.; Molefe, M. N.; Frost, J. W. *J. Am. Chem. Soc.* **2003**, *125*, 12998-12999.
- (42) Schiebener, P.; Straub, J.; Sengers, J. M. H. L.; Gallagher, J. S. *J. Phys. Chem. Ref. Data* **1990**, *19*, 677-717.
- (43) Harvey, A. H.; Gallagher, J. S.; Sengers, J. M. H. L. *J. Phys. Chem. Ref. Data* **1998**, *27*, 761-774.
- (44) Stanton, B. W., Ultrathin, Multilayered Polyelectrolyte Films as Nanofiltration Membranes, M.S. Thesis, Department of Chemistry, Michigan State University, **2003**
- (45) Please note that the swelling for Film 2 is relative to dry films in <5% RH, while the swelling for Film 1 is relative to dry films in 40% RH.). However, film thicknesses increase in the presence of water vapor, as ellipsometry experiments with 4-bilayer PSS/PDADMAC films show that they swell 20% on going from <5% to 55% RH. Thus, Film 1 likely possesses greater than 380% swelling.,
- (46) Rmaile, H. H.; Farhat, T. R.; Schlenoff, J. B. *J. Phys. Chem. B* **2003**, *107*, 14401-14406.

Chapter 5

CONCLUSIONS AND FUTURE WORK

5.1 Conclusions

This body of work demonstrates that novel polymeric films are capable of effecting separations in nanofiltration (NF). Polyelectrolyte multilayers (PEMs) assembled by a simple layer-by-layer technique can cover porous alumina supports with just a few bilayers. In addition, simple adjustments to synthesis variables such as the constituent polyelectrolytes, deposition conditions, and the capping-layer choice (polyanion or polycation) result in films with molecular weight cutoffs (MWCOs) ranging from 100 to >20000. These PEMs possess higher NF fluxes than commercially available membranes and can separate sugars, salts from sugars, and even proteins.

This dissertation also investigates how swelling of PEMs relates to polyelectrolyte structure and solute transport. In situ ellipsometry experiments reveal that the swelling of PEMs in water is directly related to polyelectrolyte charge density. Assembling PEM films from polyelectrolytes that have a low charge density results in films that swell more, which in turn leads to higher MWCOs. PEM swelling can also be top-layer dependent, as poly(styrene sulfonate) (PSS)/poly(diallyldimethylammonium chloride) (PDADMAC) films swell 4 times more when the polycation is the capping layer as opposed to the polyanion. Additionally, swelling correlates to permeability, as films with greater

water uptake have lower NF rejections and higher sugar fluxes than PEMs that swell less.

Moreover, one can tailor membranes for specific applications. The selectivities and overall fluxes in oligosaccharide fractionation and the separation of salt from sugar can be optimized by simple adjustments to the PEM deposition system. For example, the NaCl/sucrose selectivity of PSS/PDADMAC films can be increased by a factor of 10 by simply capping these coatings with 1.5-bilayers of PSS/poly(allylamine hydrochloride) (PAH).

5.2 Future Work

There are a number of research paths available with PEM films. One of the most interesting directions involves optimization of the previously described hyaluronic acid (HA)/chitosan films. Chapter 2 describes them as possessing a MWCO between 20 and 70 kDa with fluxes much higher than any other membrane system studied. As the functional groups of these polyelectrolytes are primary amines and carboxylic acids, such films may be susceptible to crosslinking. Formation of covalent amide bonds would likely limit the mobility of the polymer chains, reducing swelling and decreasing the MWCO. Thus, stoichiometric or temporal control of the crosslinking reaction could result in various transport properties. The crosslinking could be performed chemically via an 1-ethyl-3-(3-dimethylaminopropyl)-carbodiimide (EDC)/N-hydroxysuccinimide (NHS) coupling as shown in Figure 5.1.¹ Reaction progress could be monitored by changes in film swelling or by FT-IR studies of crosslinked films deposited

Figure 5.1: Simplified mechanism for the crosslinking reaction of HA and chitosan by EDC/NHS coupling.

on Al or Au-coated silicon wafers. Heating the PEM may be another way to produce a crosslinked system,² though membrane decomposition may be a concern.

Another interesting application of PEMs would be their use as sizestationary phases in electrochromatography.^{3,4} exclusion Capillary electrophoresis cannot separate neutral solutes without buffer additives. Even with the addition of a stationary phase, neutral solutes with similar polarities may still be challenging to resolve. However, utilizing the size-selective properties of PEMs could facilitate these separations by excluding larger solutes while allowing small molecules to partition into the stationary phase, increasing their retention time. Additionally, PEMs are charged so electroosmosis could still be employed as a driving force for flow. 5,6 PSS/PDADMAC films could be ideal for this application, as they do not reject small organics like glycerol, but exclude sucrose and raffinose (see Tables 2.2 and 2.3). However, thick films with a sufficient phase ratio to effect separations may take considerable time to deposit. To combat this possible limitation, exponentially growing PSS/PDADMAC films deposited from high ionic strength could be used, though the transport properties of these films are currently unknown. Additionally, non-polar solutes could be driven into the stationary phase by modifying the PEM film with hydrophobic groups.8

One final project involving PEMs would be a study of the effect of ionic strength on the transport of neutral molecules. Several previous studies report that PEM swelling is directly related to the ionic strength of the surrounding

solution,⁹⁻¹¹ and Chapter 3 of this thesis suggests that transport properties are a strong function of swelling. Thus, the ionic strength of the feed solution should directly affect the sieving properties of a PEM film. In commercial applications a wide range of solution conditions may be encountered, thus knowing how rejection and flux depend on changes in ionic strength is vital.

Overall, there are numerous avenues for the future exploration of PEMs. The straightforward manipulation of PEM permselectivities as well as their ease of deposition makes them highly attractive for practical applications. With continued research and development polymeric film systems have the capacity to benefit separations of all sizes.

5.3 Works Cited

- (1) Sehgal, D.; Vijay, I. K. *Anal. Biochem.* **1994**, *218*, 87-91.
- (2) Harris, J. J.; DeRose, P. M.; Bruening, M. L. *J. Am. Chem. Soc.* **1999**, *121*, 1978-1979.
- (3) Ding, F.; Stol, R.; Kok, W. T.; Poppe, H. *J. Chromatogr., A* **2001**, *924*, 239-249.
- (4) Stol, R.; Pedersoli, J. L., Jr.; Poppe, H.; Kok, W. T. *Anal. Chem* **2002**, **74**, 2314-2320.
- (5) Sui, Z.; Schlenoff, J. B. *Langmuir* **2003**, *19*, 7829-7831.
- (6) Stanton, B. W.; Harris, J. J.; Miller, M. D.; Bruening, M. L. *Langmuir* **2003**, *19*, 7038-7042.
- (7) McAloney, R. A.; Sinyor, M.; Dudnik, V.; Goh, M. C. *Langmuir* **2001**, *17*, 6655-6663.
- (8) Dai, J.; Balachandra, A. M.; Lee, J. I.; Bruening, M. L. *Macromolecules* **2002**, *35*, 3164-3170.
- (9) Sukhorukov, G. B.; Schmitt, J.; Decher, G. Berichte der Bunsen-Gesellschaft 1996, 100, 948-953.
- (10) Gao, C.; Leporatti, S.; Moya, S.; Donath, E.; Möhwald, H. *Chem.--Eur. J.* **2003**, *9*, 915-920.
- (11) Burke, S. E.; Barrett, C. J. Biomacromolecules 2005, 6, 1419-1428.

